

**Molecular mechanisms of the cytokine-dependent  
induction of the heme oxygenase-1 gene: *in vivo*  
and *in vitro* studies**

Dissertation  
zur Erlangung des Doktorgrades  
der Mathematisch-Naturwissenschaftlichen Fakultäten  
der Georg-August-Universität zu Göttingen

vorgelegt von  
Kyrylo Tron  
aus Zhytomyr, Ukraine

Göttingen 2004

D7

Referent: Prof. Dr. Rüdiger Hardeland

Korreferent: Prof. Dr. Kurt von Figura

Tag der mündlichen Prüfung: 30.06.2004

# Contents

<b>Abbreviations .....</b>	<b>VI</b>
<b>Summary.....</b>	<b>1</b>
<b>1. Introduction .....</b>	<b>3</b>
<b>1.1 Heme: an essential catalyst of biological oxidation processes .....</b>	<b>3</b>
<b>1.2 Heme oxygenases (HO), key enzymes for heme catabolism.....</b>	<b>3</b>
1.2.1 Mammalian isoforms of HO.....	3
1.2.2 The oxidative cleavage of heme by HO-1 .....	4
1.2.3 HO-1, the “inducible” isozyme among the HO family .....	6
<b>1.3 The biological significance of the HO system .....</b>	<b>7</b>
1.3.1 Carbon monoxide (CO), a second messenger gas .....	7
1.3.2 Biliverdin and bilirubin as potent antioxidants .....	9
1.3.3 “Free” iron: a regulator of mRNAs expression.....	10
<b>1.4 Acute phase response (APR) and its mediators .....</b>	<b>11</b>
1.4.1 APR: a systemic reaction of an organism to maintain its integrity.....	11
1.4.2 Mediators of the hepatic APR .....	12
1.4.3 Acute phase proteins and their regulation.....	13
1.4.4 Models of the APR .....	15
<i>Animal models of the APR .....</i>	<i>15</i>
<i>In vitro models of the APR .....</i>	<i>15</i>
<b>1.5 Aim of the study .....</b>	<b>16</b>
<b>2. Materials.....</b>	<b>18</b>
<b>2.1 Animals.....</b>	<b>18</b>
<b>2.2 Bacterial strain, vectors and plasmid constructs.....</b>	<b>18</b>
2.2.1 Bacterial strain .....	18
2.2.2 Vectors.....	18
<i>pBS-KSII vector .....</i>	<i>18</i>
<i>pcDNA3.1 vector.....</i>	<i>19</i>
<i>pGL3-basic vector.....</i>	<i>21</i>
2.2.3 Plasmid constructs .....	21
<i>HO-1 promoter constructs.....</i>	<i>21</i>
<i>Vector expressing GFP.....</i>	<i>22</i>
<b>2.3 Oligonucleotides and cDNA probes.....</b>	<b>23</b>

2.3.1 Oligonucleotides .....	23
2.3.2 cDNA probes.....	23
<b>2.4 Antibodies .....</b>	<b>24</b>
<b>2.5 Proteins, enzymes and protein standards.....</b>	<b>25</b>
<b>2.6 Protease inhibitors .....</b>	<b>25</b>
<b>2.7 Detection, purification and synthesis systems (kits) .....</b>	<b>25</b>
<b>2.8 Stock solutions .....</b>	<b>26</b>
<b>2.9 Chemicals.....</b>	<b>28</b>
<b>2.10 Other materials .....</b>	<b>30</b>
<b>2.11 Instruments .....</b>	<b>31</b>
<b>3. Methods .....</b>	<b>34</b>
<b>3.1 Methods of cell biology.....</b>	<b>34</b>
3.1.1 Isolation of rat hepatocytes .....	34
<i>Liver perfusion .....</i>	<i>34</i>
<i>Preparation of the hepatocyte suspension .....</i>	<i>34</i>
3.1.2 Isolation of rat Kupffer cells.....	36
<i>Liver perfusion and preparation of cell suspension .....</i>	<i>36</i>
<i>Separation of nonparenchymal liver cells.....</i>	<i>36</i>
<i>Purification of Kupffer cells by counterflow elutriation .....</i>	<i>37</i>
3.1.3 Primary culture treatment and harvesting of rat liver cells.....	40
<i>Primary culture of rat hepatocytes.....</i>	<i>40</i>
<i>Culturing of Kupffer cells.....</i>	<i>41</i>
<b>3.2 Methods of molecular biology.....</b>	<b>42</b>
3.2.1 Transformation of <i>E. coli</i> .....	42
3.2.2 Purification of plasmid DNA .....	43
3.2.3 Amplification of DNA by polymerase chain reaction (PCR).....	45
3.2.4 Agarose gel electrophoresis of DNA .....	48
3.2.5 Radioactive labeling of DNA .....	49
<i>DNA labeling by nick translation method.....</i>	<i>49</i>
<i>DNA labeling by random priming reaction .....</i>	<i>50</i>
<i>Purification of labeled DNA .....</i>	<i>50</i>
<i>Measurement of <math>\beta</math>-radioactivity .....</i>	<i>51</i>
3.2.6 Isolation of total RNA .....	51
<i>RNA isolation procedure using silicate columns .....</i>	<i>51</i>

<i>Isolation of RNA by density-gradient ultracentrifugation</i> .....	53
3.2.7 Northern blot analysis .....	55
<i>Preparation of RNA samples</i> .....	55
<i>Electrophoresis conditions</i> .....	56
<i>Transfer of RNA to nylon membrane</i> .....	56
<i>Hybridization of RNA with radiolabeled cDNA probe</i> .....	57
3.2.8 Transient transfection of primary rat hepatocytes .....	60
3.2.9 Detection of luciferase activity.....	61
<i>Preparation of cell lysates</i> .....	61
<i>Luciferase detection</i> .....	62
<b>3.3 Biochemical methods</b> .....	<b>62</b>
3.3.1 Protein extraction from liver tissue and cultured hepatocytes .....	62
<i>Preparation of tissue homogenates</i> .....	62
<i>Preparation of cell lysates</i> .....	63
3.3.2 Western blot analysis .....	65
<i>Sample preparation</i> .....	65
<i>Casting of SDS-polyacrylamide gel</i> .....	65
<i>SDS-polyacrylamide gel electrophoresis (SDS-PAGE) and</i> <i>electrophoretic transfer</i> .....	66
<i>Staining the membrane with Ponceau S</i> .....	66
<i>Immunovisualization</i> .....	67
3.3.3 Enzyme-Linked Immunosorbent Assay (ELISA) .....	71
3.3.4 Immunohistochemical analysis .....	73
<i>Preparation and fixation of tissue sections</i> .....	73
<i>Inhibition of endogenous peroxidases and blocking of nonspecific</i> <i>binding</i> .....	74
<i>Incubation with antibodies</i> .....	74
<i>Visualization of immune complexes</i> .....	74
3.3.5 Statistical analysis.....	76
3.3.6 Safety measures .....	76
<b>4. Results</b> .....	<b>77</b>
<b>4.1 Studies <i>in vivo</i>: HO-1 expression in a turpentine oil (TO) model of</b> <b>the acute phase response (APR) in rats</b> .....	<b>77</b>

4.1.1 HO-1 expression in the liver and extrahepatic tissues during a turpentine oil (TO)-induced acute phase response (APR) in rats.....	77
<i>Expression of hepatic HO-1 mRNA and protein during a turpentine oil (TO)-induced acute phase reaction .....</i>	<i>77</i>
<i>Expression of HO-1 mRNA in extrahepatic rat tissues during a turpentine oil (TO)-induced acute phase reaction .....</i>	<i>79</i>
4.1.2 Distribution of HO-1 within the liver and injured muscle during a turpentine oil (TO)-induced acute phase response (APR) in rats.....	81
<i>HO-1 distribution in the livers of untreated and turpentine oil (TO)-treated rats.....</i>	<i>81</i>
<i>HO-1 distribution in injured muscle during a turpentine oil (TO)-induced acute phase reaction .....</i>	<i>83</i>
4.1.3 Assessment of IL-6 mRNA expression in various tissues and serum levels of IL-6 during a turpentine oil (TO)-induced acute phase response (APR) in rats.....	85
<i>Expression of IL-6 mRNA occurred only in muscle during a turpentine oil (TO)-induced acute phase reaction .....</i>	<i>85</i>
<i>Serum IL-6 levels in rats during a turpentine oil (TO)-induced acute phase reaction.....</i>	<i>87</i>
<b>4.2 Studies <i>in vitro</i>: HO-1 expression in primary cultures of rat hepatocytes treated with proinflammatory cytokines.....</b>	<b>88</b>
4.2.1 Regulation of HO-1 mRNA expression in primary rat hepatocytes by proinflammatory cytokines .....	88
<i>Dose-dependent induction of HO-1 mRNA expression in primary rat hepatocytes by proinflammatory cytokines .....</i>	<i>88</i>
<i>Time-dependent induction of HO-1 mRNA expression in primary rat hepatocytes by proinflammatory cytokines .....</i>	<i>90</i>
4.2.2 Regulation of HO-1 mRNA and protein expression by IL-6 in primary rat hepatocytes .....	92
<i>Dose-dependent induction of HO-1 mRNA and protein expression by IL-6 in primary rat hepatocytes.....</i>	<i>94</i>
<i>Time-dependent induction of HO-1 mRNA and protein expression by IL-6 in primary rat hepatocytes.....</i>	<i>94</i>

4.2.3 Regulation of transfected HO-1 promoter luciferase gene constructs by IL-6 in primary rat hepatocytes .....	96
<i>Sequence analysis of the rat HO-1 promoter</i> .....	97
<i>Induction of the rat HO-1 promoter controlled luciferase expression in primary rat hepatocytes by IL-6 treatment</i> .....	97
<b>5. Discussion</b> .....	<b>101</b>
<b>5.1 Regulation of HO-1 expression in turpentine oil (TO) model of the acute phase response (APR) in rats</b> .....	<b>101</b>
<b>5.2 Expression of IL-6 after turpentine oil (TO) administration and its possible role in HO-1 induction in the liver</b> .....	<b>102</b>
<b>5.3 Cell type specificity of HO-1 induction and its possible role in turpentine oil (TO)-induced acute phase response (APR)</b> .....	<b>104</b>
<b>5.4 Cytokine-dependent regulation of HO-1 in cultured hepatocytes</b> .....	<b>106</b>
<b>5.5 Molecular mechanisms of HO-1 regulation under inflammatory conditions</b> .....	<b>108</b>
<b>5.6 Conclusions and future directions</b> .....	<b>110</b>
<b>References</b> .....	<b>112</b>

## Abbreviations

Ab	Antibody
AMP	Adenosine monophosphate
AP-1	Activating protein 1
APP	Acute phase proteins
APR	Acute phase response
APS	Ammonium persulfate
ATP	Adenosine triphosphate
BCA	Bicinchoninic acid
bp	Base pair
BR	Bilirubin
BSA	Bovine serum albumin
BV	Biliverdin
BV-R	Biliverdin reductase
C/EBP $\beta$	CCAAT/enhancer binding protein $\beta$
cAMP	Cyclic adenosine-3',5'-monophosphate
cDNA	Copy desoxyribonucleic acid
CDTA	<i>trans</i> -1,2-Diaminocyclohexane -N, N, N', N'-tetraacetate
cGMP	Cyclic guanosine monophosphate
Ci	Curie
CNTF	Ciliary neurotrophic factor
CO	Carbon monoxide
CRE	cAMP response element
CRP	C-reactive protein
dd H <sub>2</sub> O	Double distilled water
DEPC	Diethylpyrocarbonate
DMSO	Dimethylsulfoxide
dNTP	Deoxyribonucleoside triphosphate
DTT	Dithiothreitol
<i>E. coli</i>	Escherichia coli
E-box	Enhancer box element
EDTA	Ethylendiaminetetraacetic acid
EGTA	Ethylenglycol-bis-(2-aminoethylether)-N, N'-tetraacetate



ELISA	Enzyme-linked immunosorbent assay
FCS	Fetal calf serum
g	Gravity
GAPDH	Glyceraldehyde-3-phosphate dehydrogenase
GFP	Green fluorescent protein
gp	Glycoprotein
GRE	Glucocorticoid response element
HEPES	2-(4-(2-hydroxyethyl)-piperazinyl)-1-ethansulfonate
HO	Heme oxygenase
HPLC	High performance liquid chromatography
HRP	Horseradish peroxidase
HSE	Heat shock element
hsp32	32 kDa heat-shock protein
IgG	Immunoglobulin G
IL	Interleukin
IL-6-RE	IL-6 response element
Ins	Insulin
IRP	Iron regulatory protein
I $\kappa$ B	NF $\kappa$ B inhibitory subunit
JAK	Janus kinase
kb	Kilobase
kDa	Kilodalton
LB	Luria Bertani
LIF	Leukemia inhibitory factor
LPS	Lipopolysaccharide
Luc	Luciferase
$\alpha$ 2-M	$\alpha$ 2-macroglobulin
MAPK	Mitogen-activated protein kinase
MOPS	3-(N-Morpholino)-propanesulfonic acid
NAD(P) <sup>+</sup>	Nicotinamide adenine dinucleotide (phosphate) oxidized
NAD(P)H	Nicotinamide adenine dinucleotide (phosphate) reduced
NF- $\kappa$ B	Nuclear factor $\kappa$ B
NO	Nitric oxide
OD	Optical density

OSM	Oncostatin M
PBS	Phosphate buffered saline
pBS	Plasmid Bluescript
PCR	Polymerase chain reaction
PGJ-2	Prostaglandin J <sub>2</sub>
pHO	Heme oxygenase promoter
PMSF	Phenylmethyl sulfonylfluoride
RNase	Ribonuclease
ROS	Reactive oxygen species
rpm	Revolutions per minute
RT	Room temperature
RT-PCR	Reverse transcriptase-PCR
SAA	Serum amyloid A
SBE	STAT binding element
SDS	Sodium dodecylsulfate
SDS-PAAG	SDS-polyacrylamide gel
SDS-PAGE	SDS-polyacrylamide gel electrophoresis
SEM	Standard error of the mean
sGC	Soluble guanylate cyclase
SSC	Standard saline citrate
STAT	Signal transducer and activator of transcription
TAE	Tris acetate EDTA buffer
TEMED	N, N, N', N'-tetramethylethylenediamine
TNF- $\alpha$	Tumor necrosis factor $\alpha$
TO	Turpentine oil
Tris	Tris-(hydroxymethyl)-aminomethane
UV	Ultraviolet
WB	Western blot

## Summary

Heme oxygenase-1 (HO-1) is the inducible and rate-limiting enzyme which catalyses the oxidative degradation of heme. This reaction yields carbon monoxide (CO), divalent iron ( $\text{Fe}^{2+}$ ), and biliverdin. For these products, a broad range of anti-inflammatory, anti-apoptotic and anti-proliferative activities has been discussed. In this regard HO-1 has been proposed to be involved in the acute phase response (APR), the defense reaction of the organism directed against any damaging or injuring agents. However, the mechanisms of the HO-1 regulation under inflammatory conditions are poorly understood. Especially, it remains unclear, whether the induction of HO-1 *in vivo* occurs as a response to the cytokines released by inflammatory cells. It is also a matter of debate which cell type(s) within the liver contribute(s) to HO-1 up-regulation in the course of inflammation. Moreover, it is not known whether the induction of HO-1 during inflammation is a liver-specific, direct consequence of the APR or just a matter of accompanying oxidative stress and occurs in other organs to the similar extent. Furthermore, on the level of signal transduction, the pathways for cytokine-dependent HO-1 induction are not yet elucidated.

Therefore it was the aim of the present study, by the use of a turpentine oil model of the acute phase response in rats, to examine the HO-1 expression in the liver and in extrahepatic tissues and to evaluate the role of IL-6, the principle mediator of inflammation, in this process. Further, the investigation of spatial and cell type-specific induction of HO-1 within the liver and injured muscle was intended. In addition, it was also the purpose to study regulation of HO-1 expression by various proinflammatory cytokines using primary cultures of isolated rat hepatocytes and to perform a functional analysis of the rat HO-1 promoter to define DNA elements involved in the cytokine-dependent HO-1 gene regulation.

The present study has demonstrated that during turpentine oil-induced localized inflammation in rats, the expression of HO-1 was strongly up-regulated at early time points in injured muscle, the initiating site of the acute phase reaction, and in the liver, the major source of serum acute phase proteins. In other internal organs investigated, only moderate changes were observed. As revealed by immunohistochemical analysis, in injured muscle the induction of HO-1 was

attributed to macrophages, whereas in the liver, hepatocytes were the major source of the elevated HO-1 levels during the acute phase response.

Among various tissues examined under inflammatory conditions by Northern blot, muscular tissue at the site of turpentine oil injection was found to be the only source of IL-6, the principle mediator of the acute phase response in rats. The up-regulation of IL-6 mRNA levels was followed by elevated plasma levels of this cytokine, as measured by the rat IL-6-specific ELISA. The elevated plasma IL-6 concentrations correlated with hepatic HO-1 induction in the course of inflammation, suggesting that IL-6 derived from injured muscle is most likely responsible for the HO-1 induction in the rat liver.

Studies in primary rat hepatocytes further underlined the pivotal role of IL-6 in hepatic HO-1 induction under inflammatory conditions. As demonstrated by Western and Northern blot analyses, among the proinflammatory cytokines (IL-6, IL-1 $\beta$ , and TNF- $\alpha$ ) used for the treatment of primary cultured rat hepatocytes, IL-6 was the most potent inducer of HO-1 expression in time- and dose-dependent experiments. Sequence analysis of the rat HO-1 promoter revealed the presence of several putative binding sites for transcription factors of the STAT-family, the major transducers of IL-6 signalling. Furthermore, the functional analysis of the rat HO-1 promoter by means of the luciferase reporter gene assay, using deletion and mutation approaches, identified one of the putative STAT binding sites, S3BE, as an active element of the IL-6-dependent HO-1 gene regulation, which does not require cooperation with AP-1 binding site for its action.

Taken together, these data indicate that HO-1 might be referred to as an intracellular positive acute phase protein that plays an important role in cytoprotection of hepatocytes, which might become damaged during their clearance function. Moreover, at the site of local injury, up-regulation of HO-1 in macrophages can participate in the resolution of inflammation.

# 1. Introduction

## 1.1 Heme: an essential catalyst of biological oxidation processes

Heme (Fe-protoporphyrin IX) is a ubiquitous molecule containing an active iron linked to the four nitrogen atoms of a tetrapyrrole macrocycle (Maines, 1997). Since the active iron in a reduced ferrous state has a high affinity for molecular oxygen and can donate electrons, the heme molecule promotes most biological oxidation processes and, thus, performs vital functions in aerobic metabolism (Ryter and Tyrrell, 2000).

Heme serves as a prosthetic moiety for various heme proteins involved in oxygen transport (hemoglobin) and storage (myoglobin), mitochondrial respiration (cytochromes), oxidative modification of xenobiotics (cytochrome P450 family), cellular antioxidant defenses (peroxidases, catalase, other enzyme systems), and signal transduction processes (nitric oxide synthase, soluble guanylate cyclase) (Ryter and Tyrrell, 2000; Dennery, 2000).

On the other hand, heme may catalyze the production of cytotoxic reactive oxygen species which, in turn, cause DNA damage, lipid peroxidation and protein denaturation resulting in cellular damage. Therefore, the cellular heme pool needs to be tightly controlled by heme synthesis (provided by  $\delta$ -aminolevulinate synthase) and degradation (carried out by heme oxygenase) (Immenschuh and Ramadori, 2000).

## 1.2 Heme oxygenases (HO), key enzymes for heme catabolism

Heme oxygenases (HO) perform the oxidative cleavage of the heme molecule, an essential reaction in diverse physiological processes in various species. Thus expression and regulation of these enzymes might play an important role in maintaining cellular homeostasis (Otterbein and Choi, 2000).

### 1.2.1 Mammalian isoforms of HO

Three isoforms of HO (HO-1, HO-2, and HO-3) have been described in mammals as the products of separate genes (Maines et al., 1986; Shibahara et al., 1993; McCoubrey, Jr. et al., 1997b). HO-1, also known as the major 32-kDa heat-shock protein (hsp32), is widely expressed in tissues and highly inducible in virtually all

cell types by a variety of stimuli (Maines, 1997). Under physiological conditions, HO-1 expression is highest in the spleen, a major organ for destruction of senescent erythrocytes (Dennerly, 2000). Constitutively synthesized HO-2, a 36-kDa protein, is known to be abundant in brain, testis, and unstimulated liver of rodents and humans (Cruse and Maines, 1988). HO-2 is so far unresponsive to any of known HO-1 inducers and therefore functions mainly in normal heme metabolism (Shibahara et al., 1993; McCoubrey, Jr. and Maines, 1994; Maines, 1997). The recently discovered HO-3 isozyme (33 kDa in size) displays a high sequence homology with HO-2 but it is nearly devoid of catalytic activity (McCoubrey, Jr. et al., 1997b). Besides the catalytic domain, both HO-2 and HO-3 contain two additional heme binding sites which might be relevant to the regulatory role of these isoforms in heme-dependent cellular processes (McCoubrey, Jr. et al., 1997a; McCoubrey, Jr. et al., 1997b). Although functions and regulation of HO-3 are not completely understood, there is evidence that it may serve as heme binding/transporting protein (McCoubrey, Jr. et al., 1997b).

### **1.2.2 The oxidative cleavage of heme by HO-1**

Heme oxygenase-1 (EC 1.14.99.3) catalyzes the initial and rate-limiting reaction in the catabolism of heme (iron-protoporphyrin IX) yielding equimolar amounts of biliverdin, carbon monoxide (CO), and free ferrous iron ( $\text{Fe}^{2+}$ ) (Figure 1) (Tenhunen et al., 1968; Tenhunen et al., 1969). HO-1 is found in the endoplasmic reticulum in a complex with NADPH cytochrome P450 reductase and degrades heme in a multi-step, energy-requiring system (Yoshida and Kikuchi, 1979). This system utilizes molecular oxygen ( $\text{O}_2$ ) and requires NADPH as a source of the reducing equivalents, which are transferred to HO-1 by cytochrome P450 reductase and used for activation of  $\text{O}_2$  and reduction of heme iron from  $\text{Fe}^{3+}$  to  $\text{Fe}^{2+}$  and/or maintenance of iron in the  $\text{Fe}^{2+}$  state (Maines, 1997). The conversion reaction of one heme molecule requires the input of three  $\text{O}_2$  molecules and a total of seven electrons (Figure 1) (Wilks, 2002).

The cleavage of heme by HO-1 is regioselective and occurs at the  $\alpha$ -meso-carbon to form biliverdin IX $\alpha$  as the sole enzymatic product (Tenhunen et al., 1969). This reaction consists of three mono-oxygenation cycles; in each of them the reduced iron binds molecular oxygen that accepts the second electron from NADPH. The first cycle forms  $\alpha$ -meso-hydroxyheme, the second cycle eliminates the  $\alpha$ -methene

bridge carbon as CO producing  $\alpha$ -verdoheme, and the third cycle forms a ferribiliverdin IX $\alpha$  complex, BV-Fe<sup>3+</sup>. An additional NADPH is consumed for reduction of the BV-Fe<sup>3+</sup> followed by dissociation of Fe<sup>2+</sup> from biliverdin (Ryter and Tyrrell, 2000).

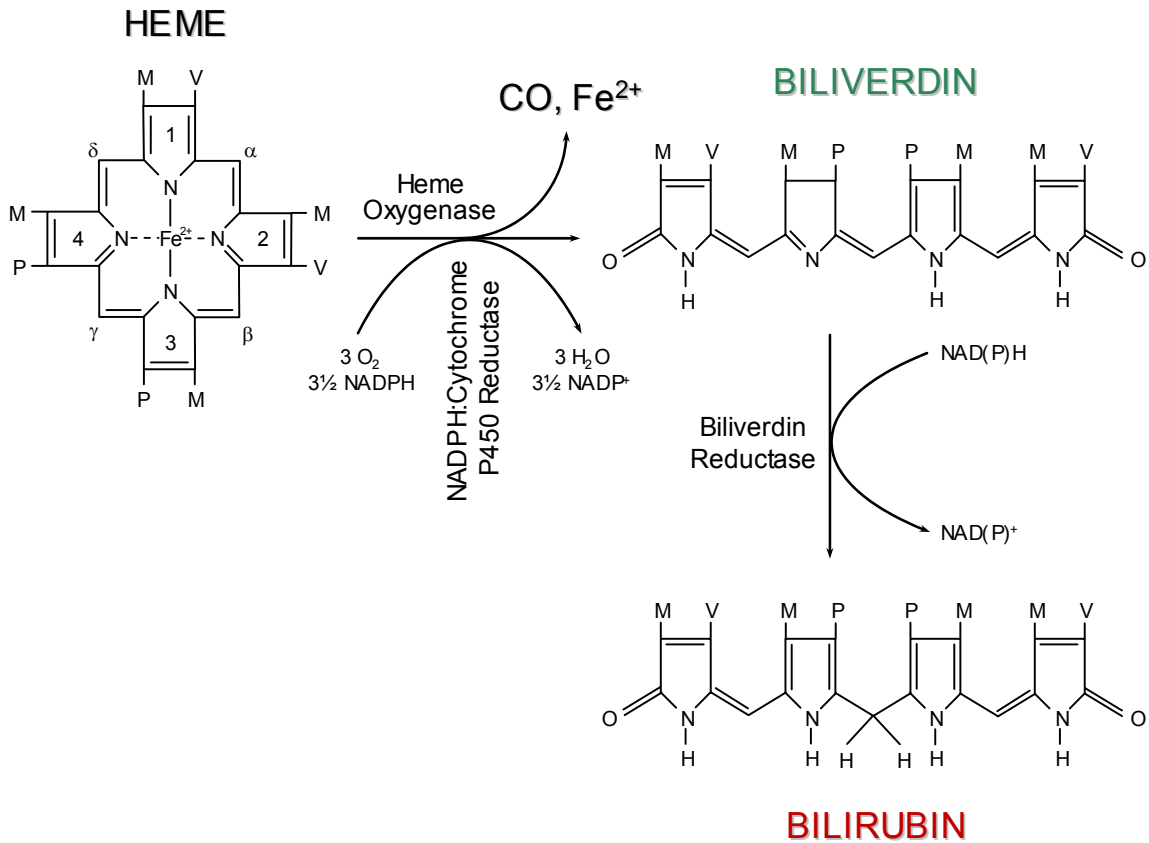


**Figure 1. Enzymatic conversion of heme to bilirubin.** Oxidative cleavage of the  $\alpha$ -*meso*-carbon bridge of a b-type heme molecule by heme oxygenase yields equimolar quantities of biliverdin IX $\alpha$  and carbon monoxide (CO), while the central iron is released. Biliverdin is subsequently converted to bilirubin by biliverdin reductase. Abbreviations are as follows: M, methyl; V, vinyl; P, propionate. The heme pyrrole rings are labeled 1-4 and the *meso*-carbons  $\alpha$ - $\gamma$ .

In most mammalian species, biliverdin is subsequently reduced to bilirubin (BR) by the action of the cytoplasmic enzyme NAD(P)H biliverdin reductase (Figure 1), (Tenhunen et al., 1969) while the free iron is promptly sequestered into ferritin (Balla et al., 1992). The BR formed in the various tissues effluxes into the blood, where it forms a 1:1 complex with albumin. The circulating BR, in turn, is absorbed by the liver parenchyma, subsequently conjugated with sugars (mainly glucuronic acid) by uridine diphosphate-glucuronosyl transferase and then excreted into the bile (Ryter and Tyrrell, 2000).

### 1.2.3 HO-1, the “inducible” isozyme among the HO family

HO-1 expression is induced not only in response to its substrate heme (Tenhunen et al., 1970), but also by various stress stimuli such as hydrogen peroxide (H<sub>2</sub>O<sub>2</sub>), xenobiotics, nitric oxide, ultraviolet-A radiation, heavy metals, hypoxia, hyperoxia, heat shock, glutathione depletion, sodium arsenite, prostaglandins (Elbirt and Bonkovsky, 1999; Ryter and Choi, 2002), ischemia/reperfusion (Maines et al., 1993; Bauer et al., 1998), shear stress (Wagner et al., 1997; Pillar and Seitz, 1999), bacterial endotoxins (Rizzardini et al., 1994; Immenschuh et al., 1999), and proinflammatory cytokines (Cantoni et al., 1991; Mitani et al., 1992; Rizzardini et al., 1998; Oguro et al., 2002).

Despite the great variety of HO-1 inducers, most, if not all, of them exert their effects on HO-1 gene expression at the transcriptional level (Elbirt and Bonkovsky, 1999; Bauer and Bauer, 2002). However, the broad spectrum and chemical diversity of HO-1 inducers argues against the possibility that all agents utilize a single transcription activation pathway. Indeed, various transcriptional enhancer elements have been identified within the 5′-flanking region of the mouse, rat, human and chicken HO-1 genes (Choi and Alam, 1996; Elbirt and Bonkovsky, 1999). In most cases, these motifs are equivalent to or a variation of recognition sites for known DNA-binding proteins, including those for activator protein-1 (AP-1) and nuclear factor κB (NF-κB) as well as hypoxia response, cadmium response, heat-shock response, and metal response elements (Bauer and Bauer, 2002).

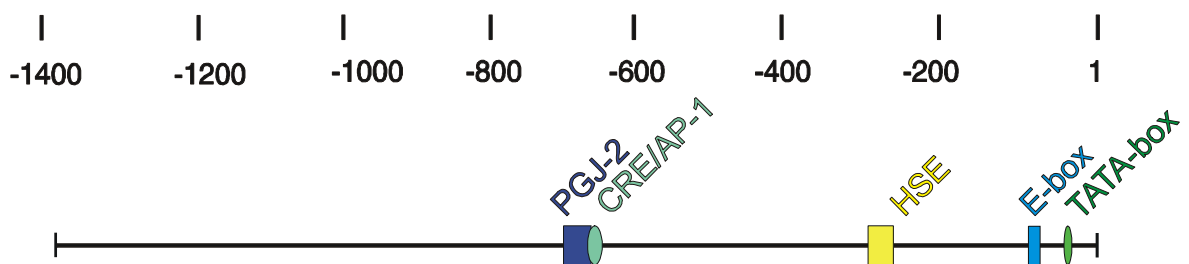


**Figure 2. Scheme of the rat HO-1 gene promoter.** The known functional response elements are indicated as: TATA-box element; E-box, enhancer box element; HSE, heat shock response element; CRE/AP-1, cAMP response element / activator protein-1 binding site; PGJ-2, prostaglandin J<sub>2</sub> response element. The promoter length is indexed on top by negative numbers in bp, starting from the transcription initiation site.

Among mammalian HO-1 genes, the most detailed description is given to the mouse one. The majority of functional inducer-responsive sequences identified to



date were found in the promoter, proximal enhancer and two distal enhancers within 12 kb of the 5'-flanking region of the mouse HO-1 gene (Choi and Alam, 1996). Being located 4 and 10 kb upstream from the transcription initiation site, the distal enhancers exhibit a potent cooperation with the HO-1 promoter in mediating HO-1 gene transcription in response to various stimuli (Alam et al., 1994; Camhi et al., 1995; Lee et al., 2000).

Although the gene coding for rat HO-1 has been cloned as early as 1987 by Müller and colleagues (Muller et al., 1987), the rat HO-1 gene promoter region is poorly investigated (Figure 2). Only a few functional inducer-responsive sequences were identified within 1387 bp of the 5'-flanking region of the rat HO-1 gene. Among them are: enhancer box (Kietzmann et al., 2003), heat shock response element (Okinaga and Shibahara, 1993), activator protein-1 binding site (Immenschuh et al., 1998), and prostaglandin J<sub>2</sub> response element (Koizumi et al., 1995).

### **1.3 The biological significance of the HO system**

The potential toxicity of heme points to a critical role for heme degradation in cellular metabolism. This function is provided by the HO system, which thus participates in cellular defense. An increasing number of evidences reveals the protective role of HOs, particularly HO-1 due to its inducibility, by virtue of anti-inflammatory, anti-apoptotic and anti-proliferative activities of the products released by the heme breakdown reaction (Figure 3) (Otterbein et al., 2003; Wunder and Potter, 2003; Alcaraz et al., 2003).

#### **1.3.1 Carbon monoxide (CO), a second messenger gas**

Carbon monoxide (CO) was known for a long time as poisonous gas, lethal at high enough doses, and metabolic waste compound. Indeed, due to its strong affinity for hemoglobin and myoglobin, CO is able to prevent oxygen delivery to the tissues and organs, creating hypoxia (Otterbein and Choi, 2000). However, recent studies have shown that physiological concentrations of CO generated from HO activity can regulate vasomotor tone as well as neurotransmission (Verma et al., 1993; Maines, 1997; Suematsu and Ishimura, 2000).

Currently it is known that CO is an endogenous monoxide that, similar to nitric oxide (NO), activates soluble guanylate cyclase (sGC) by binding to the heme moiety of this enzyme, thereby functioning as a second messenger gas

(Christodoulides et al., 1995). Despite CO being a 50-100 times less potent activator of sGC than NO, it appears to provide the major control of the sinusoidal vascular tone in the liver (Wunder and Potter, 2003). This might be due to the fact that in contrast to NO, which is extremely labile and in reaction with superoxide forms peroxynitrite (a potent cytotoxic oxidant), CO is a stable gas and does not form radicals (Motterlini et al., 2002; Hartsfield, 2002). Therefore, CO can accumulate in the cell to levels that are presumably much higher than those of NO (Otterbein and Choi, 2000). The sGC activity leads to the generation of cyclic guanosine monophosphate (cGMP) which, in turn, mediates various physiological functions, e. g., smooth muscle relaxation (Wang et al., 1997).

In addition, CO may influence vascular resistance independently of cGMP via activation of calcium-dependent potassium channels, leading to smooth muscle cells relaxation (Wang et al., 1997), or by inhibiting the cytochrome P450-mediated production of endothelin-1, a vasoactive compound known to cause contraction of the hepatic stellate cells, thereby increasing sinusoidal resistance in the liver (Wunder and Potter, 2003).

As to the liver, CO is involved in the regulation of hepatobiliary function through altering the bile acid-dependent bile flow and the contractility of the bile canaliculus. Moreover, HO-1-derived CO has been shown to protect hepatic microcirculation under stress conditions (Suematsu and Ishimura, 2000).

CO may also possess potent anti-inflammatory effects such as the ability to prevent platelet aggregation by activation of sGC and subsequent generation of cGMP (Brune and Ullrich, 1987). Furthermore, CO has been shown to suppress the proinflammatory cytokine production and to promote increased interleukin (IL)-10 expression by macrophages both *in vitro* and *in vivo* through a pathway involving the mitogen-activated protein (MAP) kinases (Otterbein et al., 2000). Moreover, CO mediates the anti-inflammatory effects of IL-10 via a MAP kinase-dependent pathway (Lee and Chau, 2002). It was also reported that CO prevented apoptosis in several cell types, including endothelial cells, fibroblasts and hepatocytes, utilizing cGMP and/or MAP kinase signalling systems, depending on the cell type (Otterbein et al., 2003).

Thus, CO is one of the most important from HO-1 downstream mediators with a broad range of physiological functions (Figure 3).

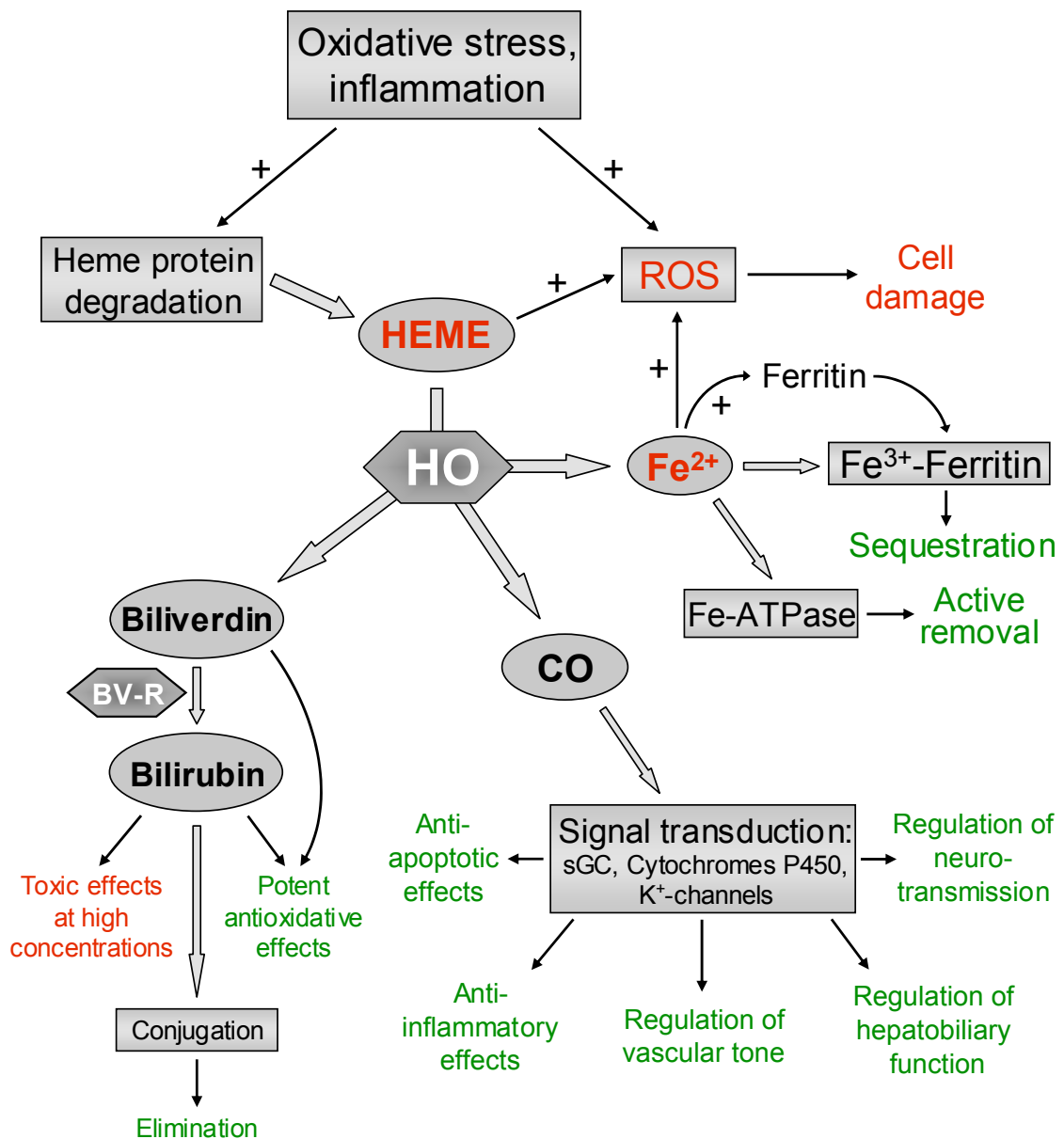


**Figure 3. Significance of the heme oxygenase reaction for cellular homeostasis.** Under inflammatory or oxidative stress conditions, heme, a potent oxidant released from heme containing proteins, becomes available for enzymatic degradation. The degradation of heme by heme oxygenase (HO) results in the release of several by-products like carbon monoxide (CO), divalent iron ( $\text{Fe}^{2+}$ ), and biliverdin with a broad range of biological activities. Biliverdin is subsequently converted into bilirubin by the action of cytosolic biliverdin reductase (BV-R). Beneficial consequences of heme oxygenase activity are shown in green color. Potentially deleterious effects and compounds are indicated in red. ROS, reactive oxygen species; sGC, soluble guanylate cyclase; "+" indicates activation.

### 1.3.2 Biliverdin and bilirubin as potent antioxidants

Cytoplasmic NAD(P)H biliverdin reductase reduces the water soluble biliverdin (BV) to the hydrophobic bilirubin IX $\alpha$  (BR) (Tenhunen et al., 1968). Dissociation of BR from serum albumin, which serves as a principle transporter of unconjugated

BR, represents a rate-limiting step in absorption of BR by hepatocytes (Zucker et al., 1999). Once absorbed, BR undergoes phase-II glucuronidation, forming water-soluble mono- and di-glucuronides which are eliminated by bile and faeces (Figure 3) (Wunder and Potter, 2003). The excess accumulation of unconjugated BR in plasma is known to induce neurotoxicity and can cause hemolysis (Ryter and Tyrrell, 2000). In contrast, BR at nannomolar concentrations protects neuronal cultures against oxidative stress injury (Dore et al., 1999). Administration of BV to mice prolonged survival of cardiac allografts and islets transplanted into allogeneic recipients (Otterbein et al., 2003). Administrated to rats, BV appeared to modulate lipopolysaccharide-induced P- and E-selectin expression in the vascular system, acting as an anti-inflammatory agent (Otterbein and Choi, 2000). BR was reported to provide a protective effect on the transplanted liver grafts via inhibition of lipid peroxidation in hepatocytes (Kato et al., 2003).

BR and BV are thought to exert their protective (including anti-inflammatory and anti-apoptotic) effects largely because of their antioxidant properties (Otterbein et al., 2003). This hypothesis originates from observations of bile pigment antioxidant activity *in vitro*. It has been clearly shown for both BR and BV to prevent the oxidation of polyunsaturated fatty acids in multilamellar liposomes at least as effectively as  $\alpha$ -tocopherol (Stocker et al., 1987). While BR functioned as a chain breaking antioxidant (peroxyl radical reductant), the BV acted as a peroxyl radical trap (Stocker et al., 1987). Exogenous free and albumin-bound BR has also been shown to inhibit plasma and low density lipoprotein lipid peroxidation after the depletion of endogenous circulating antioxidants (Neuzil and Stocker, 1994).

Although it is evident that BR has antioxidant effects in extracellular fluids *in vivo* and some *in vitro* model systems, it remains uncertain to what extent this metabolic waste product is significant as a chain breaking antioxidant at the cellular level (Ryter and Tyrrell, 2000).

### **1.3.3 “Free” iron: a regulator of mRNAs expression**

Reduced iron ( $\text{Fe}^{2+}$ ), released by HO-1 from the core of the heme molecule, is a potent prooxidant, which exhibits its cytotoxic effect via production of reactive oxygen species by Fenton chemistry (Immenschuh and Ramadori, 2000). However, the potential catalysis of oxidative reactions by this compound is limited through its chelation by the iron-sequestering protein ferritin as well as via its

active removal from the cell by the specific Fe-ATPase pump (Figure 3) (Ferris et al., 1999; Baranano et al., 2000).

Expression of ferritin was originally reported to be the mechanism by which HO-1 conferred resistance to oxidative stress in endothelial cells (Balla et al., 1992). HO-1 induction by heme demonstrated ferritin-mediated protective effect in a model of hyperoxic lung injury (Taylor et al., 1998).

Ferritin is a heterooligomeric protein consisting of 24 subunits with a high capacity for iron sequestration (~4500 Fe<sup>3+</sup> ions per holoferritin). The ferroxidase activity intrinsic to ferritin maintains the iron as Fe<sup>3+</sup> (Ryter and Tyrrell, 2000). The synthesis of ferritin is regulated by a post-transcriptional mechanism, which utilizes iron released from HO activity (Eisenstein and Munro, 1990). An iron regulatory protein (IRP) binds to and inhibits the translation of ferritin mRNA. Cytoplasmic iron, as it becomes available, binds to the IRP, releasing the Fe-IRP from ferritin mRNA and thus de-repressing its translation (Eisenstein and Munro, 1990). Similar regulatory mechanisms were found to control synthesis of other proteins involved in iron redistribution, such as transferrin receptor and  $\delta$ -aminolevulinate synthase (Hentze and Kuhn, 1996), divalent cation transporter-1 (Gunshin et al., 1997), and, probably, Fe-ATPase (Baranano et al., 2000).

Thus, the cytoprotective action of ferritin under the stress conditions is triggered by HO-1 induction with subsequent release of “regulatory” iron from heme.

## **1.4 Acute phase response (APR) and its mediators**

The acute phase reaction comprises a variety of systemic changes in response to tissue injury and infection.

### **1.4.1 APR: a systemic reaction of an organism to maintain its integrity**

The acute phase response (APR) is the defense reaction of the organism directed to restrict the area of damage and to eliminate, or at least isolate, the damaging agent. Every agent, which leads to loss of tissue integrity, induces a local reaction, known as inflammation (Ramadori and Christ, 1999).

Different injury agents (e.g., bacterial or viral infections, trauma or extensive surgery, thermal injury, intoxication, etc.) can induce more or less similar signs and symptoms of the APR, such as fever, neurological and hormonal alterations, loss of appetite, muscular pain, leucocytosis, hypoferrremia, hyperglycemia, and

increased protein metabolism in muscles with consequent transfer of amino acids to the liver to maintain synthesis of acute phase proteins (Ramadori and Christ, 1999). The purposes of these systemic and metabolic changes are to control the defense mechanisms, to maintain vital functions in the course of inflammation, and, finally, to restore homeostasis (Moshage, 1997).

#### 1.4.2 Mediators of the hepatic APR

Cells of the inflammatory infiltrate produce and/or induce the production of cytokines, the main soluble factors responsible for the onset, progression and resolution of the APR, whereas the liver is the primary target organ of the host defense reaction (Streetz et al., 2001). The cytokines of the APR can be classified according to similarities in transduction of their signals via specific receptors into two major groups (Table 1).

**Table 1. Cytokines of the acute phase response**

IL-1-type cytokines	Role in the APR	IL-6-type cytokines	Role in the APR
IL-1 $\alpha$	Modulation	IL-6	Induction
IL-1 $\beta$	Induction	CNTF	Modulation
TNF- $\alpha$	Induction	OSM	Modulation
TNF- $\beta$	Modulation	LIF	Modulation
		Cardiotropin 1	Modulation
		IL-11	Modulation

CNTF, ciliary neurotrophic factor; IL, interleukin; LIF, leukemia inhibitory factor; OSM, oncostatin M; TNF, tumor necrosis factor.

Interleukin (IL)-6 itself from the group of IL-6-type cytokines and IL-1 $\beta$  together with tumor necrosis factor (TNF)- $\alpha$  from the IL-1-type cytokine group are considered to be the major mediators of the APR. At the inflammatory sites, IL-6 is produced by macrophages, endothelial cells, and fibroblasts (Ramadori and Christ, 1999). The release of mature IL-1 $\beta$  by macrophages seems to take place only during or after cell death (Perregaux and Gabel, 1998). TNF- $\alpha$  is synthesized mainly by mononuclear phagocytes recruited at the sites of damage and by tissue macrophages (Ramadori and Christ, 1999). While IL-6, IL-1 $\beta$ , and TNF- $\alpha$  are the

inducers of acute phase protein gene expression, other cytokines (Table 1) were shown to modulate this expression (Moshage, 1997).

### **1.4.3 Acute phase proteins and their regulation**

Various plasma proteins synthesized by the liver parenchymal cells exhibit quantitative changes after onset of the APR. Proteins with a transient increase in synthesis and plasma concentration are called positive acute phase proteins (APP), e.g.,  $\alpha$ 2-macroglobulin in rats, C-reactive protein (CRP) and serum amyloid A (SAA) in humans. Proteins whose synthesis decreases under inflammatory conditions are referred to as negative APP, e.g., albumin, transferrin,  $\alpha$ -1 lipoprotein (Ramadori and Christ, 1999). The APPs could be also divided into two classes according to their ability to be regulated by certain cytokines acting via their specific signalling pathways (Figure 4).

IL-6-type cytokines use the common receptor  $\beta$ -subunit (gp130) for signal transduction which in some cases requires an  $\alpha$ -receptor subunit (IL-6, IL-11, CNTF) but in other does not (OSM, LIF) (Heinrich et al., 1998). After ligand binding, dimerization of two  $\beta$ -subunits leads to the activation of the receptor-associated Janus kinases (JAKs), which, in turn, phosphorylate transcription factors from the signal transducer and activator of transcription (STAT) family, namely STAT1, 3, and 5 (Heinrich et al., 2003). After homo- or heterodimerization, activated STATs are translocated to the nucleus, where they bind to target sequences in the promoters of type II APP genes, stimulating synthesis of corresponding proteins (Figure 4). Among STAT factors, STAT3 is considered to play a pivotal role in the regulation of the APR, since STAT3 binding sites were shown in the promoters of various APP genes induced by IL-6 (Streetz et al., 2001).

Activation of TNF/IL-1 receptors after interaction with their ligands initiates the conversion of membrane sphingomyelin to ceramide via sphingomyelinase (Kolesnick and Golde, 1994). Subsequently, ceramide-activated protein kinases connect to several signalling pathways which lead to activation and translocation of transcription factors, such as activating protein (AP)-1 and nuclear factor (NF)- $\kappa$ B (Moshage, 1997). NF- $\kappa$ B is activated and translocated to the nucleus after phosphorylation and degradation of inhibitory subunit I $\kappa$ B (Streetz et al., 2001). Many type I APP genes contain NF- $\kappa$ B and AP-1 response elements in their promoter regions (Figure 4) (Kolesnick and Golde, 1994).

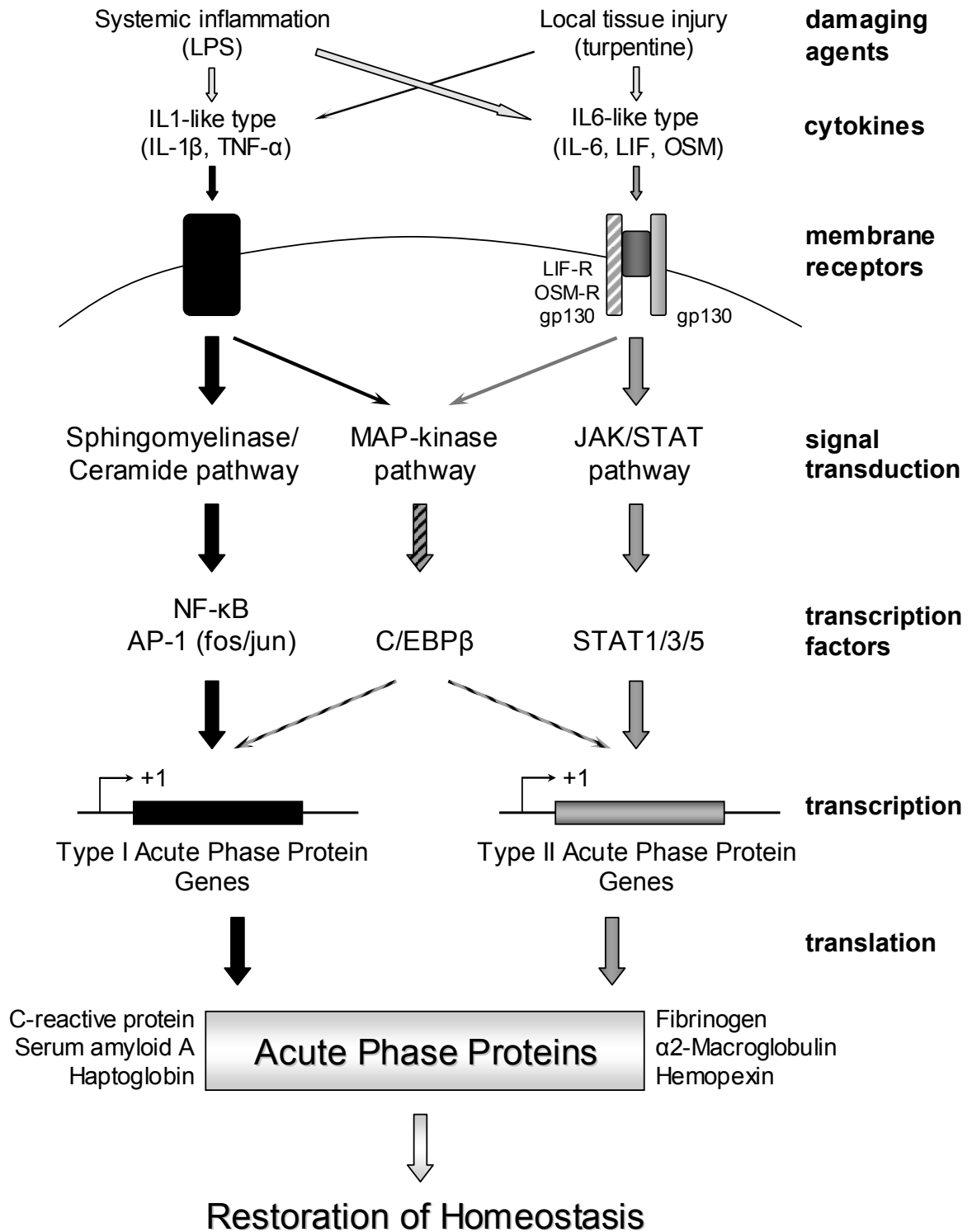


**Figure 4. Induction of the acute phase response.** Damaging agents cause local or systemic inflammation, resulting in increased expression of cytokines. Binding of the ligands to cytokine receptors initiate signalling events, leading to activation of several transcription factors. These factors bind to their response elements in the promoter regions of acute phase genes. Transcription of acute phase genes is induced and acute phase proteins are secreted. In the extracellular environment, acute phase proteins function to restore homeostasis.



An overlapping signalling involving both cytokines families is provided by the mitogen activated protein (MAP) kinase pathway activating the transcription factors of the CCAAT/enhancer binding protein  $\beta$  (C/EBP $\beta$ ) family, which may recognize target sequences in the promoters of type I and II APPs (Figure 4) (Ramadori and Armbrust, 2001).

#### **1.4.4 Models of the APR**

##### *Animal models of the APR*

To study APR *in vivo*, two types of animal models are generally used (Ramadori and Christ, 1999). In the first model, APR is induced in rodents by intraperitoneal or intravenous administration of the bacterial lipopolysaccharide (LPS). It is characterized by systemic inflammation and rapid circulatory increase of all three major proinflammatory cytokines: IL-6, IL-1  $\beta$  and TNF- $\alpha$  (Ulich et al., 1990; Ulich et al., 1991; Luster et al., 1994). In the second model, induction of a sterile abscess in rats by subcutaneous or intramuscular injection of turpentine oil (TO) causes a local inflammation with a subsequent systemic APR (Fey and Fuller, 1987). This model is characterized by local increase in IL-1 $\beta$  and TNF- $\alpha$ , and circulatory increase in IL-6 (Luheshi et al., 1997).

##### *In vitro models of the APR*

Once it became obvious that the liver is a primary target organ for the APR, the individual liver cell types were introduced in culture to investigate a hierarchy of the events triggering the full APR in the liver. Besides the ability to respond to the cytokine action, different cell types within the liver are also able to express IL-1 $\beta$ , TNF- $\alpha$ , IL-6, and other modulatory cytokines of the hepatic APR (Ramadori and Christ, 1999). However, despite limited evidence on the production of cytokines by hepatic sinusoidal endothelial cells (Feder et al., 1993) and hepatic stellate cells (Ramadori and Armbrust, 2001), Kupffer cells are by far the most active intrahepatic “amplifiers” of the systemic APR in the liver by liberating a second wave of proinflammatory cytokines, promoting autocrine stimulation and paracrine hepatocyte stimulation (Decker, 1990).

Hepatocytes express a great variety of receptors for cytokines, growth factors, and prostaglandins and represent therefore the major target for a multiple set of mediators involved in both systemic and local host defense reactions. Hepatocytes

are also known to express and secrete the cytokines of the APR, which might further stimulate adjacent hepatocytes and neighboring Kupffer cells (Rowell et al., 1997).

### 1.5 Aim of the study

Despite single reports appeared over the last one and a half decade of years suggesting the involvement of HO-1 in the acute phase response, the mechanisms of the HO-1 regulation under inflammatory conditions are poorly understood. Although hepatic HO-1 induction has been shown in different models of the APR (Cantoni et al., 1991; Rizzardini et al., 1998; Bauer et al., 1998; Lyoumi et al., 1998a), it remains unclear whether induction of HO-1 *in vivo* occurs as a response to the cytokines released by inflammatory cells. It is also not clear which cell type(s) within the liver is/are the main contributor(s) to HO-1 up-regulation during inflammation. Moreover, it is even not known whether the induction of HO-1 during inflammation is a liver-specific, direct consequence of the APR or just a matter of accompanying oxidative stress and occurs also in other organs to the similar extent. Even though it has been shown that HO-1 was up-regulated by proinflammatory cytokines in different cell types (Mitani et al., 1992; Choi and Alam, 1996; Terry et al., 1998), the role of individual cytokines in the elevation of HO-1 expression *in vivo* is still a matter of debates (Oguro et al., 2002; Song et al., 2003b). Furthermore, the signal transduction pathways of the cytokine-dependent HO-1 induction are not known in detail. Therefore, the aim of the present study was:

1. using a turpentine oil model of the acute phase response in rats:
  - a) to study HO-1 expression in the liver and extrahepatic tissues under inflammatory conditions;
  - b) to investigate spatial and cell type-specific induction of HO-1 within the liver (and other organs) during acute phase reaction;
  - c) to evaluate the role of interleukin-6, the principle mediator of inflammation, in the HO-1 induction *in vivo*;
2. using primary cultures of isolated rat hepatocytes:
  - a) to study regulation of HO-1 expression by various proinflammatory cytokines in a dose- and time-dependent experiments;

- b) to perform a functional analysis of the rat HO-1 promoter by means of luciferase reporter gene assay in order to define the molecular mechanisms of the cytokine-dependent HO-1 gene regulation.

## 2. Materials

### 2.1 Animals

Male Wistar rats (about 200 g body weight) were purchased from Harlan-Winkelmann (Borchen, Germany) and kept under standard conditions with 12-hour light/dark cycles and access to fresh water and food pellets *ad libitum* at room temperature of 19-23°C. The rats consumed 12-15 g food (rat diet "ssniff", Spezialitäten GmbH, Soest, Germany) and 12-25 ml water per day and had a 30-40 g gain of weight per week.

Animals were used for the experiments not earlier than 6 days after arrival. The preparation of hepatocytes was performed during the first 3 h of the light phase. Rats were anesthetized by intraperitoneal injection of pentobarbital (400 mg/kg body weight). For *in vivo* investigations, an acute phase reaction was induced by intramuscular injection with 5 ml/kg body weight turpentine oil (TO) into the right and left hind limb of ether-anesthetized rats; control animals received no injection. Animals were sacrificed at time points, ranging from 30 minutes to 48 hours after TO administration under pentobarbital anesthesia. Different organs and muscle tissue from the hind limb were excised, rinsed with physiological sodium saline, snap-frozen in liquid nitrogen and stored at -80°C until use.

All animals received humane care in accordance with the institution's guidelines, the German Convention for Protection of Animals and the National Institutes' of Health guidelines.

### 2.2 Bacterial strain, vectors and plasmid constructs

#### 2.2.1 Bacterial strain

*E. coli* DH5 $\alpha$  strain [genotype: supE44, thi-1, recA1, relA1, hsdR17(rK-mK+), thi-1,  $\Delta$ lacU169( $\Phi$ 80 lacZ $\Delta$ M15), endA1, gyrA (Nal<sup>r</sup>)] (Stratagene /Heidelberg, Germany) was used for plasmid transformation.

#### 2.2.2 Vectors

##### *pBS-KSII* vector

For the amplification of the specific cDNA fragments used for Northern blot analysis, the plasmid vector pBluescript (pBS-KS II) (Stratagene, Heidelberg) was

used. The vector, derived from the vector pUC19, consists of 2961 bp. It contains T3 and T7 RNA polymerase promoters, necessary for the *in vitro* transcription, a multiple cloning site (polylinker), containing the sites for different restriction endonucleases, and primer sequences (universal and reverse primers) necessary for DNA sequencing (Figure 5). Moreover, the multiple cloning site, where a cDNA of interest could be cloned, is flanked by the sequences for T3 and T7 standard primers, which were used in the current work for the PCR-amplification of the cDNAs of interest.

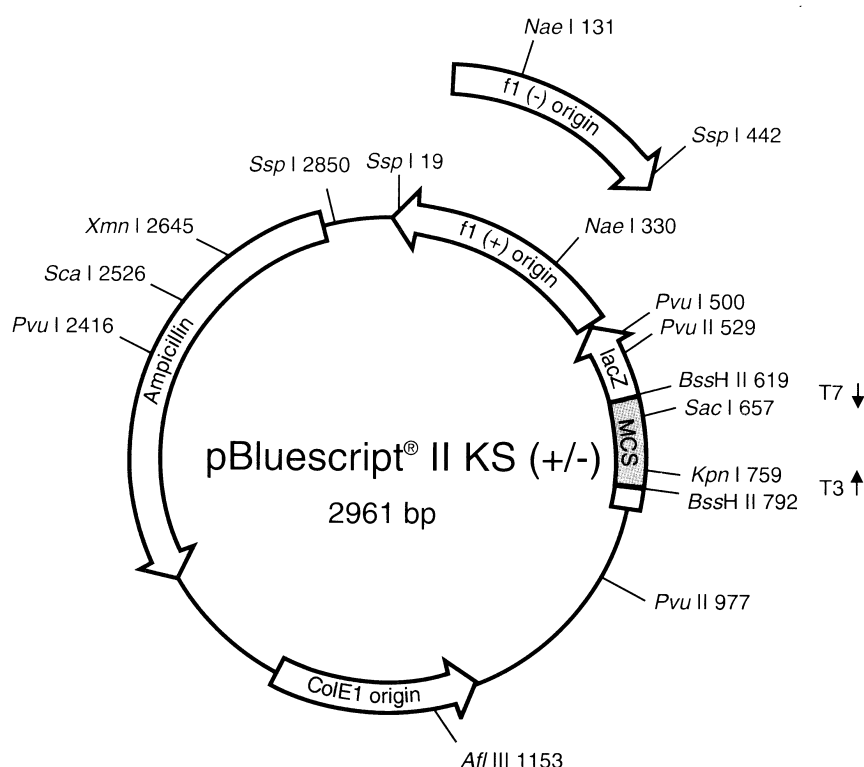


**Figure 5. Structure of the pBluescript vector (pBS-KSII).** The vector contains the origin of replication ColE1 ori, the ampicillin resistance gene for antibiotic selection, and the LacZ gene coding for  $\beta$ -galactosidase, which provides the possibility for blue/white color selection of recombinant clones. The multiple cloning site is flanked by T3 and T7 promoters and by the sequences for T3 and T7 primers, KS and SK primers, universal (M13) and reverse sequencing primers.

#### *pcDNA3.1 vector*

To assess the transfection efficiency of primary rat hepatocytes, a reporter vector pcDNA3.1 (Invitrogen /Karlsruhe, Germany), containing the GFP gene cloned between EcoR I and Xho I restriction endonuclease sequences of the plasmid multiple cloning site (polylinker), was used. The vector consists of 5428 bp and contains human cytomegalovirus (CMV) promoter followed by the polylinker in

forward orientation (+) with T7 promoter and the sites for different restriction endonucleases (Figure 6). The CMV promoter permits efficient, high-level expression of the recombinant protein of interest cDNA cloned in the polylinker. Bovine growth hormone (BGH) polyadenylation signal is needed for efficient transcription termination and polyadenylation of the respective mRNA. T7 promoter/priming site allows for *in vitro* transcription in the sense orientation and sequencing through the insert. pUC origin permits high-copy number replication and growth in *E. coli*, and ampicillin resistance gene ( $\beta$ -lactamase) allows selection of vector in *E. coli*.

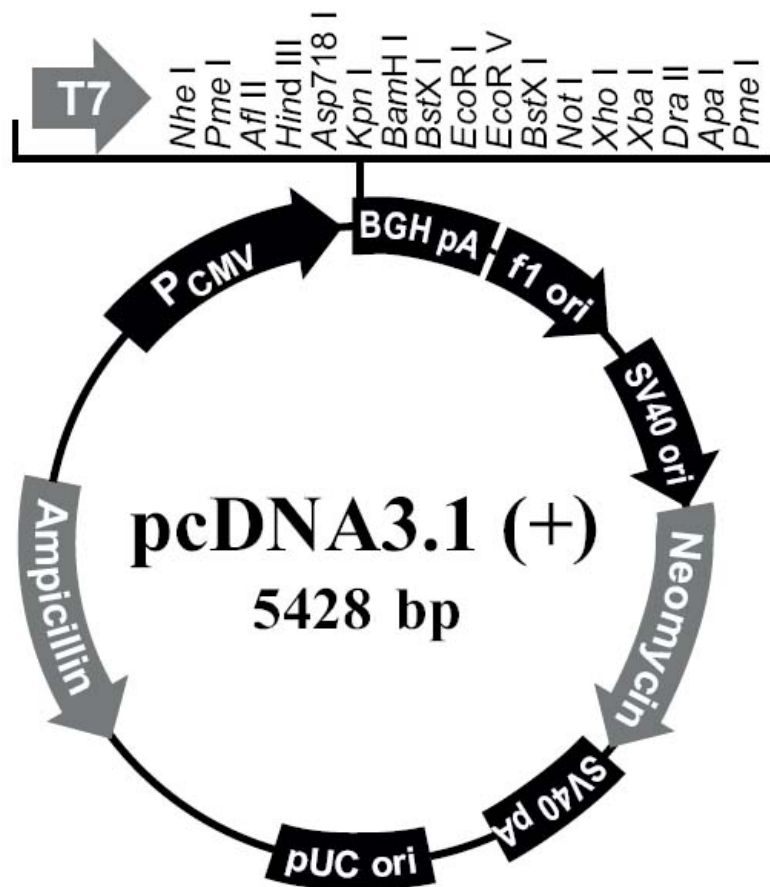


**Figure 6. Structure of the pcDNA3.1 (+) vector.** The multiple cloning site (polylinker) is flanked by the sequences for T7 forward and BGH reverse priming sites. CMV promoter and BGH polyadenylation (polyA) sequences are located directly before and after the polylinker, respectively. The SV40 early promoter with origin and SV40 early polyA signal are flanking the neomycin resistance gene. The plasmid also contains the ampicillin resistance gene ( $\beta$ -lactamase) and two other origins of replication, pUC ori and f1 ori. The gene of interest and the neomycin gene are transcribed clockwise whereas ampicillin gene is transcribed counterclockwise.

### *pGL3-basic vector*

For the luciferase reporter gene assay, primary rat hepatocytes were transfected with constructs, containing various rat HO-1 promoter sequences in front of the luciferase (Luc) gene, based on the pGL3-basic vector (Promega /Mannheim, Germany). The vector consists of 4818 bp. The HO-1 promoter sequences were cloned in the multiple cloning site (polylinker) of pGL3-basic. The polylinker is flanked by the primer sequences GL2, RV4 and RV3, which are necessary for DNA sequencing. The vector contains the firefly luciferase gene (Luc+) as a reporter gene to estimate the promoter activity, and two polyadenylation signals. The vector pGL3 basic also contains the gene responsible for ampicillin resistance and two origins of replication ColE1 ori and f1 ori, the second of which is necessary for the production of single-stranded DNA (ssDNA) (Figure 7).

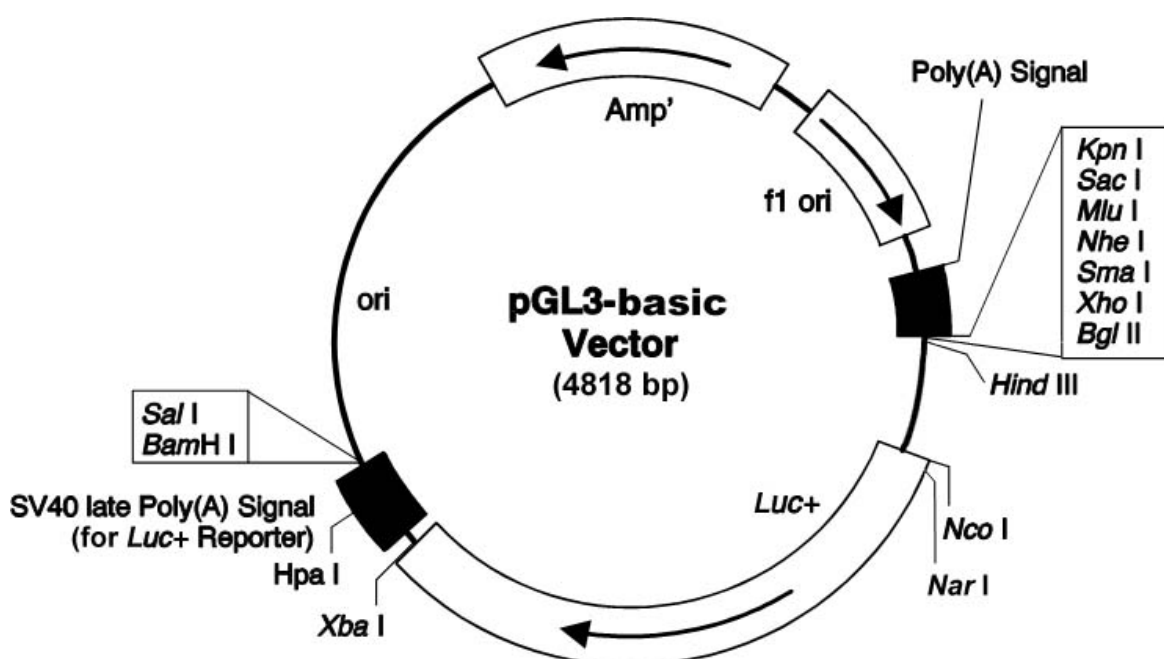


**Figure 7. Structure of the pGL3-basic vector.** The multiple cloning site (41 bp) is followed by the firefly luciferase gene (Luc+, 1649 bp) and the SV40 late polyA signal (221 bp). Another, upstream polyA signal (153 bp), is located directly before the multiple cloning site. The plasmid also contains the ampicillin resistance gene ( $\beta$ -lactamase; Amp'; 857 bp) and two origins of replication, ColE1 ori and f1 ori (454 bp). The Luc+ gene is transcribed clockwise whereas Amp' is transcribed counterclockwise.

### **2.2.3 Plasmid constructs**

#### *HO-1 promoter constructs*

To investigate regulation of the rat HO-1 promoter, primary rat hepatocytes were transiently transfected with luciferase (Luc) gene constructs driven by wild-type

1387, 754, and 347 bp of the rat HO-1 promoter (pHO-1387, pHO-754, and pHO-347) or the 754-bp promoter mutated at the CRE/AP-1 site (pHO-754 $\Delta$ AP1) or at the STAT3 site (pHO-754 $\Delta$ S3BE) (Figure 8).



**Figure 8. HO-1 promoter luciferase gene constructs.** The denominations of the pGI3-HO-1 Luc constructs are indicated on the left. In pHO-754 $\Delta$ AP1 and pHO-754 $\Delta$ S3BE, the wild-type HO-1 promoter sequence is shown on the upper strand, and the mutated sequence is shown on the lower strand: deleted bases are indicated by “-”, mutated bases are shown in lowercase letters and indicated by asterisks.

The HO-1 promoter luciferase gene constructs were generously provided by Dr. Thomas Kietzmann and Dr. Anatoly Samoylenko.

#### *Vector expressing GFP*

The bioluminescent jellyfish *Aequorea victoria* produces light when energy is transferred from Ca<sup>2+</sup>-activated photoprotein aequorin to green fluorescent protein (GFP) (Morin and Hastings, 1971). The cloning of the wild-type GFP gene (Prasher et al., 1992; Inouye and Tsuji, 1994) and its subsequent expression in heterologous systems (Chalfie et al., 1994; Inouye and Tsuji, 1994; Wang and Hazelrigg, 1994) established GFP as a novel genetic reporter system. When expressed in either eukaryotic or prokaryotic cells and illuminated by blue or UV light, GFP yields a bright green fluorescence. Light-stimulated GFP fluorescence is species-independent and does not require any cofactors, substrates, or additional



gene products from *A. victoria*. Additionally, detection of GFP and its variants can be performed in living cells and tissues as well as fixed samples.

In the current study, a plasmid construct pcDNA3.1-GFP was used to assess the transfection efficiency of primary rat hepatocytes. In this vector, the GFP gene is cloned between EcoR I and Xho I restriction endonucleases sequences of the plasmid multiple cloning site. The pcDNA3.1-GFP construct was kindly provided by Dr. Thomas Armbrust.

## 2.3 Oligonucleotides and cDNA probes

### 2.3.1 Oligonucleotides

For PCR-amplification of the cDNAs cloned in pBS-KSII vector, standard T3 and T7 primers were used:

T3: 5'-AAT TAA CCC TCA CTA AAG GG-3'

T7: 5'-GTA ATA CGA CTC ACT ATA GGG C-3'

Northern blot hybridization with the following 28S rRNA-specific oligonucleotide probe was used to control equal loading of total RNA (Barbu and Dautry, 1989):

Oligonucleotide complementary to 28S rRNA:

5'-AAC GAT CAG AGT AGT GGT ATT TCA CC-3'

### 2.3.2 cDNA probes

Two of the cDNA probes used for Northern blot were amplified from respective clones (based on pBS-KSII vector) by polymerase chain reaction (PCR) using standard T3 and T7 primers:

- an 883 base pair (bp) *EcoR* I - *Hind* III insert of clone pBS-HO-1 coding for the rat HO-1 (Shibahara et al., 1985);

- a 901 bp *Pst* I - *BamH* I fragment of a rat IL-6 clone (Northemann et al., 1989).

In order to control development of the APR in the rat liver, a rat  $\alpha$ 2-macroglobulin-specific cDNA clone (Gehring et al., 1987) and a clone carrying a 700 bp fragment of mouse albumin cDNA (Kioussis et al., 1981) were used.

To validate quantitative Northern blot results, a clone carrying the rat glyceraldehyde-3-phosphate dehydrogenase (GAPDH) cDNA was used (Fort et al., 1985).

## 2.4 Antibodies

### Anti-Heme-Oxygenase-1 Ab (SPA-895)

For the detection of HO-1 using immunoblotting, rabbit polyclonal anti-serum raised against recombinant rat HO-1 was used (Stressgen Biotechnologies Corp. /Victoria, BC, Canada). Species reactivity: SPA-895 detects HO-1 from human, mouse, rat, monkey, rabbit, hamster, guinea pig, sheep, and canine tissues.

### Anti-Heme-Oxygenase-1 Ab (OSA-111)

For the detection of HO-1 using immunohistochemical analysis, mouse monoclonal antibody (HO-1-2 clone) raised against rat HO-1 was used (Stressgen Biotechnologies Corp. /Victoria, BC, Canada). Species reactivity: OSA-111 detects HO-1 in mouse and rat.

### Anti- $\beta$ -actin Ab

For the detection of  $\beta$ -actin, mouse monoclonal antibody (AC-15 clone) raised against N-terminal peptide of  $\beta$ -actin was used (Sigma /Munich, Germany). This antibody recognizes  $\beta$ -isoform (nonmuscle) of actin in human, bovine, sheep, pig, rabbit, dog, mouse, rat, guinea pig, chicken, carp, and fruit fly tissues. The antibody does not cross react with skeletal and cardiac isoform ( $\alpha$ -isoform) of actin.

### Anti-rat ED1 Ab (MCA341R)

For the detection of rat tissue macrophages in immunohistochemical analysis, mouse monoclonal antibody raised against rat spleen cells was used (Serotec /Düsseldorf, Germany). This antibody recognizes a single chain glycoprotein of 90-100 kDa expressed by the majority of tissue macrophages in rat.

### Anti-rat ED2 Ab (MCA342R)

For the detection of rat Kupffer cells in immunohistochemical analysis, mouse monoclonal antibody raised against rat spleen cell homogenate was used (Serotec /Düsseldorf, Germany). This antibody recognizes a membrane antigen on Kupffer cells in rat.

Secondary Ab (horse radish peroxidase conjugated):

rabbit anti-mouse affinity purified Ig, Dako /Copenhagen, Denmark;

donkey anti-rabbit whole Ig, Amersham Pharmacia Biotech /Freiburg, Germany.

**2.5 Proteins, enzymes and protein standards**

Bovine serum albumin (BSA)	PAA /Linz, Austria
Collagenase type I	Biochrom /Berlin, Germany
Collagenase H	Roche /Mannheim, Germany
DNase I	Roche /Mannheim, Germany
Glucose oxidase	Sigma /Munich, Germany
Insulin, porcine	Sigma /Munich, Germany
Pronase E	Merck /Darmstadt, Germany
Rainbow™ colored protein molecular weight markers	Amersham Pharmacia Biotech / Freiburg, Germany
Recombinant rat IL-6	PeproTech Inc. /Rocky Hill, USA
Taq DNA polymerase	Invitrogen /Karlsruhe, Germany

**2.6 Protease inhibitors**

Antipain	Sigma /Munich, Germany
Benzamidine	Sigma /Munich, Germany
Chymostatin	Sigma /Munich, Germany
Leupeptin	Sigma /Munich, Germany
Pepstatin A	Sigma /Munich, Germany
PMSF	Sigma /Munich, Germany

**2.7 Detection, purification and synthesis systems (kits)**

BCA Protein Assay, Pierce /Bonn, Germany

EndoFree™ Plasmid Maxi Kit, Qiagen /Hilden, Germany

Liquid DAB+ Substrate Chromogen System, Dako /Copenhagen, Denmark

Luciferase Assay Kit, Berthold /Pforzheim, Germany

Nick translation kit, Invitrogen /Karlsruhe, Germany

NEBlot<sup>®</sup> Kit, New England Biolabs /Schwalbach, Germany

NucleoSpin<sup>®</sup> RNAII kit, Macherey-Nagel /Düren, Germany

SuperSignal<sup>®</sup> West Pico Chemiluminescent Substrate, Pierce /Bonn, Germany

Quantikine<sup>®</sup> M rat IL-6 immunoassay kit, R&D Systems /Wiesbaden, Germany

## 2.8 Stock solutions

All stock solutions were prepared either in double distilled water or (for experiments with RNA) in RNase-free water; the pH values of stock solutions are presented as the values at 25°C.

### APS 10%

	For 10 ml	Final concentration
APS	1 g	10%
ddH <sub>2</sub> O	to 10 ml	

The solution was dispensed into 100 µl aliquots and stored at -20°C.

### Citric acid 0.25 M

	For 100 ml	Final concentration
Citric acid	4.8 g	0.25 M
RNase-free H <sub>2</sub> O (Ampuwa <sup>®</sup> )	to 100 ml	

The solution was stored at room temperature.

### EDTA 0.5 M

	For 100 ml	Final concentration
EDTA (disodium salt)	18.61 g	0.5 M
RNase-free H <sub>2</sub> O (Ampuwa <sup>®</sup> )	to 100 ml	

pH was adjusted with 5N NaOH to 8.0. The solution was sterile filtered and stored at room temperature.

### PBS 10X

	For 1 l	Final concentration
NaCl	81.82 g	1.4 M

KCl	2 g	27 mM
Na <sub>2</sub> HPO <sub>4</sub>	14.2 g	100 mM
KH <sub>2</sub> PO <sub>4</sub>	2.45 g	18 mM
ddH <sub>2</sub> O	to 1 l	

pH was adjusted with HCl to 7.3. The solution was sterile filtered and stored at room temperature.

#### SDS 20%

	For 100 ml	Final concentration
SDS	20 g	20%
ddH <sub>2</sub> O	to 100 ml	

In the case of precipitation of SDS, the solution was warmed until clear.

#### Sodium acetate 2 M

	For 100 ml	Final concentration
Sodium acetate	16.408 g	2 M
RNase-free H <sub>2</sub> O (Ampuwa <sup>®</sup> )	to 100 ml	

pH was adjusted with acetic acid to 5.4. The solution was stored at 4°C.

#### Sodium citrate 0.25 M

	For 100 ml	Final concentration
Sodium citrate	7.35 g	0.25 M
RNase-free H <sub>2</sub> O (Ampuwa <sup>®</sup> )	to 100 ml	

pH was adjusted with 0.25 M citric acid to 7.0; the solution was stored at room temperature.

#### Tris-HCl 2 M

	For 1 l	Final concentration
Tris-HCl	315.2 g	2 M
RNase-free H <sub>2</sub> O (Ampuwa <sup>®</sup> )	to 1 l	

pH was adjusted with HCl to 7.4. The solution was sterile filtered and stored at 4°C.

## 2.9 Chemicals

All chemicals were of analytical grade and obtained from commercial sources as indicated.

Amersham Pharmacia Biotech /Freiburg, Germany

[ $\alpha$ -<sup>32</sup>P]-labeled deoxy-cytidine-triphosphate (specific activity 3,000 Ci/mmol),  
Ficoll<sup>®</sup> 400

Biochrom /Berlin, Germany

M199, fetal calf serum, Trypan blue

Bioline /Luckenwalde, Germany

dNTP master mix

Bio-Rad /Munich, Germany

Tween 20, mixed bed resin AG 501-X8(D)

Böhringer /Mannheim, Germany

Ampicillin

Difco Laboratories /Detroit, MI, USA

LPS from *Salmonella Minnesota*, bactoagar, bacto-trypton, yeast extract

Fresenius /Bad Homburg, Germany

Ampuwa<sup>®</sup> water

Invitrogen /Karlsruhe, Germany

Agarose, guanidine isothiocyanate

MBI Fermentas /Vilnius, Lithuania

6X loading dye solution, GeneRuler<sup>™</sup> 100bp DNA Ladder Plus, GeneRuler<sup>™</sup> 1kb  
DNA Ladder Plus

Merck /Darmstadt, Germany

All usual laboratory chemicals, acetic acid glacial, acetone, bromphenol blue, ethanol, 37% formaldehyde, formamide, glucose, glycerol, Kaiser's glycerol gelatin, Meyer's hemalaun, methanol,  $\beta$ -mercaptoethanol, penicillin G, streptomycin, TEMED

Merial /Hallbergmoos, Germany

Pentobarbital sodium (Narcoren<sup>®</sup>)

Nyegaard /Oslo, Norway

Nycodenz<sup>®</sup>

PAA /Linz, Austria

L-Glutamine

Paesel and Lorei /Frankfurt, Germany

Cesium chloride

Promega /Mannheim, Germany

Luciferase assay cell lysis reagent

Roth /Karlsruhe, Germany

Rotiphorese Gel 30 (30% acrylamide stock solution with 0.8% bisacrylamide in proportion 37.5:1), glycine, sodium dodecyl sulfate (SDS)

Serva /Heidelberg, Germany

Ponceau S, Tris-HCl

Sigma-Aldrich Chemie /Munich, Germany

All usual laboratory chemicals, ammonium persulfate, antifoam A, CDTA, citric acid, dexamethasone, DMSO, DTT, EDTA, ethidium bromide, HEPES, MOPS, N-lauroylsarcosyl, sodium acetate, sodium citrate, Triton X-100

Stratagene /Heidelberg, Germany)

QuikHyb<sup>®</sup> Hybridization Solution

Universitaets Apotheke Goettingen /Göttingen, Germany

Turpentine oil

Zinsser Analytic /Frankfurt, Germany

Scintillation liquid

## **2.10 Other materials**

Braunules 2G14, Braun /Melsungen, Germany

Cover-slips, 24x55 mm, Menzel-Gläser /Braunschweig, Germany

Culture dishes (60 mm), serological pipettes (2, 5, 10, 25 ml), transfer pipettes, plastic tubes (15 and 50 ml), Sarstedt /Germany

Hybond N nylon membrane, disposable NICK columns prepacked with Sephadex<sup>®</sup> G-50 DNA grade, Amersham Pharmacia Biotech /Freiburg, Germany

Hybridization glass tubes, Biometra /Göttingen, Germany

Microscope glass slides, 76x26 mm, Menzel-Gläser /Braunschweig, Germany

Nitrocellulose Transfer Membrane, 0.45  $\mu\text{m}$ , PROTRAN<sup>®</sup>, Whatman 3MM paper, Schleicher and Schuell /Dassel, Germany

Polyallomer thin-walled centrifuge tubes (5 ml), Beckman /Munich, Germany

Safe-Lock tubes (0.2, 0.5, 1.5 and 2 ml), Eppendorf /Hamburg, Germany

Scintillation vials (5 ml), Zinsser Analytic /Frankfurt, Germany

Sterile filter Nalgene, 0.2  $\mu\text{m}$ , Sartorius /Göttingen, Germany

Sterile filter pipette tips, Biozym /Oldendorf, Germany



96-well microtiter plates, Nunc Inc. /Naperville, IL, USA

X-ray films, Fuji /Düsseldorf, Germany

X-ray films X-Omat AR, Kodak /Rochester, USA

## 2.11 Instruments

Automatic pipettes, type Reference<sup>®</sup>, Eppendorf /Hamburg, Germany

Automatic pipettes, type Pipetman, Gilson /Bad Camberg, Germany

Centrifuges and rotors:

Bench-top, high speed and ultracentrifuges	
Beckman model J2-21 centrifuge Beckman rotor JE-6B	Beckman /Munich, Germany
Centricon T-2070 ultracentrifuge Centricon rotor TST55.5 – 55000 rpm	Kontron Instruments/Neufahrn, Germany
Eppendorf bench-top centrifuge, type MiniSpin 5415C	Eppendorf /Hamburg, Germany
Hettich Mikro Rapid/K centrifuge Hettich Rotina 3850 centrifuge Hettich Rotina 48RS centrifuge Hettich Rotixa/RP centrifuge	Hettich /Tuttlingen, Germany
Minifuge GL centrifuge	Heraeus-Christ /Osterode, Germany
Sigma 3K30 centrifuge Rotor Nr 12156 – 16500 rpm Rotor Nr 12153 – 22000 rpm	Sigma Laboratory Centrifuges /Osterode, Germany

Cryostat for tissue section preparation, Frigocut 2800 E, Reichert-Jung /Bensheim, Germany

Eagle Eye™ system with built-in ultraviolet emitter, video camera and frame integrator, Stratagene Europe /Amsterdam, The Netherlands

Electroblotting apparatus, type Mini Trans-Blot®, Bio-Rad /Munich, Germany

Electrophoresis apparatus, type Mini-Protean® III, Bio-Rad /Munich, Germany

Gas controlled incubators, Heraeus-Electronic /Hannover, Germany

Horizontal gel electrophoresis system, Horizon® 11-14, Gibco BRL /Gaithersburg, MD, USA

Hybridization oven, Biometra /Göttingen, Germany

Ice machine, Ziegra /Isernhagen, Germany

Incubator with shaking for cell culture, model 3-25, New Brunswick Scientific Co., Inc. /Edison, New Jersey, USA

Liquid scintillation counter Wallac 1409 / Turku, Finland

Magnetic mixer with warming, type M21/1 Framo-Gerätetechnik /Germany

Microwave oven, Siemens /Germany

Microplate reader MRX, Dynatech Laboratories /Chantilly, VA, USA

Microscope Axiovert 25, Zeiss /Oberkochen, Germany

Microscope Axioscop with fotocamera MC 100 Spot, Zeiss /Oberkochen, Germany

Peristaltic pump P-1, Amersham /Freiburg, Germany

pH-Meter 761 Calimatic, Knick /Berlin, Germany

Power supply, Power Pac 300, Bio-Rad /Munich, Germany

Rocking platform, Biometra /Göttingen, Germany

Savant Speed Vac<sup>®</sup> concentrator, ThermoLife Sciences /Egelsbach, Germany

Scanning densitometer, Molecular Analyst, Bio-Rad /Hercules, CA, USA

Sterile bench, type Lamin Air, TL 2472, Heraeus /Hanau, Germany

Sterile bench, type MRF 0.612-GS, Prettl Laminarflow und Prozesstechnik / Bempflingen, Germany

Thermocycler, type Mastercycler<sup>®</sup> gradient, Eppendorf /Hamburg, Germany

Thermomixer 5436, Eppendorf /Hamburg, Germany

Thermostat, Heraeus /Hanau, Germany

Ultra-Turrax TP 18/10 homogenizer, Janke & Kunkel /Staufen, Germany

Ultraviolet emitter, 312 nm, Bachofer /Reutlingen, Germany

UV spectrophotometer, RNA/DNA Calculator GeneQuant II, Pharmacia Biotech / Freiburg, Germany

UV-light crosslinker, Stratalinker<sup>™</sup> 180, Stratagene /Heidelberg, Germany

Vortex, Genie 2<sup>™</sup>, Bender and Hobein /Zurich, Switzerland

Vortex, with platform, Schütt Labortechnik /Göttingen, Germany

Water bath 1083, GFL /Burgwedel, Germany

X-ray film cassettes 10×18, Siemens /Germany

X-ray film-developing machine SRX-101A, Konica Europe /Hohenbrunn, Germany

## 3. Methods

### 3.1 Methods of cell biology

#### 3.1.1 Isolation of rat hepatocytes

Hepatocytes were isolated from male Wistar rats by circulating perfusion with collagenase essentially as described previously (Seglen, 1973; Katz et al., 1979).

##### *Liver perfusion*

After laparotomy, the *vena portae* was cannulated, *vena cava inferior* was ligated above the diaphragm to prevent flow of the perfusion media into a whole body circulation. Finally, the *vena cava inferior* was cut beneath the liver and cannulated. The liver was perfused in non-recirculative mode through the portal vein with 150-200 ml CO<sub>2</sub>-enriched preperfusion medium at a flow rate of 30 ml/min until the liver was free from blood. To break down components of extracellular matrix, the liver was perfused in recirculative mode with collagenase perfusion medium until it started to feel soft (about 7-11 min).

##### *Preparation of the hepatocyte suspension*

After perfusion, the liver was excised and transferred into a sterile glass beaker filled with culture medium M 199 with additives. Glisson's capsule, i. e. collagen tissue around the liver, was carefully removed and discarded. To obtain a cell suspension, the tissue was disrupted mechanically using sterile forceps. Connective tissue and remainder of the liver capsule as well as big cell aggregates were removed by filtration of the primary cell suspension through a nylon mesh (pore size 79 µm). Non-parenchymal cells and cell debris were removed by numerous selective sedimentations (20 g, 2 min, 4°C) in wash medium. After the last centrifugation, hepatocytes were suspended in medium M 199 with additives. 50 ml of M 199 was added per 1 g of wet weight of the sedimented cells; the cell suspension typically had a density of about 10<sup>6</sup>/2.5 ml.

##### Media and solutions for hepatocyte preparation and culture

All media and solutions for cell culture were prepared in double distilled water, further purified by sterile filtration and stored at 4°C. All solutions were prepared not more than one day before the isolation.

Krebs-Ringer stock solution

	For 1 l	Final concentration
NaCl	7 g	120 mM
KCl	0.36 g	4.8 mM
MgSO <sub>4</sub> ×7H <sub>2</sub> O	0.296 g	1.2 mM
KH <sub>2</sub> PO <sub>4</sub>	0.163 g	1.2 mM
NaHCO <sub>3</sub>	2.016 g	24.4 mM
ddH <sub>2</sub> O	to 1 l	

The solution was equilibrated with carbogen and pH was adjusted to 7.35.

Preperfusion medium

	For 1 l	Final concentration
EGTA	95.1 mg	0.25 mM
Krebs-Ringer stock solution	to 1 l	

Collagenase perfusion medium

	For 100 ml	Final concentration
HEPES	360 mg	15 mM
CaCl <sub>2</sub> ×2H <sub>2</sub> O	58.8 mg	4 mM
Collagenase	50 mg	
Krebs-Ringer stock solution	to 100 ml	

The medium was prepared directly prior to isolation, equilibrated with carbogen for 30 min and finally sterile filtered.

Wash medium

	For 1 l	Final concentration
HEPES/NaOH pH 7.4	4.77 g	20 mM
NaCl	7.00 g	120 mM
KCl	0.36 g	4.8 mM
MgSO <sub>4</sub> ×7H <sub>2</sub> O	0.30 g	1.2 mM
KH <sub>2</sub> PO <sub>4</sub>	0.16 g	1.2 mM
Bovine serum albumin	4.00 g	0.4%
ddH <sub>2</sub> O	to 1 l	

Medium M 199 with additives

	For 1 l	Final concentration
M199 with Earle's salts		
without NaHCO <sub>3</sub>	1 l	
Glucose×H <sub>2</sub> O	1.1 g	5.5 mM
HEPES	3.6 g	15 mM
NaHCO <sub>3</sub>	1.5 g	18 mM
Bovine serum albumin	4.0 g	0.4%

The medium was equilibrated with carbogen until pH reached a value of 7.35.

Finally, the medium was sterile filtered.

**3.1.2 Isolation of rat Kupffer cells**

Rat liver macrophages (Kupffer cells) were isolated according to the method of Knook and Sleyster (Knook and Sleyster, 1976) as previously described with slight modifications.

*Liver perfusion and preparation of cell suspension*

The laparotomy and canulation were performed essentially as described above (see 3.1.1). The liver was perfused with preperfusion medium containing Gey's Balanced Salt Solution (GBSS) and sodium hydrocarbonate, followed by perfusion with enzyme solution 1 containing pronase with subsequent change to enzyme solution 2 containing pronase and collagenase.

After perfusion, the liver was excised and placed into the sterile Petri dish filled with enzyme solution 3 containing pronase, collagenase and DNase I and was mechanically disrupted with sterile forceps. The cell suspension obtained was stirred in the same perfusion solution for 30 min with simultaneous control of pH (7.5) and finally filtered through the sterile sieve and collected in 50 ml polypropylene tubes. To separate big cell aggregates and major part of the parenchymal liver cells, the suspension was centrifuged for 4 min at 35 g (4°C). The supernatant was recentrifuged for 5 min at 640 g (4°C), the pellet was resuspended in 50 ml of GBSS containing 100 µl DNase I.

*Separation of nonparenchymal liver cells*

Nonparenchymal liver cells were separated using Nycodenz<sup>®</sup> density gradient as follows: the cell suspension was transferred into four sterile 50 ml polypropylene

tubes and centrifuged for 5 min at 640 g (4°C). The supernatant was discarded and the pellets were resuspended in small volume (5-6 ml) of GBSS with 100 µl DNase I and pooled together in one sterile 50 ml polypropylene tube. 14 ml of 30% Nycodenz was added and the volume was adjusted to 24 ml with GBSS. This mixture was divided between four sterile 15 ml polypropylene tubes and GBSS (1.5 ml per tube) was carefully layered over the content of the tubes. The gradient was centrifuged for 15 min at 1,800 g (4°C). Afterwards, the interphase brown layer between Nycodenz and GBSS containing nonparenchymal liver cells was carefully transferred into sterile 50 ml polypropylene tube and centrifuged for 5 min at 640 g (4°C).

#### *Purification of Kupffer cells by counterflow elutriation*

To obtain pure Kupffer cells, nonparenchymal liver cells were fractionated by centrifugal counterflow elutriation according to (Knook and Sleyster, 1976). The nonparenchymal liver cell pellet obtained in previous step was resuspended in 5-6 ml of 0.4% BSA/GBSS, collected in a sterile 10 ml syringe and injected in the elutriation system. Using JE-6B elutriation rotor assembled according to the manufacturer's instructions and spun at 2,500 rpm in a J2-21 centrifuge (Beckman Instruments), fractions enriched with sinusoidal endothelial cells, myofibroblasts and Kupffer cells were collected at flow rates of 19 ml/min, 23 ml/min and 55 ml/min, respectively.

The Kupffer cell fraction was sedimented by centrifugation (5 min at 640 g, 4°C), counted in a Neubauer chamber and, after assessment of cell viability by Trypan blue staining, taken up in a culture medium.

#### Media and solutions for Kupffer cell preparation and culture

All media and solutions for cell culture were prepared in double distilled water, further purified by sterile filtration and stored at 4°C, unless otherwise indicated.

#### 10X GBSS (Gey's Balanced Salt Solution)

	For 1 l
NaCl	80 g
KCl	3.7 g
MgSO <sub>4</sub> ×7H <sub>2</sub> O	0.7 g

NaH <sub>2</sub> PO <sub>4</sub> ×H <sub>2</sub> O	1.7 g
CaCl <sub>2</sub> ×2H <sub>2</sub> O	2.2 g
KH <sub>2</sub> PO <sub>4</sub>	0.3 g
MgCl <sub>2</sub> ×6H <sub>2</sub> O	2.1 g
Glucose	10 g
ddH <sub>2</sub> O	to 1 l

#### Preperfusion medium

	For 1 l
NaHCO <sub>3</sub>	227 mg
10X GBSS	100 ml
ddH <sub>2</sub> O	to 1 l

The solution was prepared directly prior to isolation; pH was adjusted to 7.4.

#### 1X GBSS without NaCl

	For 1 l
KCl	370 mg
MgSO <sub>4</sub> ×7H <sub>2</sub> O	70 mg
NaH <sub>2</sub> PO <sub>4</sub> ×H <sub>2</sub> O	170 mg
CaCl <sub>2</sub> ×2H <sub>2</sub> O	220 mg
NaHCO <sub>3</sub>	227 mg
KH <sub>2</sub> PO <sub>4</sub>	30 mg
MgCl <sub>2</sub> ×6H <sub>2</sub> O	210 mg
Glucose	1 g
ddH <sub>2</sub> O	to 1 l

pH was adjusted to 7.4.

#### 30% Nycodenz<sup>®</sup>

	For 100 ml
Nycodenz <sup>®</sup>	30 g
1X GBSS without NaCl	to 100 ml

The solution was dispensed into 14 ml aliquots and stored at -20°C.



0.4% BSA/GBSS

	For 500 ml
BSA	2 g
1X GBSS	to 500 ml

Enzyme solutions

All enzymes were dissolved in GBSS for 30 min at room temperature, agitating occasionally.

Enzyme solution 1

	For 60 ml
Pronase E	120 mg
1X GBSS	to 60 ml

Enzyme solution 2

	For 150 ml
Pronase E	75 mg
Collagenase H	80 mg
1X GBSS	to 150 ml

Enzyme solution 3

	For 100 ml
Pronase E	20 mg
Collagenase H	60 mg
DNase I stock	300 $\mu$ l
1X GBSS	to 100 ml

The DNase I was added to the solution immediately before application.

DNase I stock

	For 10 ml
DNase I	100 mg
ddH <sub>2</sub> O	to 10 ml

The solution was dispensed into 1 ml aliquots and stored at  $-20^{\circ}\text{C}$ .

### **3.1.3 Primary culture treatment and harvesting of rat liver cells**

The cultures of rat hepatocytes and Kupffer cells were performed on 60 mm polystyrol dishes and maintained at 37°C in a 95% air/ 5% CO<sub>2</sub> atmosphere and saturated humidity.

#### *Primary culture of rat hepatocytes*

Immediately after preparation, fetal calf serum (4 ml/100 ml suspension) was added to the hepatocyte suspension in order to make the cell adhesion to the polystyrol dishes more efficient. Furthermore, the antibiotics (1 ml of pen/strep stock solution per 100 ml cell suspension) together with 10<sup>-7</sup> M dexamethasone and 10<sup>-9</sup> M insulin as permissive hormones were added. Rat hepatocytes were plated onto 60-mm plastic dishes at a density of 1 × 10<sup>6</sup> and 2 × 10<sup>6</sup> cells per dish for transfection and RNA/protein isolation experiments, respectively.

After the initial 4 h attachment phase (for transfected cells 5 h) the medium was changed, and the hepatocytes were further cultured in medium M 199 with the same concentrations of hormones and antibiotics as before but without fetal calf serum. A volume of 2.5 ml medium per 60 mm culture dish and 6 ml per 100 mm culture dish were added. After 24 h the medium was changed again.

Primary rat hepatocytes were usually treated with various proinflammatory cytokines of different concentrations on the next day after plating. The medium was changed 6 h prior to treatment, the stimuli were diluted to the required concentrations in the culture medium and added directly to the culture dishes by pipetting. The same amount of normal culture medium was pipetted to the dishes with cells which served later as experimental controls.

To stop the culture, dishes with cells were taken from the incubator, the cells were washed with phosphate buffered saline, pH 7.4 and frozen at -80°C for subsequent RNA or protein isolation. Alternatively, the transfected cells were subjected to lysis immediately after washing with subsequent detection of the luciferase activity. The fluorescence of GFP-transfected hepatocytes was observed by vital microscopy.

#### **Hormone and antibiotics stock solutions**

All solutions were sterile filtered, aliquoted and stored at -20°C.

Pen/strep stock

	For 100 ml
Penicillin G (sodium salt)	0.64 g
Streptomycine sulfate	1.17 g
0.9% NaCl	to 100 ml

Dexamethasone (100 µM)

	For 100 ml
Dexamethasone	3.92 g
0.9% NaCl	to 100 ml

Dexamethasone was first dissolved in 0.3 ml of ethanol and then adjuted to 100 ml with 0.9% NaCl.

Insulin (10 µM)

	For 100 ml
Insulin	6 mg
BSA	100 mg
0.9% NaCl	to 100 ml

Insulin was dissolved at pH 2.5, neutrilized and then BSA was added.

*Culturing of Kupffer cells*

Rat Kupffer cells were taken up in the culture medium M 199 containing 15% fetal calf serum, 100 U/mL penicillin, 100 µg/mL streptomycin, and 1% L-glutamine and plated onto 60-mm plastic dishes at a density of  $6 \times 10^6$  cells per dish.

Treatment of Kupffer cells with bacterial lipopolysaccharide (500 ng/ml) was carried out in a serum-reduced medium (0.3% FCS) containing the same amount of antibiotics and L-glutamine for 24 h, afterwards the cells were washed with phosphate buffered saline, pH 7.4 and frozen at  $-80^{\circ}\text{C}$  for subsequent RNA isolation. Total cellular RNA isolated from LPS-treated Kupffer cells served as a positive control for detection of IL-6-specific transcripts.

Culture medium

	For 100 ml
Pen/strep stock	1 ml

FCS	15 ml
L-Glutamine	1 ml
M 199	to 100 ml

## 3.2 Methods of molecular biology

### 3.2.1 Transformation of *E. coli*

Competent *E. coli* DH5 $\alpha$  cells, capable of taking up linear or circular (plasmid) double stranded DNA, were used for transformation.

The competent bacteria (100  $\mu$ l) were thawed on ice. Next, 100 ng of plasmid DNA was added directly to the competent cells and the mixture was incubated on ice for 30 min. Cells were subjected to heat shock by incubating at 42°C for 2 min and subsequently incubated on ice for 2 min. Afterwards, 300  $\mu$ l of SOC medium was added to the cells followed by 40 min incubation at 37°C under continuous shaking at 225 rpm. After chilling on ice, transformed cells (50  $\mu$ l) were spread over a LB-ampicillin agar dish and incubated for 18 h at 37°C.

#### Media and solutions used for *E. coli* transformation

##### SOC medium

0.5% yeast extract
2% bacto-trypton
10 mM NaCl
2.5 mM KCl
10 mM MgSO <sub>4</sub>
10 mM MgCl <sub>2</sub>
20 mM glucose

##### Luria Bertani (LB) medium

	For 1 l
Bacto-trypton	10 g
Yeast extract	5 g
NaCl	5 g
ddH <sub>2</sub> O	to 1 l

pH was adjusted with NaOH to 7.3, the medium was sterilized by autoclaving and stored at 4°C. Just prior to use, ampicillin was added to the medium at the final concentration of 50-100 µg/ml.

#### LB-ampicillin agar dishes

Bactoagar was added to the LB medium to a final concentration of 1.5% followed by autoclaving. Afterward the medium was let to cool down to 55°C and ampicillin was added to a final concentration of 50 µg/ml. This medium was poured into 10 cm sterile Petri-dishes and left undisturbed for about 30 min to solidify. LB-Agar dishes were stored in the dark at 4°C.

#### Ampicillin stock solution

Ampicillin	100 mg/ml
------------	-----------

The powder was dissolved in sterile ddH<sub>2</sub>O; the pH was adjusted with HCl to 7.0; 500 µl aliquots were stored at -20°C.

#### **3.2.2 Purification of plasmid DNA**

Purification of plasmid DNA from transformed bacteria was performed using EndoFree™ Plasmid Maxi Kit (Qiagen).

Qiagen plasmid purification protocol is based on a modified alkaline lysis procedure, followed by binding of plasmid DNA to Qiagen Anion-Exchange Resin under appropriate low-salt and pH conditions. RNA, proteins, and low-molecular-weight impurities are removed by a medium-salt wash. Plasmid DNA is eluted in a high-salt buffer and then concentrated and desalted by isopropanol precipitation.

A single colony of transformed *E. coli* was picked from LB-ampicillin agar dish and inoculated into 2 ml of ampicillin-containing LB medium, followed by incubation for 12 h at 37°C with vigorous shaking at 300 rpm. Afterwards, 850 µl aliquot of bacteria suspension was mixed with 150 µl of sterile 87% glycerol and stored at -80°C as a bacterial stock, other portion of this starter culture was diluted 1:1,000 in LB medium, i.e. 100 µl of bacterial suspension was inoculated into 100 ml of LB medium, and bacteria were grown at 37°C for 12-16 h with vigorous shaking at 300 rpm to a density of approximately  $3-4 \times 10^9$  cells per ml, which corresponds to OD<sub>600</sub> of 1-1.5. The bacterial cells were harvested by centrifugation at 6,000 g for

15 min at 4°C. The supernatant was discarded and bacterial pellet was resuspended in 10 ml of P1 buffer, containing RNase A, by pipetting up and down until no cell clumps remained.

To lyse the cells, 10 ml of P2 buffer was added and mixed by gentle inverting (the mixture should not be vortexed to avoid shearing of genomic DNA). After 5 min of incubation at RT, 10 ml of chilled P3 buffer was added to the lysate to precipitate genomic DNA, proteins and cell debris. Immediately after precipitation, lysate was transferred into the barrel of QIAfilter Cartridge and incubated there for 10 min at room temperature, which is essential for optimal performance of the QIAfilter Maxi Cartridge. During this 10-min incubation, floating layer of a precipitate was formed on top of the lysate. Subsequently, the lysate was cleared by pushing the liquid through the filter of the QIAfilter Maxi Cartridge using the plunger. After adding 2.5 ml of ER buffer, the filtered lysate was incubated on ice for 30 min, and later on applied to a Qiagen-tip 500 column equilibrated with 10 ml of QBT buffer. After the entire volume of lysate had entered the resin, the column was washed twice with 30 ml of QC buffer. For all subsequent steps endotoxin-free reagents and plasticware were used. The plasmid DNA was eluted with 15 ml of QN buffer. To precipitate the DNA, the eluate was mixed with 10.5 ml of room-temperature isopropanol and centrifuge immediately at 15,000 *g* for 30 min at 4°C. The supernatant was discarded and the DNA pellet was washed from precipitated salt with 5 ml of endotoxin-free, room-temperature 70% ethanol, followed by centrifugation at 15,000 *g* for 10 min. The supernatant was carefully decanted; the DNA pellet was air-dried for 5-10 min and redissolved by pipetting up and down in a suitable volume (100-500  $\mu$ l depending on the size of the pellet) of endotoxin-free TE buffer.

To determine DNA concentration and the presence of protein in the probes, the OD at 260 nm (DNA) and 280 nm (protein) was measured. 1 OD at 260 nm  $\approx$  50  $\mu$ g DNA/ml. In a protein-free solution, the ratio OD<sub>260</sub>/OD<sub>280</sub> is 2. For the given experiments it was typically higher than 1.8.

The integrity and purity of the obtained plasmid DNA was controlled by agarose gel analysis (see 3.2.4 )

### **Solutions used for plasmid DNA purification**

P1 buffer (resuspension buffer )	50 mM Tris·Cl, pH 8.0 10 mM EDTA 100 µg/ ml RNase A
P2 buffer (lysis buffer)	200 mM NaOH 1% SDS
P3 buffer (neutralization buffer)	3.0 M potassium acetate, pH 5.5
QBT buffer (equilibration buffer)	750 mM NaCl 50 mM MOPS, pH 7.0 15% isopropanol 0.15% Triton X-100
QC buffer (washing buffer)	1 M NaCl 50 mM MOPS, pH 7.0 15% isopropanol
QN buffer (elution buffer)	1.6 M NaCl 50 mM MOPS, pH 7.0 15% isopropanol
TE buffer	10 mM Tris·HCl, pH8.0 50 mM MOPS, pH 7.0 15% isopropanol

### **3.2.3 Amplification of DNA by polymerase chain reaction (PCR)**

The polymerase chain reaction allows to amplify fragments due to repetitive cycles of DNA synthesis (Figure 9). The reaction uses two specific synthetic oligonucleotides (primers), that hybridize to sense and antisense DNA strands of the DNA fragment to be amplified, four deoxyribonucleotide triphosphates (dNTP's) and a heat-stable DNA polymerase. Each cycle consists of three reactions that take place under different temperatures. First, the double-stranded DNA is converted into its two single strands (denaturation at 95°C). They serve as templates for the synthesis of new DNA. After heating, the reaction is cooled (45-60°C) to allow the annealing (hybridization) of primers to the complementary DNA strands. Starting from the primers, DNA polymerase extends both DNA strands at 72°C (DNA synthesis) (Figure 9A). Since the DNA molecules synthesized in each

cycle can serve as a template in the next cycle, the number of target DNA copies approximately doubles every cycle. Already after the third cycle, double stranded DNA molecules of the size corresponding to the distance between two primers are synthesized (Figure 9B). The repeating cycles of heating and cooling take place in a thermocycler.

The PCR reaction was performed with standard T3- and T7-specific primers to amplify rat HO-1, IL-6, and GAPDH cDNAs cloned into pBluescript II KS (+/-) vector for subsequent labeling and use in Northern blot analysis. The PCR lasted for 35 cycles under the following conditions:

1. 45 sec denaturation at 95°C
2. 45 sec annealing at 50°C
3. 60 sec at 72°C DNA synthesis

The denaturation step at 95°C before the first cycle was extended for 2 min. After the last cycle the synthesis step was prolonged for 10 min at 72°C to finish synthesis of incompletely synthesized DNA strands.

The PCR was performed with the *Taq* DNA-polymerase (5 U/μl) (Invitrogen). The specific buffers and solutions were received with polymerase. dNTP master mix from Bioline was used.

PCR reaction mixture:

- 10 μl 10X PCR buffer (500 mM Tris-HCl, pH 9.1, 140 mM (NH<sub>4</sub>)<sub>2</sub>SO<sub>4</sub>)
- 4 μl MgCl<sub>2</sub> (50 mM)
- 0.8 μl 100 mM dNTP mix (25 mM of each dATP, dCTP, dGTP, dTTP)
- 1.5 μl (150 pmol) T3 primer
- 1.5 μl (150 pmol) T7 primer
- 1 μl template (100 ng plasmid DNA)
- 0.5 μl *Taq* polymerase (2.5 units)
- 100 μl volume was adjusted with sterile ddH<sub>2</sub>O



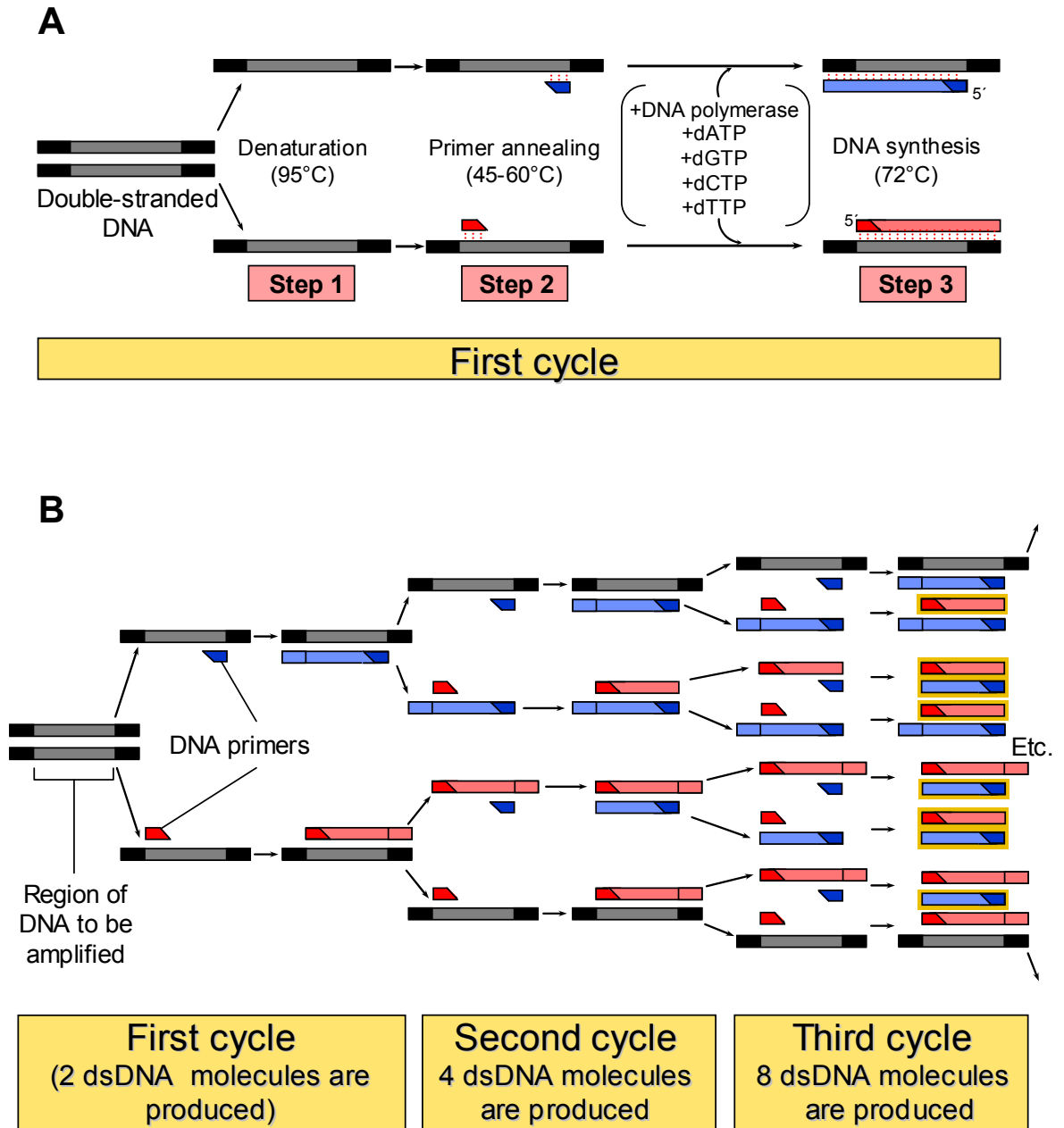


**Figure 9. Amplification of DNA using the PCR technique.** (A) After strand separation (step1), cooling of the DNA allows primers to hybridize to complementary sequences in the two DNA strands (step 2). In the presence of DNA polymerase and the four dNTPs, DNA is synthesized, starting from the two primers (step 3). (B) In the example illustrated, three cycles of reaction produce 16 DNA chains, 8 of each (boxed in yellow) are the same length as and correspond exactly to one or the other strand of the original bracketed sequence shown at the far left; the other strands contain extra DNA downstream of the original sequence, which is replicated in the first few cycles. After several more cycles, essentially all of the DNA strands have this unique length.

To check the size of the PCR product and to control its purity and integrity, an 8  $\mu$ l aliquot of the PCR reaction was electrophoretically analyzed in a 1.25% agarose gel.

### 3.2.4 Agarose gel electrophoresis of DNA

For preparation of a 1.25% gel, 1.25 g of agarose was dissolved by heating in 100 ml of 1X TAE buffer. For visualization of the bands, 8  $\mu$ l of ethidium bromide (10 mg/ml) was added to the mixture. After mixing, the gel was poured into the prepared gel plate. In the mean time of the polymerization, the samples were prepared for loading by mixing of 8  $\mu$ l of DNA probe with 2  $\mu$ l of 6X Loading Dye Solution (MBI Fermentas).

After polymerization, the gel was placed into an electrophoresis chamber filled with 1X TAE buffer, the samples were loaded, and the electrophoresis was performed at 60 V.

DNA bands, intercalating ethidium bromide, were visualized by UV detection. Ethidium bromide is a fluorescent dye which contains a planar group that intercalates between the stacked bases of the DNA. The fixed position of this group and its close proximity to the bases cause dye, bound to DNA, to display an increased fluorescence yield compared to that of the dye in free solution. Ultraviolet radiation at 254 nm is absorbed by the DNA and transmitted to the dye; radiation at 302 nm and 366 nm is absorbed by the bound dye itself. In both cases, the energy is reemitted at 590 nm in the red orange region of the visible spectrum. Hence, DNA can be visualized under a UV transilluminator. The gel was photographed using Eagle Eye™ system (Stratagene), a setup containing UV transilluminator, intensity control unit, video camera and printer.

#### 20X Tris/acetate/EDTA (TAE) buffer

	For 1 l	Final concentration
Tris base	122 g	1 M
Sodium acetate	32 g	0.4 M
EDTA	14 g	40 mM
ddH <sub>2</sub> O	to 1 l	

After EDTA was completely dissolved, pH was adjusted with acetic acid to 7.4; the buffer was autoclaved and stored at room temperature.

1X TAE buffer

	For 1 l
20X TAE buffer	50 ml
ddH <sub>2</sub> O	To 1 l

**3.2.5 Radioactive labeling of DNA**

For radioactive labeling of a full-length plasmid containing cDNA of interest, nick translation method was used. Alternatively, random primed DNA labeling was utilized for relatively short specific cDNA fragments.

*DNA labeling by nick translation method*

DNA labeling by nick translation method was performed using Nick Translation System kit (Invitrogen).

Nick translation requires the activity of two different enzymes. DNase I is used to cleave (nick) phosphodiester bonds at random sites in both strands of a double-stranded target DNA. *E. coli* DNA polymerase I is used to add deoxynucleotides to the 3'-hydroxyl termini created by DNase I. In addition to its polymerizing activity, DNA polymerase I carries a 5'→3' exonucleolytic activity that removes nucleotides from the 5' side of the nick. The simultaneous elimination of nucleotides from the 5' side and the addition of radiolabeled nucleotides to the 3' side result in movement of the nick (nick translation) along the DNA, which becomes labeled to high specific activity (Kelly et al., 1970). The reaction is carried out at low temperature (15°C).

In sterile 1.5 ml tube placed on ice, nuclease free H<sub>2</sub>O was added to the solution containing 1 µg of template DNA to bring the volume to 35 µl. Consequently the following reagents were added to the DNA in the indicated order:

5 µl dNTP mix (dATP, dTTP and dGTP)

5 µl α-<sup>32</sup>P-dCTP (3,000 ci/mmol, 50 µCi)

5 µl Pol I/DNase I mix

The components were mixed gently but thoroughly and centrifuged briefly in an Eppendorf bench-top centrifuge. The mixture was incubated at 15°C for 60 min. Afterwards, 5 µl of stop buffer was added to terminate the reaction.

### *DNA labeling by random priming reaction*

Random primed DNA labeling was performed using NEBlot<sup>®</sup> Kit (New England Biolabs) designed to produce labeled DNA probes using the method of Feinberg and Vogelstein (Feinberg and Vogelstein, 1983), where random sequence octadeoxynucleotides serve as primers for DNA synthesis *in vitro* from denatured double-stranded template DNA by the Klenow Fragment of *E. coli* polymerase I. One labeled deoxyribonucleotide is used in the dNTP reaction mixture and is incorporated during primer directed DNA synthesis by DNA polymerase. The resulting labeled DNA is used as hybridization probe in Northern blot.

50-100 ng of template DNA was dissolved in nuclease free H<sub>2</sub>O (the volume of added water should not exceed 33  $\mu$ l). The DNA was denatured by heating at 95°C for 5 min and subsequently chilled on ice for 5 min. The following reagents were added to the DNA in the indicated order:

- 5  $\mu$ l 10X labeling buffer (includes Random Octadeoxyribonucleotides)
- 6  $\mu$ l dNTP mixture (2  $\mu$ l of dATP, dTTP and dGTP were mixed previously)
- 5  $\mu$ l  $\alpha$ -<sup>32</sup>P-dCTP (3,000 ci/mmol, 50  $\mu$ Ci)
- 1  $\mu$ l DNA Polymerase I – Klenow Fragment (3'→5' exo<sup>-</sup>) (5 units)

The mixture was incubated at 37°C for 1 h, followed by termination of the reaction by adding 5  $\mu$ l of 0.2 M EDTA, pH 8.0.

### *Purification of labeled DNA*

Synthesized labeled DNA probe was separated from unincorporated nucleotides by gel filtration on Sephadex<sup>®</sup> G-50 using Pharmacia NICK Column (Pharmacia Biotech).

A column was opened according to the manufacturer's instructions and equilibrated with 3 ml of 1X TE buffer, pH 8.0. After the entire volume of buffer had entered the gel, random priming reaction mixture was applied onto the column, followed by adding 400  $\mu$ l of 1X TE buffer. The flowthrough was collected in the tube placed under the column and kept for further measurement of radioactivity. A new tube for sample collection was placed under the column and the purified sample was eluted with 400  $\mu$ l of 1X TE. The sample obtained was subjected to measurement of radioactivity and stored at -20°C until use for Northern blot hybridization.

10X TE

	For 1 l	Final concentration
2 M Tris-HCl, pH 7.4	50 ml	100 mM
0.5 M EDTA	20 ml	10 mM
RNase-free H <sub>2</sub> O	to 1 l	

pH was controlled and if necessary adjusted with NaOH or HCl to 7.6. The solution was sterile filtered and stored at 4°C.

1X TE

	For 500 ml
10X TE	50 ml
RNase-free H <sub>2</sub> O	to 500 ml

*Measurement of  $\beta$ -radioactivity*

After the purification step as described above, the radioactivity of labeled cDNA samples was measured using Wallac 1409 liquid scintillation  $\beta$ -counter (Turku /Finland). 2  $\mu$ l aliquots from the flowthrough and elution fractions were transferred to screw-lid plastic tubes containing 5 ml of scintillation liquid, mixed by inverting and subjected to radioactivity measurements.  $\beta$ -Radioactivity of the samples was expressed in counts per minute (cpm). The activity value in flowthrough fraction was used as means to assess the efficiency of radioactive nucleotide incorporation. For effective labeling this value should not exceed 10% of the radioactivity value in the cDNA sample.

**3.2.6 Isolation of total RNA***RNA isolation procedure using silicate columns*

The isolation of total RNA from cultured rat hepatocytes and Kupffer cells was conducted using the NucleoSpin<sup>®</sup> RNAII kit (Macherey-Nagel) in accordance to the protocol for cultured animal cells.

NucleoSpin<sup>®</sup> RNA method utilizes the silica membrane which adsorbs the RNA from the cell lysate. Contaminating DNA, which is also bound to the membrane, is removed with a solution containing DNase. Salts, metabolites and macromolecular

cellular components are washed away in two washing steps. Pure RNA is finally eluted under low ionic strength conditions with RNase-free water.

The cells frozen on the culture dishes ( $2 \times 10^6$  cells per 6 cm culture dish) were thawed on ice. 350  $\mu$ l of RA1 buffer with freshly added  $\beta$ -mercaptoethanol was applied to the dish, and cells were scraped with a disposable scraper, transferred to RNase-free 1.5 ml tubes and homogenized by passing 5 times through a 22 G injection canula connected to a syringe. This step was performed rapidly to prevent degradation of the RNA. Next, lysates were pipetted directly onto NucleoSpin<sup>®</sup> Filter unit, sitting in 2 ml collection tubes, and centrifuged for 1 min at 11,000 *g*. This step was performed to reduce viscosity and clear the lysates. Then, 350  $\mu$ l of 70% ethanol was added to each filtered lysate and mixed by vortexing. 700  $\mu$ l of each sample was applied to a NucleoSpin<sup>®</sup> RNA II column sitting in a 2 ml collection tube, and centrifuged for 30 sec at 8,000 *g*. To desalt the columns prior to DNA digest, 350  $\mu$ l of MDB buffer was pipetted onto NucleoSpin<sup>®</sup> RNA II column, followed by centrifugation for 1 min at 11,000 *g*. To digest DNA bound to the membrane, 95  $\mu$ l of DNase reaction mixture was applied directly onto the center of the silica membrane of the column, followed by incubation at room temperature for 15 min. To wash the silica membrane, 200  $\mu$ l of RA2 buffer was added to the NucleoSpin<sup>®</sup> RNA II column followed by centrifugation for 30 sec at 8,000 *g*. To continue washing, 600  $\mu$ l of RA3 buffer was applied and columns were centrifuged for 30 sec at 8,000 *g*. The last washing step was performed with 250  $\mu$ l of RA3 buffer, followed by centrifugation for 2 min at 11,000 *g* to dry the membrane completely. Afterwards, the NucleoSpin<sup>®</sup> RNA II columns were placed into nuclease-free 1.5 collection tubes, the RNA was eluted with 60  $\mu$ l of RNase-free H<sub>2</sub>O pipetted directly onto the silica membrane and columns were centrifuged at 11,000 *g* for 1 min.

To determine the concentration and purity of the RNA obtained, the aliquot of RNA sample was diluted 1:100 in RNase-free H<sub>2</sub>O and the extinction at 260 nm and 280 nm was measured spectrophotometrically (GeneQuant II, Pharmacia Biotech). The ratio of the OD at 260 nm and at 280 nm served as a measure of RNA purity. In a protein-free solution, the ratio  $OD_{260}/OD_{280}$  is 2. Due to minor protein contaminations this coefficient is usually somewhat lower. In our experiments it was typically higher than 1.8.

### **Solutions used for RNA isolation**

All solutions used for RNA isolation were provided in the NucleoSpin® RNAII kit and their detailed composition is not described. Buffers RA1, RA2 and MDB contain thiocyanate.

#### **RA1 buffer**

RA1 buffer (Macherey-Nagel)	1000 µl
β-Mercaptoethanol	10 µl

#### **DNase reaction mixture**

	For 1 sample
DNase I (Macherey-Nagel)	10 µl
DNase reaction buffer (Macherey-Nagel)	90 µl

#### **RA3 buffer**

RA3 buffer (concentrate, Macherey-Nagel)	12.5 ml
100% ethanol	50 ml

#### ***Isolation of RNA by density-gradient ultracentrifugation***

Total RNA was isolated from different rat tissues including liver, spleen, kidney, lung, heart, skeletal muscle, small and large intestine by means of guanidine isothiocyanate extraction, cesium chloride density-gradient ultracentrifugation and ethanol precipitation according to method of Chirgwin (Chirgwin et al., 1979).

This method is a versatile and efficient way to extract intact RNA from most tissues and cultured cells, even if the endogenous level of RNase is high. The cells are rapidly lysed in guanidine isothiocyanate-containing buffer, which ensures inactivation of RNases. The lysate is layered onto a CsCl gradient and spun in an ultracentrifuge. Proteins remain in the aqueous guanidine portion, DNA bands in the CsCl, and RNA pellets in the bottom of the tube. The RNA is recovered by

redissolving the pellet. The recovery of RNA is usually excellent if the capacity of the gradient is not exceeded.

About 100 mg of frozen tissue was homogenized with Ultra-Turrax TP 18/10 homogenizer 3 times for 10 sec each in 3 ml of ice-cold GITC buffer with freshly added Antifoam A (Sigma). The homogenates were centrifuged for 10 min at 3,500 rpm in a Rotixa/RP centrifuge (Hettich) at 4°C to pellet connective tissue and large cell debris. Meanwhile, 2 ml of CsCl buffer was poured into 5-ml polyallomer ultracentrifuge tubes (6 per preparation). The cleared guanidine lysed samples were carefully layered on top of the CsCl buffer. The samples were centrifuged overnight (21 h) at 35,000 rpm in a Kontron TST55 rotor at 20°C. The supernatants were carefully removed by aspiration and the transparent gelatin-like RNA pellets were gently washed (preserving undisturbed) with 200 µl of 70% ethanol at room temperature.

The pellets were reconstituted in 200 µl of RNase-free water by pipetting and transferred into sterile 1.5 ml reaction tubes and the procedure was immediately continued to RNA precipitation. The RNA was precipitated with 450 µl of 100% ethanol in the presence of sodium acetate, pH 5.4 (20 µl of 2 M solution per pellet) overnight at -20°C.

The RNA precipitates were pelleted by centrifugation for 30 min at 12,000 rpm in an Eppendorf bench-top centrifuge placed in cold room (4°C). Supernatants were discarded and pellets were washed with 200 µl of ice-cold 70% ethanol to remove all traces of sodium acetate. After subsequent recentrifugation as described, the supernatants were discarded and the pellets were dried for 30 min at room temperature. Afterwards, the pellets were reconstituted in 100 µl of RNase-free water.

To determine the concentration and purity of the RNA obtained, the aliquot of RNA sample was diluted 1:100 in RNase-free H<sub>2</sub>O and the extinction at 260 nm and 280 nm was measured spectrophotometrically (GeneQuant II, Pharmacia Biotech). The ratio of the OD at 260 nm and at 280 nm served as a measure of RNA purity. In a protein-free solution, the ratio OD<sub>260</sub>/OD<sub>280</sub> is 2. Due to minor protein contaminations this coefficient is usually somewhat lower. In our experiments it was typically higher than 1.8.



GITC buffer

	For 200 ml	Final concentration
Guanidine isothiocyanate	94.53 g	4 M
0.25 M sodium citrate	20 ml	25 mM
N-lauroylsarcosyl	1 g	0.5%
RNase-free H <sub>2</sub> O	to 200 ml	

The solution was sterile filtered and stored in the dark at 4°C. β-Mercaptoethanol was added just prior to use at the quantity of 10 µl per 1 ml of GITC buffer.

CsCl buffer

	For 200 ml	Final concentration
Cesium chloride	192 g	5.7 M
0.25 M sodium citrate	20 ml	25 mM
0.5 M EDTA	40 ml	100 mM
RNase-free H <sub>2</sub> O	to 200 ml	

pH was adjusted with 0.25 M citric acid to 7.5; the solution was sterile filtered and stored at room temperature.

**3.2.7 Northern blot analysis**

Northern blot analysis is a method to quantify RNA expression. The RNA is separated in a denaturing formaldehyde/agarose gel, transferred by capillary transfer to a nylon membrane and fixed by UV crosslinking. The RNA of interest is identified by hybridization with a specific radiolabeled cDNA probe.

All solutions used for the Northern blot were autoclaved, the electrophoresis and blot chambers, gel plates and combs were kept in freshly prepared 0.1% DEPC solution for 10-20 min before use to inactivate RNases.

*Preparation of RNA samples*

Each RNA probe (5-10 µg of total RNA) in a volume not more than 5 µl was mixed with 7.5 µl of sample buffer. If the volume of probe exceeded 5 µl, the sample was concentrated in a vacuum centrifuge until the volume was reduced to 5 µl. RNA probes mixed with sample buffer were denatured by heating at 65°C for 10 min. Afterwards, the samples were briefly chilled on ice and centrifuged for 1 min at 10,000 rpm in an Eppendorf bench-top centrifuge. Each sample was mixed with 3

µl of loading buffer and recentrifuged for 1 min at 10,000 rpm in an Eppendorf bench-top centrifuge.

#### *Electrophoresis conditions*

The denatured formaldehyde/agarose gel (1%) was prepared as follows: at first, 1 g of agarose was dissolved in 72.2 ml of RNase-free water (Ampuwa<sup>®</sup>) by heating in microwave oven and then slightly cooled to approximately 70°C, followed by sequential adding 10 ml of 10X running buffer and 16.7 ml of 37% formaldehyde. Next, 8 µl of ethidium bromide (10 mg/ml) was added to the mixture for visualization of 28S and 18S rRNA bands served for estimation of apparent molecular weight of the RNAs of interest in further hybridization steps. The mixture was poured into the prepared gel plate and let to polymerize under a fume hood for 20-30 min.

Immediately after preparation, the samples were loaded onto the gel, and the electrophoresis was performed at constant voltage of 80 V for 1-1.5 h.

After electrophoresis, the quality of RNA was estimated under UV transilluminator built-in Eagle Eye™ system (Stratagene); the gel was photographed, and the procedure was immediately continued to blotting.

#### *Transfer of RNA to nylon membrane*

After the separation of RNA in the gel, it was transferred to a nylon membrane by capillary transfer. The system for transfer was assembled as depicted on Figure 10. A plastic tray was filled with 500 ml of 20X SSC. A piece of Whatman 3MM filter was soaked in 20X SSC and draped over the glass plate placed over the tray with both ends hanging into buffer to act as wick. Any bubbles between the filter and glass plate were smoothed out. The gel was carefully placed upside down over the filter. The bubbles between the gel and wick were carefully removed. The nylon membrane wetted in 2X SSC was placed on top of the gel and smoothed. Two other pieces of Whatman 3MM filters wetted in 2X SSC were sequentially flat laid on top of nylon filter and smoothed. A stack of paper towels was placed on top, covered with another glass plate and pressed with 1 kg blotting weight. The transfer was carried out overnight.

After the transfer, RNA was fixed on the membrane by UV crosslinking for 2 min from both sides using Stratalinker™ 180 (Stratagene) set at “autocrosslink” mode.

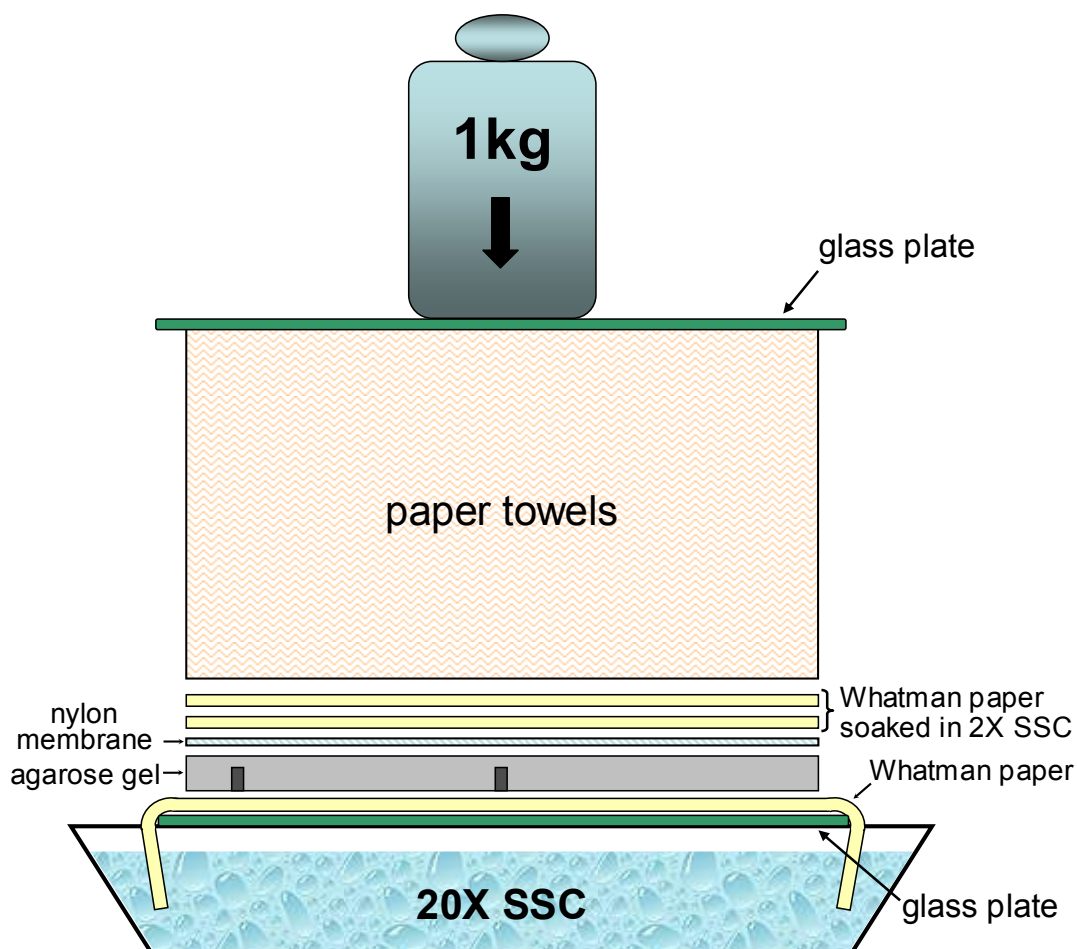


**Figure 10. Scheme of the system for capillary transfer of RNA on nylon membrane.**  
For explanations, see the text.

#### *Hybridization of RNA with radiolabeled cDNA probe*

After crosslinking, the nylon membrane was rinsed with 1X TE buffer to wash away any traces of agarose. Afterwards, the membrane was placed into a hybridization tube, and any bubbles between the membrane and internal wall of the tube were carefully removed. The prehybridization which is necessary to prevent unspecific binding was performed for 1 h with 10 ml of QuikHyb<sup>®</sup> hybridization solution at 68°C in a hybridization oven. Radiolabeled probe prepared as described in 3.2.5 was mixed with double volume of salmon sperm DNA and afterwards denatured for 5 min at 95°C. After chilling on ice, the DNA probe was mixed with QuikHyb<sup>®</sup> solution in the hybridization tube. The hybridization was carried out for 1 h at 68°C in a hybridization oven.

After hybridization, the membrane was rinsed in the tube with 30 ml of 2X SSC/0.1% SDS, next portion of 2X SSC/0.1% SDS was added followed by

washing for 30 min at 55°C in a hybridization oven. Afterwards, the membrane was transferred to a plastic tray and further washed in 2X SSC/0.1% SDS with shaking at room temperature. The radioactivity was controlled and when it reached approximately 100 cpm, the washing was stopped. The membrane was wrapped in a cling film, placed in an X-ray film cassette and exposed to X-ray film, which was developed afterward according to the manufacturer's instructions.

#### 10X running buffer

	For 500 ml	Final concentration
MOPS	20 g	200 mM
2M sodium acetate	12.5 ml	50 mM
0.5 M EDTA	10 ml	10 mM
RNase-free H <sub>2</sub> O (Ampuwa <sup>®</sup> )	to 500 ml	

pH was adjusted with 5N NaOH to 7.0; the solution was sterile filtered and stored in the dark at 4°C.

#### 1X running buffer

	For 1 l
10X running buffer	100 ml
RNase-free water (Ampuwa <sup>®</sup> )	to 1 l

The solution was stored at room temperature for 1-2 weeks.

#### Sample buffer

Deionized formamide	500 µl
37% formaldehyde	169 µl
10X running buffer	100 µl

The solution was dispensed into 1 ml aliquots and stored at -20°C for 2-3 months.

#### Deionized formamide

Formamide	100 ml
Mixed Bed Resin AG 501-X8 (D)	10 g

The mixture was stirred for 30 min in the dark at room temperature, afterwards it was sterile filtered, dispensed into 50 ml aliquots and stored in the dark at  $-20^{\circ}\text{C}$ .

### Loading buffer

10X running buffer	5 ml
RNase-free H <sub>2</sub> O (Ampuwa <sup>®</sup> )	3 ml
Ficoll 400	1.5 g
Bromophenol blue	10 mg

The solution was dispensed into 0.5 ml aliquots and stored for 2-3 months at  $-20^{\circ}\text{C}$

### 20X SSC

	For 2 l
NaCl	350.6 g
Sodium citrate $\times 2\text{H}_2\text{O}$	176.4 g
ddH <sub>2</sub> O	to 1 l

The solution was autoclaved and stored at room temperature.

### 2X SSC

	For 500 ml
20X SSC	50 ml
ddH <sub>2</sub> O	to 500 ml

### 10X TE

	For 1 l	Final concentration
2 M Tris-HCl, pH 7.4	50 ml	100 mM
0.5 M EDTA	20 ml	10 mM
RNase-free H <sub>2</sub> O	to 1 l	

pH was controlled and if necessary adjusted with NaOH or HCl to 7.6. The solution was sterile filtered and stored at  $4^{\circ}\text{C}$ .

1X TE

	For 500 ml
10X TE	50 ml
RNase-free H <sub>2</sub> O	to 500 ml

2X SSC/0.1% SDS

	For 500 ml
20X SSC	50 ml
20% SDS	2.5 ml
ddH <sub>2</sub> O	to 500 l

In the case of precipitation of the SDS, the solution was warmed until clear.

**3.2.8 Transient transfection of primary rat hepatocytes**

For transfection of primary hepatocytes, the calcium phosphate precipitation method was used. All the protocols for calcium phosphate precipitation, including the protocol used in the present study, are modifications of the protocol from Graham and van der Eb (Graham and van der Eb, 1973). The principle of the method is that the DNA forms together with calcium phosphate small precipitates which are taken up by cells via the process of endocytosis. The precipitate is obtained when the DNA/calcium chloride solution is mixed with a solution containing phosphate.

The transfection mixture was prepared in polystyrol tubes to prevent adhesion of the DNA to the walls of the vessel. After pipetting, the components were mixed and left for 5-10 min at RT. During this time the DNA/calcium phosphate precipitates were formed, which was observed as a light turbidity of the solution. Finally, 250  $\mu$ l of the mixture was added to  $1 \times 10^6$  hepatocytes freshly plated in 2.5 ml of medium on 60 mm culture dish. The cells were incubated at 37°C in humid atmosphere with 5% CO<sub>2</sub>. The medium was changed 5 h post transfection and the cells were further cultured under the serum-free conditions.

Transfection mixture

Transfection mixture was prepared in the following order: 2  $\mu$ g of plasmid DNA was diluted in appropriate volume of ddH<sub>2</sub>O and subsequently mixed with CaCl<sub>2</sub>. Afterwards, the obtained mixture was added dropwise to equal volume of 2X HBS.

	For one dish (60 mm)	Final concentration
Plasmid DNA	2 $\mu$ g	
ddH <sub>2</sub> O	to 112.5 $\mu$ l	
2.5 M CaCl <sub>2</sub>	12.5 $\mu$ l	125 mM
2X HBS	125 $\mu$ l	1X

### 2X HBS

	For 100 ml	Final concentration
HEPES	1.192 g	50 mM
NaCl	1.636 g	280 mM
Na <sub>2</sub> HPO <sub>4</sub>	0.267 g	1.5 mM
ddH <sub>2</sub> O	to 100 ml	

pH was adjusted with 5N NaOH to 7.10, the buffer was dispensed in 10 ml aliquots and stored at  $-20^{\circ}\text{C}$ .

### 2.5 M calcium chloride

	For 100 ml	Final concentration
CaCl <sub>2</sub>	36.75 g	2.5 M
ddH <sub>2</sub> O	to 100 ml	

### **3.2.9 Detection of luciferase activity**

The detection of luciferase activity in the cells transfected with reporter vectors containing the luciferase gene from north american firefly (*Photinus pyralis*) was performed with the Luciferase Assay Kit (Berthold, Pforzheim). The luciferase assay is based on the enzyme-catalyzed chemiluminescence. Luciferin present in the luciferase assay reagent is oxidized by luciferase in the presence of ATP, air oxygen and magnesium ions. This reaction produces light with a wave length of 562 nm. The luminescence can be measured by a luminometer.

#### *Preparation of cell lysates*

After the desired culture time, the medium was aspirated and cells were washed twice with PBS (2 ml per 60 mm dish). Next, 300  $\mu$ l of lysis buffer was added to the dish and cells were incubated for 15 min at room temperature on a rocking platform with slow agitation. After scraping the cells with a cell-scraper, cell lysates were transferred in tubes and placed on ice with subsequent freezing them in

liquid nitrogen for about 1 min. Afterwards, the tubes were removed from liquid nitrogen; cell lysates were thawed at room temperature and centrifuged at 14,000 rpm in Eppendorf benchtop MiniSpin centrifuge for 1 min at room temperature. Aliquots of obtained supernatants were used for detection of luciferase activity.

#### *Luciferase detection*

20  $\mu$ l of the supernatant from the cell lysate, obtained as described above, was automatically mixed in the luminometer with 100  $\mu$ l of luciferase assay reagent, prepared directly before use by mixing of equal parts of solutions A and B provided in the assay kit. The reaction was measured 10 times for 2 sec. The intensity of luminescence is constant for 20 sec and then decreases with a half-life period of 5 min. No information about the composition of solution A and B was given by the supplier.

#### 5X lysis buffer

	For 200 ml	Final concentration
2 M Tris-HCl	12.5 ml	125 mM
200 mM CDTA	10 ml	10 mM
500 mM DTT	4 ml	10 mM
85% glycerol	115 ml	50%
Triton X-100	10 ml	5%
ddH <sub>2</sub> O	to 200 ml	

pH was adjusted with H<sub>3</sub>PO<sub>4</sub> to 7.8; the solution was autoclaved.

1X lysis buffer was prepared by diluting 5X stock in ddH<sub>2</sub>O just prior to use on the basis of 300  $\mu$ l per 60 mm culture dish.

### **3.3 Biochemical methods**

#### **3.3.1 Protein extraction from liver tissue and cultured hepatocytes**

##### *Preparation of tissue homogenates*

All steps were performed at 4°C to prevent proteolytic degradation of the proteins. About 100 mg of frozen tissue was homogenized with Ultra-Turrax TP 18/10 model homogenizer 3 times for 10 sec each in 10 volumes of 50 mM Tris-HCl buffer, pH 7.4, containing 150 mM NaCl, 1 mM EDTA, 1% Triton X-100, 1mM



PMSF, 1mM benzamidine, 1µg/ml leupeptin, 10µM chymostatin, 1µg/ml antipain, 1µg/ml pepstatin A. Crude homogenates were passed 5 times through a 22 G injection canula connected to a syringe. To pellet the nuclei and particular matter, crude homogenates were centrifuged for 5 min at 10,000 g (4°C) and the protein concentration of supernatants was determined by the bicinchoninic acid (BCA) method (Smith et al., 1985) using the BCA protein assay reagent kit (Pierce, Bonn, Germany). Prepared homogenates were dispensed in aliquots and stored at -20°C until use.

#### *Preparation of cell lysates*

All steps of the procedure were performed at 4°C to prevent proteolytical degradation of the proteins. The cells frozen on the culture dishes were thawed on ice. 1X ice-cold lysis buffer, comprised of 150 mM NaCl, 1 mM EDTA, 1% Triton X-100, 50 mM Tris-HCl, pH 7.4 and supplemented with protease inhibitors, was added to the cells (360 µl per 6 cm dish) followed by incubation on ice for 10 min. Afterwards, the cells were scraped with a disposable scraper, transferred to new tubes and passed 5 times through a 22 G injection canula connected to a syringe. To pellet the nuclei and particular matter, prepared lysates were centrifuged for 5 min at 10,000 g (4°C) and the protein concentration of supernatants was determined by BCA method using the kit from Pierce. Prepared lysates were aliquoted and stored at -20°C until use.

#### 10X homogenization buffer (for tissue and cell processing)

	For 100 ml	Final concentration
2 M Tris-HCl, pH 7.4	2.5 ml	50 mM
500 mM EDTA	200 µl	1 mM
NaCl	0.877 g	150 mM
ddH <sub>2</sub> O	to 100 ml	

#### 1X homogenization buffer with additives

	For 10 ml	Final concentration
10X homogenization buffer	1 ml	1X
Triton X-100	100 µl	1%
ddH <sub>2</sub> O	9 ml	

Prior to use the following protease inhibitors were added:

	For 10 ml	Final concentration
500 mM PMSF	20 $\mu$ l	1 mM
10 mg/ml leupeptin	1 $\mu$ l	1 $\mu$ g/ml
1 M benzamidine	10 $\mu$ l	1 mM
8.25 mM chymostatin	10 $\mu$ l	8.25 $\mu$ M
1 mg/ml pepstatin	10 $\mu$ l	1 $\mu$ g/ml
10 mg/ml antipain	1 $\mu$ l	1 $\mu$ g/ml

### Protease inhibitors stocks

		Stock concentration
PMSF	87.1 mg in 1 ml DMSO	500 mM
Leupeptin	1 mg in 0.1 ml H <sub>2</sub> O	10 mg/ml
Benzamidine	313.2 mg in 2 ml H <sub>2</sub> O	1 M
Chymostatin	1 mg in 0.2 ml DMSO	8.25 mM
Pepstatin A	1 mg in 1 ml DMSO:acetic acid (9:1)	1 mg/ml
Antipain	1 mg in 0.1 ml H <sub>2</sub> O	10 mg/ml

Protease inhibitors stocks were dispensed into small aliquots and stored at  $-20^{\circ}\text{C}$ .

### Product information (Sigma)

**Antipain:** inhibits reversibly serine/cysteine proteases and some trypsin-like serine proteases. Its action resembles leupeptin, but it inhibits plasmin less and cathepsin A more than does leupeptin. Antipain also inhibits papain, trypsin, cathepsin B, cathepsin D, chymotrypsin, pepsin, and calpain I.

**Benzamidine:** inhibits reversibly trypsin-like enzymes and serine proteases. Furthermore, it is a strong competitive inhibitor of trypsin, thrombin and plasmin. Benzamidine is sensitive to oxidation and for the most part interchangeable with pepstatin A.

**Chymostatin:** inhibits strongly a lot of proteases, including chymotrypsin, chymotrypsin-like serine proteases, chymases and lysosomal cysteine proteases such as cathepsins B, H and L. Inhibits weakly human leukocyte elastase.

- Leupeptin:** inhibits reversibly and competitively serine and thiol proteases such as trypsin, plasmin, proteinase K, kallikrein, papain, thrombin and cathepsin A and B. Not affected are  $\alpha$ ,  $\beta$ ,  $\gamma$  and  $\delta$ -chymotrypsins, pepsin, cathepsin D, elastase, renin and thermolysin.
- Pepstatin A:** inhibits acid proteases (aspartyl peptidases). It forms 1:1 complex with proteases such as pepsin, renin, cathepsin D, bovine chymosin, solubilized  $\gamma$ -secretase, retroviral protease, and protease B (*Aspergillus niger*). The inhibitor is highly selective and does not inhibit thiol proteases, neutral proteases or serine proteases.
- PMSF:** inhibits serine proteases such as chymotrypsin, trypsin and thrombin as well as thiol protease papain. Does not inhibit metalloproteases, most thiol and aspartate proteases. PMSF is very unstable in the presence of water.

### 3.3.2 Western blot analysis

#### *Sample preparation*

Aliquots of prepared tissue homogenates and cell lysates were denatured in sample buffer containing 2% SDS, 10% glycerol, 50  $\mu\text{g/ml}$  bromphenol blue, 2%  $\beta$ -mercaptoethanol and 50 mM Tris-HCl, pH 6.8 by boiling at 95°C for 10 min and 15  $\mu\text{g}$  of total protein was subjected to SDS-polyacrylamide gel electrophoresis (SDS-PAGE).

#### *Casting of SDS-polyacrylamide gel*

For all applications described, a Tris/glycine SDS polyacrylamide gel (SDS-PAAG) system was used according to the method of Laemmli (Laemmli, 1970). For hand casting of the gels for vertical electrophoresis, a Mini-PROTEAN™ III Electrophoresis Cell (Bio-Rad) was used. 12.5% separating gels and 4% stacking gel were prepared as described below. The casting of the gels was performed according to the manufacturer's instructions. Precast 12% Tris/glycine SDS-PAAG (Bio-Rad) compatible with this system was used alternatively.

The separation gel (7.5 ml for 1.5 mm gel thickness) was poured between the inner (7.3×10.2 cm) and outer (8.3×10.2 cm) glass plates. The gel was carefully

overlaid with water-saturated isobutanol to create a barrier to oxygen, which inhibits the polymerization. After the gel has set (about 30 min at RT), the overlay was poured off and the top of the separating gel was washed with distilled water. The solution of stacking gel was poured directly onto the polymerized separating gel. The slots were formed by placing the appropriate comb into the gel solution. The polymerization took approximately 10 min.

#### *SDS-polyacrylamide gel electrophoresis (SDS-PAGE) and electrophoretic transfer*

The samples were loaded onto the bottom of the wells. Electrophoresis was run at constant 20 mA per gel. The Rainbow™ colored protein markers (Amersham Pharmacia Biotech) were used as molecular weight standards. Electrophoretic transfer was carried out essentially as described by Towbin (Towbin et al., 1979). Prior to stopping the gel running, fiber pads, filter paper and nitrocellulose transfer membrane (0.45 µm pore size) were soaked in transfer buffer. After electrophoresis, the gel was removed out of the plates and immersed in transfer buffer. For electrophoretic transfer of proteins from the gel to a membrane, a Mini-Trans-Blot® Cell (Bio-Rad), compatible with described system for electrophoresis, was utilized. The transblot sandwich was assembled according to the manufacturer's instructions from Bio-Rad in the following order starting from the anode side: sponge, 2 sheets of filter paper, nitrocellulose membrane, gel, 2 sheets of filter paper, sponge. The assembled transblot sandwich was inserted into the transblot cell filled with transfer buffer. Ice-cooling unit was set behind the cathode side of transblot cell. The transfer ran for 2 h at 350 mA with one change of the ice-cooling unit after the first hour.

#### *Staining the membrane with Ponceau S*

Ponceau S can be used routinely to verify quality of protein transfer from SDS-PAAG to nitrocellulose membrane. It is applied in acidic aqueous solution. Staining is rapid but not permanent; the red stain is washed away in subsequent processing. Since the binding is reversible, the stain is compatible with most antigen visualization techniques.

The membrane was immersed in freshly diluted Ponceau S solution and incubated for 5-10 min at room temperature with gentle agitation on the rocking platform. Afterwards, the membrane was destained for 1-2 min with several changes of TBS.

After visualization of distinctly visible protein bands, the dye was washed away completely with washing buffer.

### *Immunovisualization*

After transfer, the membrane was incubated on the rocking platform with blocking solution for overnight at 4°C. Next, the membrane was incubated with primary antibody diluted in antibody dilution buffer for 2 h at room temperature. After washing (six times, five min on each occasion), the membrane was incubated with HRP-conjugated secondary antibody diluted in antibody dilution buffer for 1 h at room temperature. Afterwards, the membrane was washed as before. For the chemiluminescent detection SuperSignal® West Pico Chemiluminescent Substrate (Pierce) was used. Substrate working solution was prepared by mixing of equal volumes of two substrate components. The membrane was incubated with substrate working solution for 5 min at room temperature, laid between two sheets of transparent plastic protector and exposed to X-ray film, which was developed afterward according to the manufacturer's instructions.

### 5X sample buffer

	Per 20 ml	Final concentration
Tris-HCl	0.79 g	250 mM
SDS	2 g	10%
Glycerol	10 ml	50 %

The components were dissolved in ddH<sub>2</sub>O (up to 18 ml), pH was adjusted with HCl to 6.8 and finally the following components were added:

	Per 20 ml	Final concentration
Bromphenol blue	5 mg	250 µg/ml
β-Mercaptoethanol	2 ml	10%

The solution was aliquoted and stored at -20°C. Protein samples were mixed with sample buffer in the proportion of 4:1, respectively.

### Separating gel

Components	12.5% gel	
	For 10 ml	For 15 ml
Rotiphorese Gel 30	4.17 ml	6.25 ml

4X Tris/SDS, pH 8.8	2.5 ml	3.75 ml
ddH <sub>2</sub> O	3.33 ml	5 ml
10% APS	33 µl	50 µl
TEMED	7 µl	10 µl

#### 4% stacking gel

<u>Component</u>	<u>Amount</u>
Rotiphorese Gel 30	0.67 ml
4X Tris/SDS, pH 6.8	1.25 ml
ddH <sub>2</sub> O	3.08 ml
10% APS	30 µl
TEMED	10 µl

#### 4X Tris/SDS, pH 6.8

For 100 ml

Tris base	6.05 g
SDS	0.4 g
ddH <sub>2</sub> O	to 100 ml

pH was adjusted with 37% HCl to 6.8; the solution was stored at room temperature.

#### 4X Tris/SDS, pH 8.8

For 250 ml

Tris base	45.5 g
SDS	1 g
ddH <sub>2</sub> O	to 250 ml

pH was adjusted with 37% HCl to 6.8; the solution was stored at room temperature.

5X SDS-PAGE running buffer

	For 2 l
Tris base	30.2 g
SDS	144 g
ddH <sub>2</sub> O	to 2 l

pH was adjusted with 37% HCl to 8.3; the solution was stored at room temperature.

1X SDS-PAGE running buffer

	For 2 l
5X stock	400 ml
ddH <sub>2</sub> O	to 2 l

5X transfer buffer

	For 2 l
Tris base	39.4 g
Glycine	144 g
ddH <sub>2</sub> O	to 2 l

pH was adjusted with 37% HCl to 8.3; the solution was stored at room temperature.

1X transfer buffer

	For 2 l	Final concentration
5X stock	400 ml	1X
100% methanol	400 ml	20%
20% SDS	1 ml	0.01%
ddH <sub>2</sub> O	to 2 l	

10X Ponceau S solution

	For 100 ml	Final concentration
Ponceau S	2 g	2%
Trichloroacetic acid	30 ml	30%
Sulfosalicylic acid	30 ml	30%
ddH <sub>2</sub> O	to 100 ml	

1X Ponceau S solution

	For 50 ml
10X Ponceau S	5 ml
ddH <sub>2</sub> O	to 50 ml

10X washing buffer

	For 2 l
Tris base	48.4 g
NaCl	58.48 g
ddH <sub>2</sub> O	to 2 l

pH was adjusted with HCl to 7.4; the solution was stored at room temperature.

1X washing buffer

	For 5 l	Final concentration
10X stock	500 ml	1X
Tween 20	5 ml	0.1%
ddH <sub>2</sub> O	to 5 l	

Blocking reagent

	For 50 ml	Final concentration
Nonfat dry milk	2.5 g	5%
1X washing buffer	to 50 ml	

The solution should be prepared freshly and stored at 4°C.

Antibody incubation buffer

	For 50 ml	Final concentration
5% nonfat milk	5 ml	0.5%
1X washing buffer	to 50 ml	

Primary antibodies were used in the following dilutions:

<u>Antibody</u>	<u>Used dilution</u>
anti-HO-1 rabbit polyclonal antiserum	1:2,000
anti-β-actin mouse monoclonal antibody	1:10,000



Secondary HRP-conjugated antibodies were used in the following dilution:

<u>Antibody</u>	<u>Used dilution</u>
Donkey anti-rabbit whole Ig	1:10,000
Rabbit anti-mouse Ig	1:10,000

### **3.3.3 Enzyme-Linked Immunosorbent Assay (ELISA)**

To measure IL-6 concentration in rat serum, the Quantikine<sup>®</sup> M rat IL-6 immunoassay kit (R&D Systems, Wiesbaden, Germany), based on solid phase ELISA, was used. This assay employs the quantitative sandwich enzyme immunoassay technique. A microplate is pre-coated with monoclonal antibody specific for rat IL-6. Samples are pipetted into the wells and any IL-6 present is bound by immobilized antibody. After washing away any unbound material, an enzyme-linked polyclonal antibody specific for rat IL-6 is added. Any unbound antibody-enzyme reagent is washed away, and a substrate solution is added to the wells. The enzymatic reaction yields a blue-colored product that turns yellow when the stop solution is added. The intensity of the color measured colorimetrically is proportional to the amount of rat IL-6 bound in the initial step.

#### **Reagent preparation**

Since all samples should be pipetted within 15 min, reagents needed for the assay were prepared prior to assay procedure. All reagents were provided with Quantikine<sup>®</sup> M rat IL-6 immunoassay kit.

#### **Rat IL-6 control**

The rat IL-6 control, provided with kit, was reconstituted with 1 ml double distilled water.

#### **Rat IL-6 conjugate concentrate**

	For 96 wells
Conjugate concentrate	0.5 ml
Conjugate diluent	11 ml

### Washing buffer

	For 96 wells
Washing buffer concentrate	25 ml
ddH <sub>2</sub> O	to 625 ml

### Substrate solution

Equal volumes of color reagents A and B, provided by kit, were mixed together, and solution was used with 15 min.

### Standard and sample preparation

Rat IL-6 standard was reconstituted with 2 ml of calibrator diluent RD5-16. This stock solution (2000 pg/ml) was used to prepare a dilution series ranging from 31.2 pg/ml to 2000 pg/ml. Calibrator diluent RD5-16 served as zero standard.

Blood was sampled from the *vena cava inferior* of control and treated rats, allowed to clot overnight at 4°C and centrifuged for 20 min at 2,000 *g*. Serum was collected and stored in aliquots at –20°C until use. Prior to assay, serum samples were diluted 2 fold into calibration diluent RD5-16.

### Assay procedure

The whole procedure was performed at room temperature. All samples, standards and controls were assayed in duplicates. To synchronize the reaction in each well, all reagents were pipetted using a multi-channel pipette.

50 µl of assay diluent RD1-54 was added to each well. Standards, control and samples were added in a quantity of 50 µl per well. The components were mixed by gentle tapping the plate frame for 1 min. After that, the plate was covered with the adhesive strip provided and incubated for 2 h at room temperature. Afterwards, each well was aspirated and washed with 400 µl of wash buffer using a manifold dispenser, and procedure was repeated four times for a total of five washes. For good performance, the liquid was removed completely by aspirating at each step. After washing, 100 µl of rat IL-6 conjugate was added to each well. The plate was covered with a new adhesive strip and incubated for another 2 h at room temperature. The aspiration-washing procedure was performed as described above. Subsequently, 100 µl of substrate solution was added to each well to start enzymatic reaction and plate was incubated in the dark for 30 min at room

temperature. To stop the enzymatic reaction, 100 µl of stop solution was added to each well, followed by determination of optical density of each well using a microplate reader (Dynatech Laboratories) set to dual wavelength mode (test filter – 450 nm, reference filter – 570 nm).

The calculation of results was performed with a program (Dynatech MRX software, version 1.33) created in accordance to the manual instructions (Quantikine® M rat IL-6 immunoassay kit).

### **3.3.4 Immunohistochemical analysis**

Immunoenzymatic/immunohistochemical (IHC) staining techniques allow for the visualization of tissue (cell) antigens. These techniques are based on the immunoreactivity of antibodies and the chemical properties of enzymes or enzyme complexes which react with colorless substrate-chromogens to produce a colored end-product. In the present study, indirect IHC technique where enzyme-labeled secondary antibody reacts with the antigen-bound primary antibody was used. The indirect method significantly improves the sensitivity of IHC staining compared to direct technique where enzymes are directly conjugated to the primary antibody. IHC technique can be divided into four steps, such as cell or tissue preparation, fixation, antibody binding, and detection.

#### *Preparation and fixation of tissue sections*

Preparing frozen tissue sections is the gentlest method for the preparation of samples and gives good preservation of cell structure and antigens.

Snap-frozen tissue blocks (approximately 1.0×1.0×0.5 cm) were sliced in 5 µm sections using a cryostat (Frigocut 2800 E) at the object temperature of –20°C and the chamber temperature of –23°C. The sections were placed on glass slides and air-dried for 2-3 h at room temperature. Dried sections were fixed for 10 min in ice-cold methanol followed by 10 sec fixation in ice-cold acetone and allowed to air-dry until completely dehydrated. Afterwards, the slides were proceeded with immunostaining or wrapped in aluminum foil and stored at –20°C for up to six months. Prior to immunostaining, wrapped frozen sections were equilibrated to room temperature.

Alternatively, non-fixed tissue sections were subjected to hematoxylin-eosin staining to monitor tissue structure and quality of sections. Hematoxylin-eosin staining was performed as follows: the slides were placed for 5 min in hematoxylin,

then washed for 10 min with tap water, placed afterwards for 10 sec in eosin solution and washed again for 5 min with tap water. Finally, the sections were covered with Kaiser's glycerol gelatin and coverslipped.

#### *Inhibition of endogenous peroxidases and blocking of nonspecific binding*

Prior to staining procedure, endogenous tissue peroxidases were inhibited by incubation of sections with peroxidase inhibition solution, containing glucose oxidase, sodium azide and glucose, for 20 min at room temperature. Afterwards, the sections were washed with PBS 2 times for 5 min on each occasion. Next, the slides were placed in a humidified chamber, covered with blocking solution, containing 300 µg of human IgG in 1 ml of heat inactivated FCS, and incubated for 20 min at 37°C to minimize nonspecific staining. Then washing in PBS was performed 2 times for 5 min.

#### *Incubation with antibodies*

After washing, the slides were covered with primary antibody diluted in PBS (300 µl per slide) and incubated for 60 min at room temperature in humidified chamber. For negative control, the incubation with primary antibody was omitted. Meanwhile, HRP-conjugated secondary antibody was preabsorbed with heat inactivated normal rat serum to avoid crossreactivity. For this purpose, 10 µl of rat serum was added to 50 µl of secondary antibody and incubated 60 min at 37°C, followed by centrifugation for 5 min at maximum speed of an Eppendorf bench-top centrifuge in order to pellet any precipitates. Afterwards, 50 µl of supernatant was transferred into a new tube and mixed with 350 µl of PBS and 600 µl of γ-globulin-free serum.

After incubation with primary antibody, the slides were washed in PBS 3 times for 5 min. Afterwards, the slides were covered with secondary antibody (300 µl per slide), prepared as described above, and incubated for 60 min at room temperature in a humidified chamber. Next, the washing step was performed as before.

#### *Visualization of immune complexes*

For immunovisualization, liquid DAB+ chromogen substrate (Dako) was used. Upon oxidation, DAB forms a brown end-product at the site of the target antigen. The working reagent was prepared by mixing 20 µl of the DAB Chromogen with 1 ml of Substrate buffer supplied. The slides were covered with freshly prepared

working solution (300  $\mu$ l per slide) and incubated 10 min at room temperature. Next, the slides were washed 2 times for 5 min in distilled water and the sections were counterstained with Meyer's hemalaun (Merck) for 5 min. After subsequent washing step (10 min in tap water), the sections were covered with Kaiser's glycerol gelatin and mounted with cover-slips.

#### Peroxidase inhibition solution

	For 100 ml
Glucose	180 mg
Glucose oxidase	5 mg
1M sodium azide	100 $\mu$ l
PBS	to 100 ml

The solution was prepared just prior to use. The components were dissolved in PBS, placed in prewarmed cuvette and incubated for 10 min at 37°C in water bath.

#### Blocking solution

	For 1 ml
10 mg/ml human IgG	30 $\mu$ l
Heat inactivated FCS	to 1 ml

Working solution for immunovisualization was prepared by mixing 20  $\mu$ l of DAB+ chromogen (containing 3,3'-diaminobenzidine in chromogen solution) and 1 ml of substrate buffer (containing imidazole-HCl, pH 7.5, hydrogen peroxide and an anti-microbial agent).

Primary antibodies were used in the following dilutions:

<u>Antibody</u>	<u>Used dilution</u>
anti-HO-1 mouse monoclonal antibody	1:500
anti-rat-ED1 mouse monoclonal antibody	1:100
anti-rat-ED2 mouse monoclonal antibody	1:100

Secondary HRP-conjugated antibody was used in the following dilution:

<u>Antibody</u>	<u>Used dilution</u>
Rabbit anti-mouse Ig	1:20

### **3.3.5 Statistical analysis**

Autoradiographic and immunoreactive bands after Northern and Western blots, respectively, were evaluated by densitometric scanning using Molecular Analyst scanning densitometer (Bio-Rad). The relative densities of bands were expressed as a fold of increase compared to respective controls.

Results of IL-6 plasma concentration measurements are presented as means $\pm$ SEM. Data obtained from luciferase activity measurements were analyzed by Student's *t*-test for paired values and presented as means $\pm$ SEM. A value of  $p < 0.05$  was accepted as statistically significant.

### **3.3.6 Safety measures**

All operations with genetically modified organisms and plasmid DNA were performed in accordance to the "Gentechnikgesetz" of 1990 and to the rules prescribed by the "Gentechnik-Sicherheitsverordnung" of 1990. Materials contaminated with bacterial cells were disinfected with Mucocit<sup>®</sup> (Merz /Frankfurt, Germany) and autoclaved.

Ethidium bromide, formaldehyde, DEPC and other chemicals deleterious for the environment, when used in the course of the work, were carefully managed and disposed properly in accordance with institutional guidelines.

All the operations with radioactive chemicals were performed in a radioactivity class II laboratory and the radioactive waste was disposed according to the institutional instructions.

## 4. Results

### 4.1 Studies *in vivo*: HO-1 expression in a turpentine oil (TO) model of the acute phase response (APR) in rats

An acute phase reaction in rats was induced by a single intramuscular injection of TO; control animals received no injection. Tissue and blood specimens were collected from the control and treated animals at the following time points: 0.5 h, 1 h, 2 h, 4 h, 6 h, 12 h, 24 h, 36 h and 48 h. Tissues were snap-frozen in liquid nitrogen and kept further at  $-80^{\circ}\text{C}$  for subsequent RNA, protein extraction and preparation of cryostat sections. Serum from blood samples was separated by clotting and subsequent centrifugation and stored at  $-20^{\circ}\text{C}$  until use for the rat IL-6 specific ELISA. Northern blot hybridizations of total RNA from various tissues were performed with cDNAs specific for HO-1,  $\alpha 2$ -macroglobulin, albumin, IL-6, GAPDH and with a 28S rRNA-specific oligonucleotide. Western blot analysis of hepatic protein extracts was carried out using antibodies against rat HO-1 and  $\beta$ -actin. Liver and muscular tissues were used for preparation of cryostat sections with subsequent hematoxylin/eosin staining and immunohistochemical analysis.

#### 4.1.1 HO-1 expression in the liver and extrahepatic tissues during a turpentine oil (TO)-induced acute phase response (APR) in rats

##### *Expression of hepatic HO-1 mRNA and protein during a turpentine oil (TO)-induced acute phase reaction*

To define the time-course of hepatic HO-1 mRNA expression during TO-induced acute phase reaction in rats, Northern blot analysis of total RNA prepared from whole liver tissue at various time points after single injection of TO was performed using radiolabeled HO-1 cDNA as a probe. As indicated in Figure 11A, HO-1 specific transcript levels were dramatically increased 4-6 h after TO administration with a maximum at 6 h. Since  $\alpha 2$ -macroglobulin is a well-known positive, and albumin a negative acute phase proteins in rats (Schreiber et al., 1986), hybridizations with  $\alpha 2$ -macroglobulin- and albumin-specific cDNAs were performed to ensure development of the acute phase response in the treated animals. The  $\alpha 2$ -macroglobulin mRNA levels were elevated from 4 to 24 h and albumin mRNA decreased reaching lowest levels 24 to 36 h after TO injection (Figure 11A), which

is in accordance with published data (Knittel et al., 1997). Hybridization with GAPDH-specific cDNA was used to control equal loading of RNA.

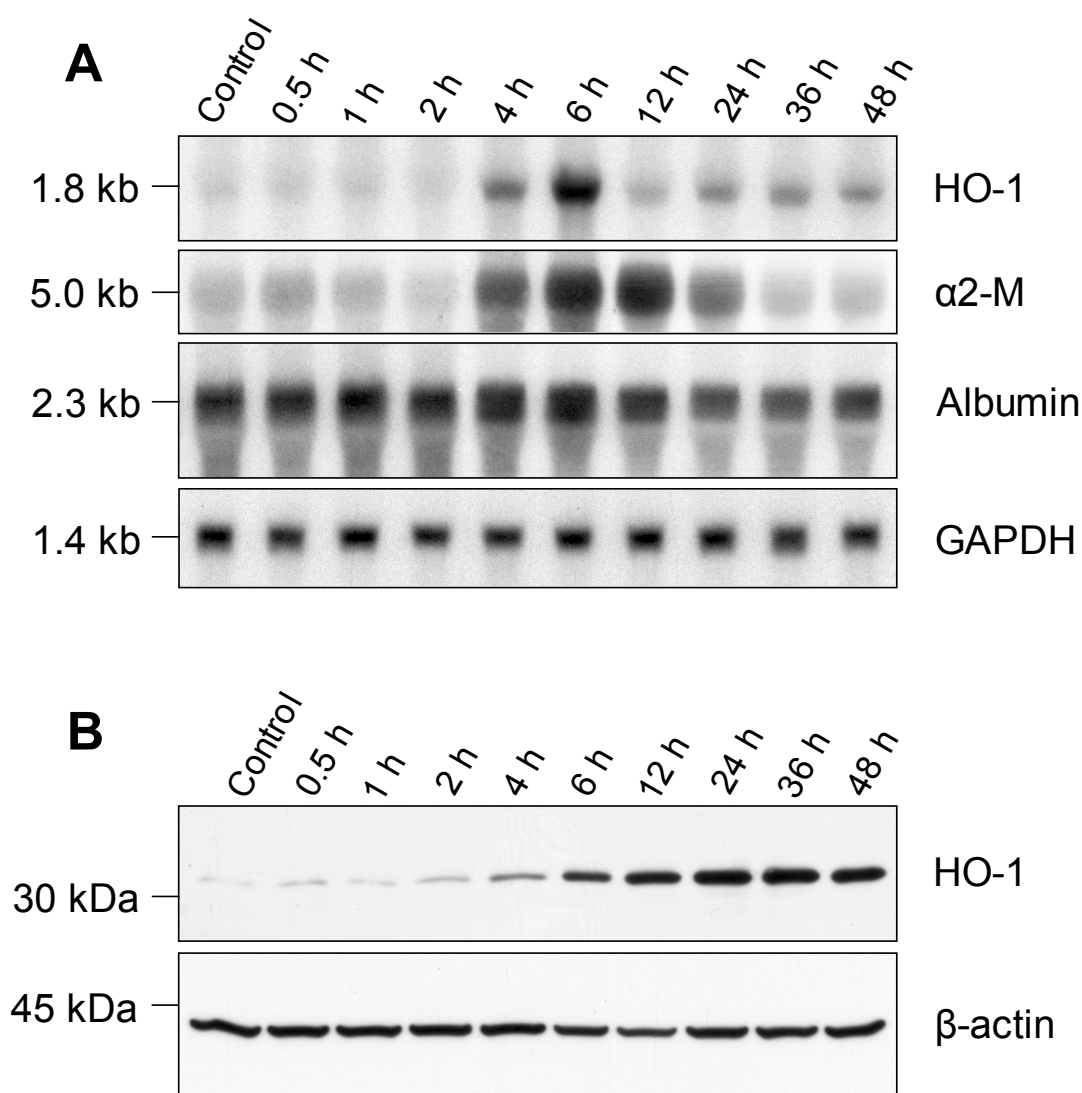


**Figure 11. Time course of hepatic HO-1 mRNA and protein expression after TO administration.** An acute phase response was induced by TO injection in rats, afterwards liver specimens were removed at the indicated time points and homogenized for RNA and protein extraction as described in Methods. **(A)** Total RNA (10 µg) from livers of control and TO-treated rats was subjected to Northern blot and sequentially hybridized with [<sup>32</sup>P]-labeled cDNAs specific for HO-1, α2-macroglobulin (α2-M), albumin and GAPDH as an internal loading control. The sizes of the transcripts (in kilobases, kb) are indicated on the left. A representative of four independent experiments is shown. **(B)** The protein samples (15 µg) from livers of control and TO-treated rats were immunoblotted and probed with a rabbit polyclonal anti-HO-1 antibody as described in Methods. Mouse monoclonal anti-β-actin antibody was used to control equal loading of protein samples. The positions of molecular weight standards (in kilodaltons, kDa) are indicated on the left. Data shown are representative of more than three independent experiments.



The enhancement of HO-1 mRNA was followed by an induction of HO-1 protein as shown by Western blot analysis. HO-1 protein levels started to increase after 4 h and remained elevated up to 48 h after TO administration (Figure 11B), indicating that in rat liver under inflammatory conditions, the life-time of the HO-1 protein seems to be considerably longer than the life-time of the HO-1 mRNA. To control equal loading of proteins, the membranes were stripped and then probed with an anti- $\beta$ -actin antibody.

*Expression of HO-1 mRNA in extrahepatic rat tissues during a turpentine oil (TO)-induced acute phase reaction*

To determine whether HO-1 induction is a liver-specific response to localized inflammation or it could also occur in other rat tissues under the given experimental conditions, Northern blot analysis of total RNA prepared from skeletal muscle, lung, heart, kidney, spleen, small and large intestine at various time points after injection of TO was performed using radiolabeled HO-1 cDNA as a probe. A strong induction of HO-1 mRNA was observed in skeletal muscle at the site of injection where the acute phase response was initiated by local inflammation. As depicted on Figure 12, HO-1-specific transcripts appeared already after 2 h, reached maximal levels by 4-6 h and slowly decreased up to 48 h after TO injection. It should be noted that HO-1 mRNA expression in injured muscle correlated with that in the liver (Figure 11A).

Figure 12 further illustrates that in the heart, kidney and large intestine, a slight induction of HO-1 mRNA was observed 6 h after TO injection, while in the lung, spleen and small intestine no changes in HO-1 expression were detected. Relatively high basal levels of HO-1 gene expression were found in the spleen (Figure 12), which is consistent with published work (Braggins et al., 1986). It is likely a consequence of permanent spleen exposure to hemoglobin released from the disrupted senescent erythrocytes.

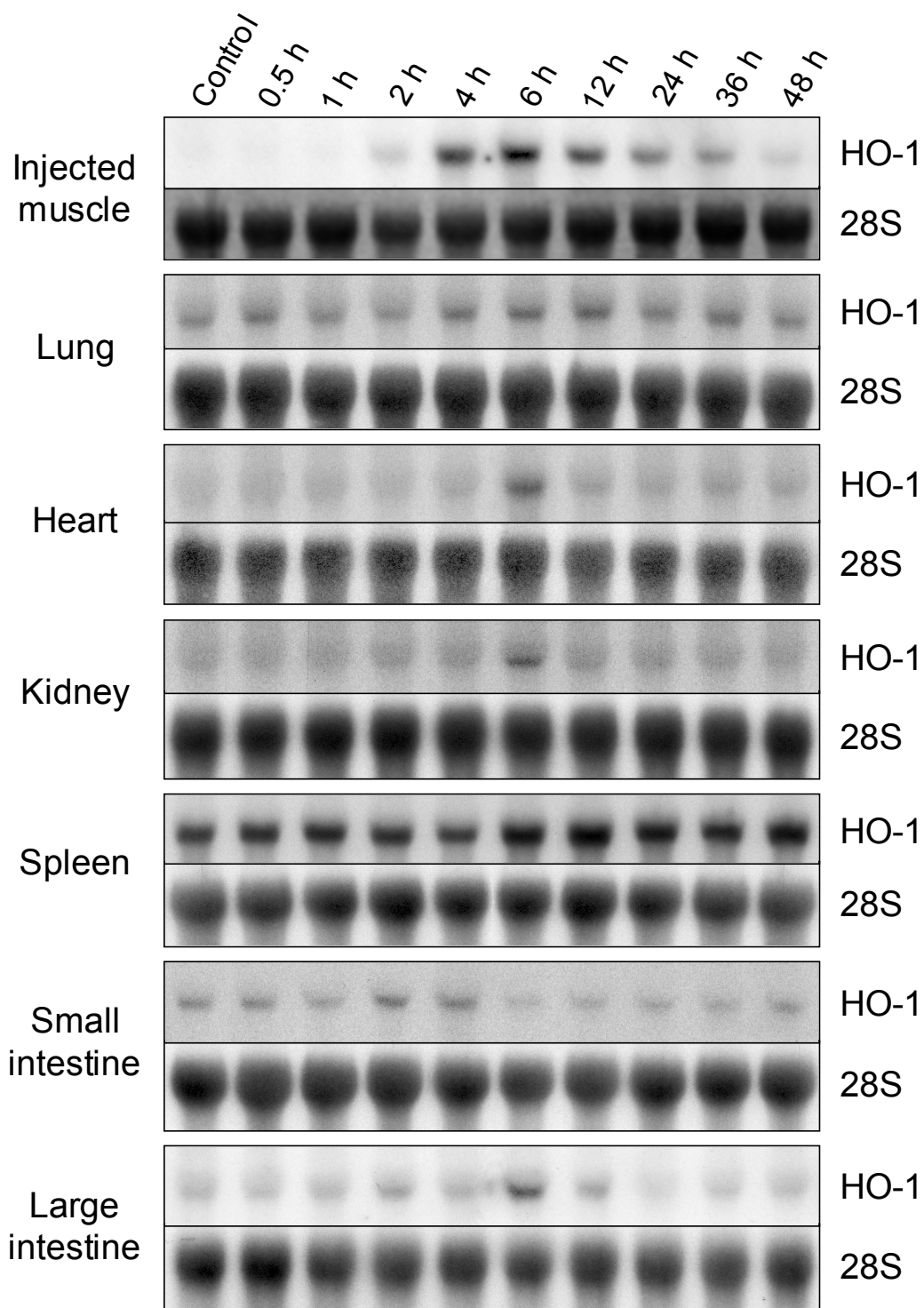


**Figure 12. Time course of HO-1 mRNA expression in extrahepatic rat tissues after TO administration.** An acute phase response was induced by TO injection in rats, and total RNA from skeletal muscle, lung, heart, kidney, spleen, small and large intestine was extracted at the indicated time points as described in Methods. Total RNA (10  $\mu$ g) from these tissues was subjected to Northern blot and hybridized with [ $^{32}$ P]-labeled cDNA specific for HO-1. A 28S rRNA-specific oligonucleotide probe was used to control equal loading. Data shown are representative of two independent experiments.

#### 4.1.2 Distribution of HO-1 within the liver and injured muscle during a turpentine oil (TO)-induced acute phase response (APR) in rats

Since the HO-1 mRNA levels were found to be markedly elevated in the liver and injured muscle, it was of interest to determine the cell types responsible for HO-1 up-regulation within these tissues during the TO-induced APR. For this purpose, histological and immunohistochemical analyses were carried out.

##### *HO-1 distribution in the livers of untreated and turpentine oil (TO)-treated rats*

Hematoxylin/eosin staining did not reveal any morphological difference between the liver of untreated and liver of TO-treated rats, suggesting that the intramuscular turpentine oil injection used for the APR induction did not cause visible liver damage (Figure 13).

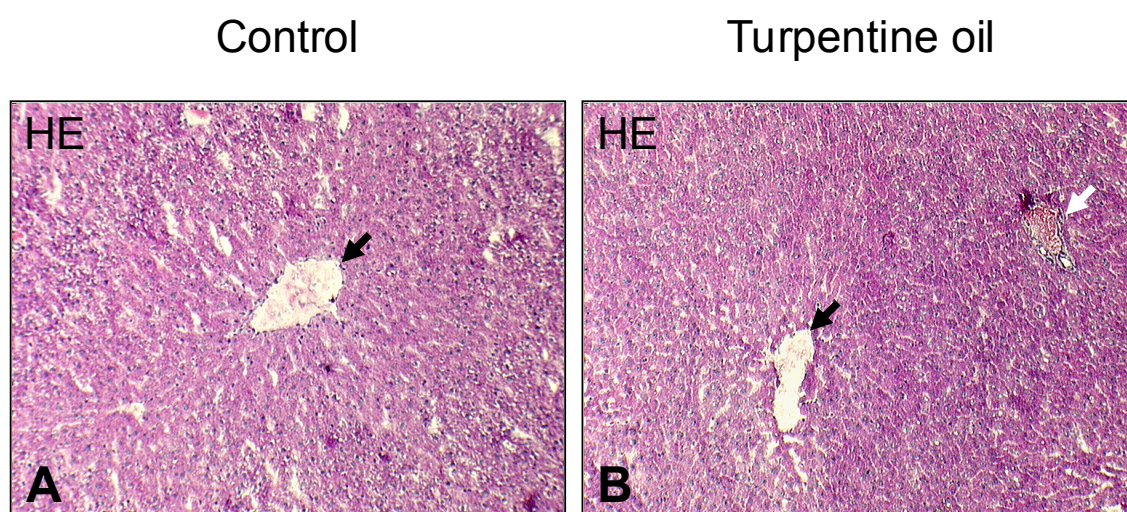


**Figure 13. Histological analysis of the livers from control and TO-treated rats.** Air-dried cryostat sections of normal rat liver (**A**) or liver excised from the rat 12 h after TO administration (**B**) were stained with hematoxylin and eosin (HE). Black arrows indicate central veins, white arrow – periportal field. Original magnification was 100-fold.

Cell type-specific expression of HO-1 in the livers obtained from control and TO-treated rats was assessed by immunohistochemical analysis of sequential cryostat sections. Under physiological conditions, the expression of HO-1 immunoreactive protein was mainly attributed to Kupffer cells, as verified by application of the antibody against the rat ED2, a well-known specific marker of resident liver

macrophages (Kupffer cells), whereas liver parenchymal cells were HO-1 negative (Figure 14A, C, D).

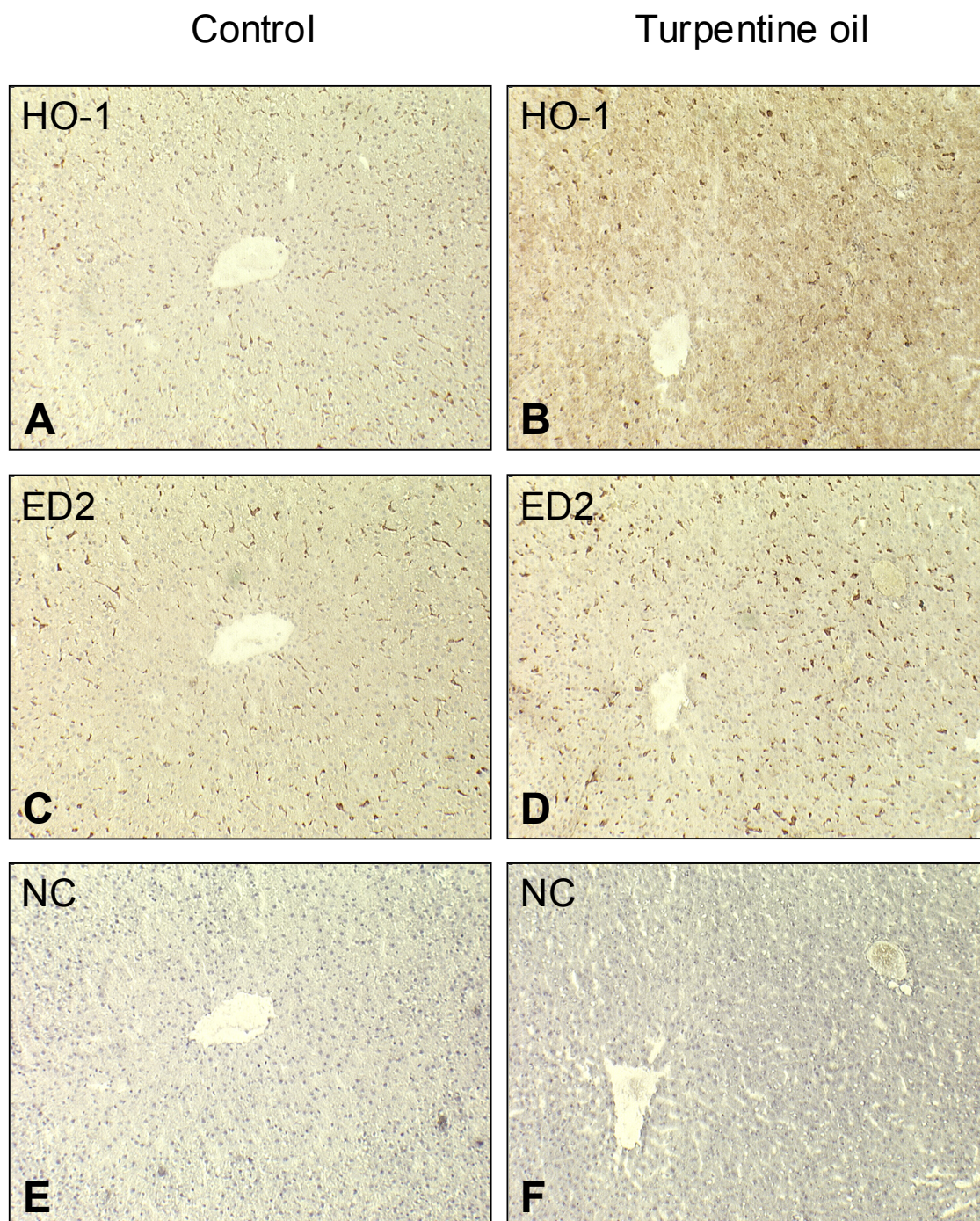


**Figure 14. Immunohistochemical analysis of the livers from control and TO-treated rats.** After blocking unspecific binding sites and endogenous peroxidase activity, sequential cryostat sections of control rat liver (**A, C, E**) or liver excised from the rat 12 h after TO administration (**B, D, F**) were stained with a monoclonal anti-rat HO-1 antibody (**A, B**) or with the monoclonal antibody against rat ED2 (**C, D**) as described in Methods. Horseradish peroxidase-linked anti-mouse immunoglobulin was applied as a secondary antibody. The positive cells are brown colored. Nuclei are counterstained in blue. The panels **E** and **F** represent negative controls (NC) obtained by omitting the primary antibody. Original magnification was 100-fold.

However, during the TO-induced inflammatory response, a prominent induction of HO-1 immunoreactivity was observed in the liver parenchyma, whereas no significant increase in the intensity and number of the HO-1-positive Kupffer cells was visible (Figure 14B). The negative controls demonstrated a specificity of the immunohistological analysis performed (Figure 14E, F).

These data suggest that under control conditions, hepatic HO-1 expression is mainly attributed to Kupffer cells, whereas the dramatic increase in the HO-1 production observed on the mRNA and protein levels in the liver during the APR (Figure 11) is most likely caused by hepatocytes.

*HO-1 distribution in injured muscle during a turpentine oil (TO)-induced acute phase reaction*

As revealed by hematoxylin/eosin staining of the injured rat muscle (6 h after TO administration), a prominent infiltration of small irregularly shaped cells with large nuclei occurred at the site of inflammation (Figure 15B). The observed cells had the morphological features of leukocytes and were absent in the muscular tissue of control animals (Figure 15A).

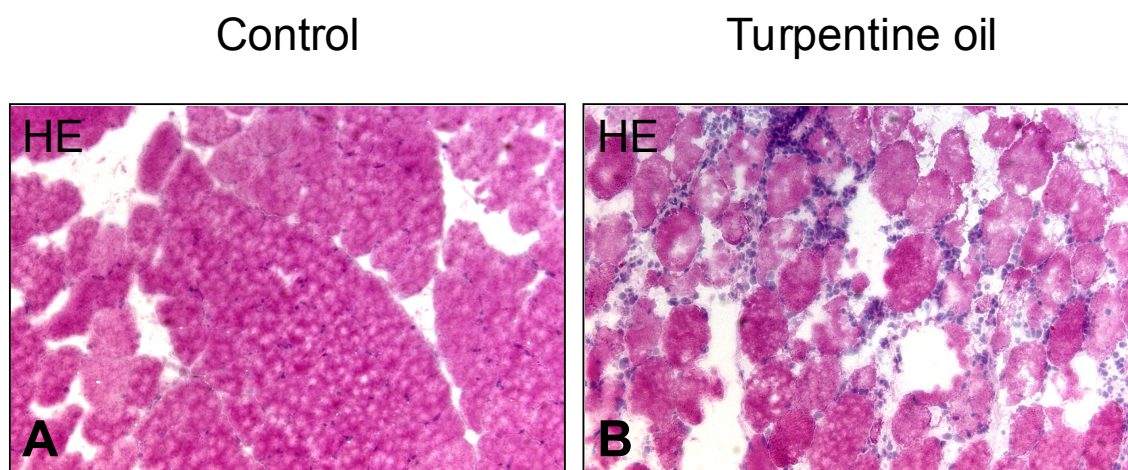


**Figure 15. Histological analysis of normal and injured muscular tissue from rat hind limb.** Air-dried cryostat sections of normal (A) or injured (6 h after TO administration) rat skeletal muscle (B) were stained with hematoxylin and eosin (HE). Original magnification was 200-fold.

Cell type-specific expression of HO-1 in normal and injured muscle from rats was assessed by immunohistochemical analysis of sequential cryostat sections. In intact muscular tissue of control animals, HO-1 immunoreactive protein was only slightly detectable in some small, elongated, irregularly shaped cells, whereas

muscle fibers were HO-1 negative (Figure 16A). However, the number of HO-1-positive cells dramatically increased in the skeletal muscle under the inflammatory conditions (Figure 16B).

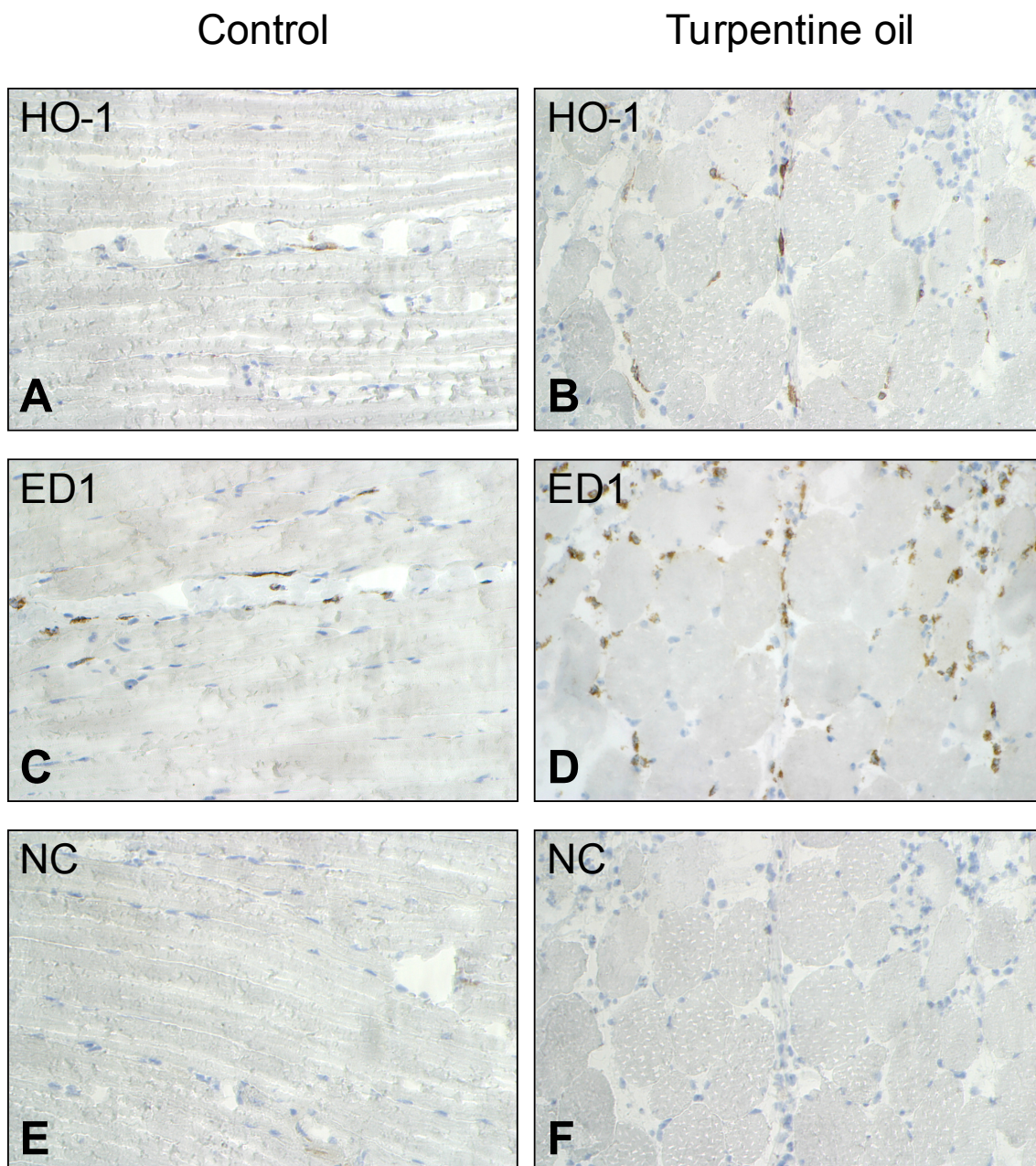


**Figure 16. Immunohistochemical analysis of normal and injured muscular tissue from rat hind limb.** After blocking unspecific binding sites and endogenous peroxidase activity, sequential cryostat sections of control (**A**, **C**, **E**) or injured (6 h after TO administration) rat muscle (**B**, **D**, **F**) were stained with a monoclonal anti-rat HO-1 antibody (**A**, **B**) or with the monoclonal antibody against rat ED1 (**C**, **D**) as described in Methods. Horseradish peroxidase-conjugated anti-mouse immunoglobulin was applied as a secondary antibody. The positive cells are brown colored. Nuclei are counterstained in blue. The panels **E** and **F** represent negative controls obtained by omitting the primary antibody. Original magnification was 250-fold.

ED1, a specific marker of myeloid cells, is expressed predominantly on the lysosomal membrane by the majority of tissue macrophages and weakly by peripheral blood granulocytes. Application of the antibody against the rat ED1 using respective subsequent sections (Figure 16C, D) demonstrated co-localization of HO-1 and ED1, suggesting that HO-1 expression is attributed to activated monocytes (i.e. macrophages) recruited to muscle tissue during inflammation. The negative controls demonstrated a specificity of the immunostainings performed (Figure 16E, F).

#### **4.1.3 Assessment of IL-6 mRNA expression in various tissues and serum levels of IL-6 during a turpentine oil (TO)-induced acute phase response (APR) in rats**

Since IL-6 is known as a key cytokine released during TO-induced APR in rats (Luheshi et al., 1997), the assessment of IL-6 specific mRNA expression in various tissues and serum levels of IL-6 in rats after TO administration was carried out.

##### *Expression of IL-6 mRNA occurred only in muscle during a turpentine oil (TO)-induced acute phase reaction*

In order to determine the source of IL-6 under the experimental conditions, Northern blot analysis of total RNA prepared from skeletal muscle, liver, lung, heart, kidney, spleen, small and large intestine at various time points after injection of TO was performed using radiolabeled IL-6 cDNA as a probe. Total cellular RNA isolated from rat Kupffer cells treated with LPS was processed in parallel and served as a positive control for IL-6-specific transcripts (Luckey et al., 2002). As depicted on Figure 17, 1.2 and 2.4 kb IL-6-specific transcripts were detectable only in injured skeletal muscle at 2 to 12 h after TO injection with maximal levels at 4-6 h. Other tissues from TO injected rats did not show any IL-6 positivity by Northern blot analysis (Figure 17), suggesting that only injured muscle is the source of IL-6 during the TO-induced acute phase response.

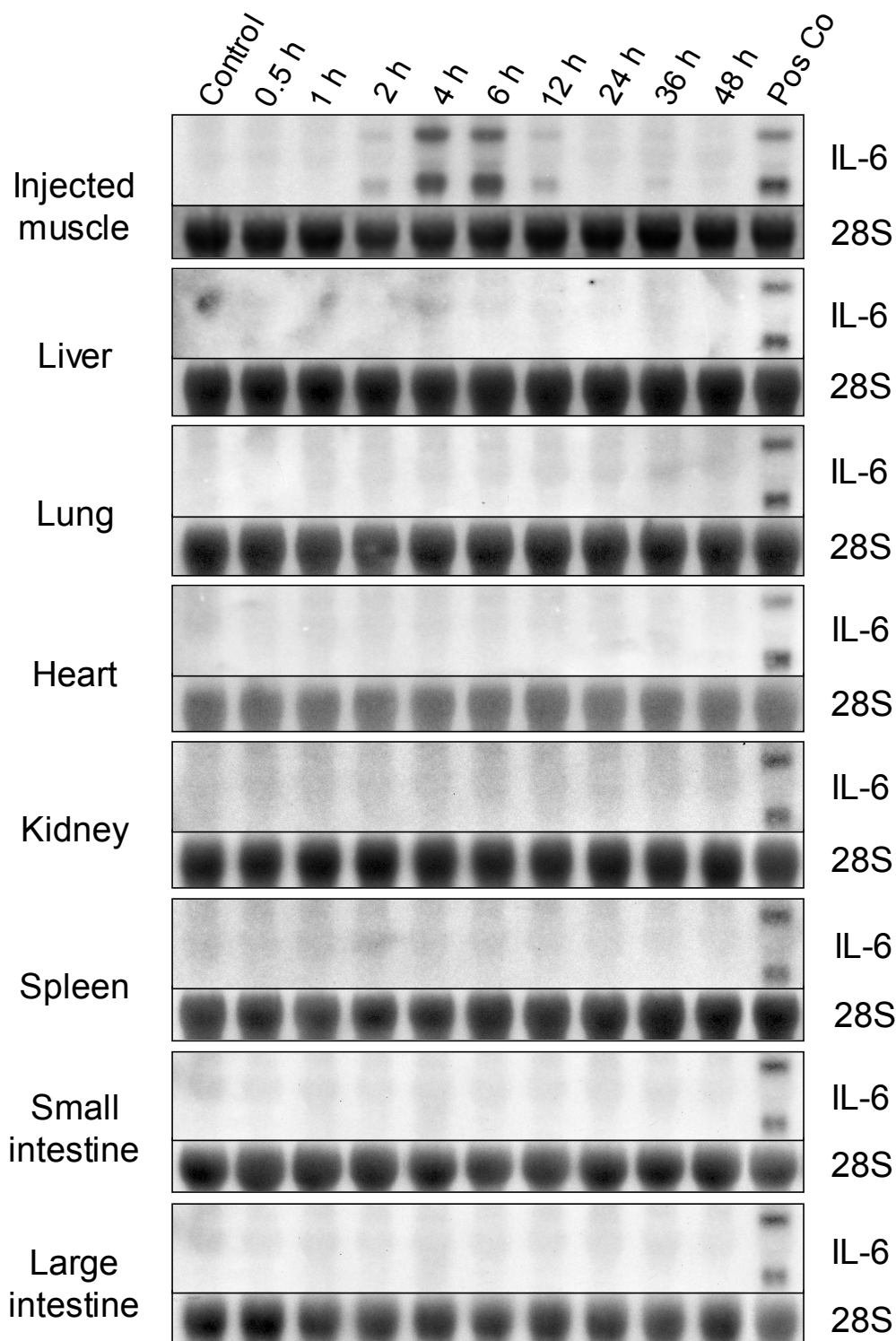


**Figure 17. Time course of IL-6 mRNA expression in various rat tissues after TO administration.** An acute phase response was induced by TO injection in rats, and RNA from skeletal muscle, liver, lung, heart, kidney, spleen, small and large intestine was extracted at the indicated time points as described in Methods. Total RNA (10  $\mu$ g) from these tissues was subjected to Northern blot analysis and hybridized with [ $^{32}$ P]-labeled cDNA specific for IL-6. 28S rRNA-specific oligonucleotide probe was used to control equal loading. Total cellular RNA (10  $\mu$ g) isolated from rat Kupffer cells treated with LPS (500 ng/ml) was processed in parallel and served as a positive control (Pos Co) for IL-6-specific transcripts. Data shown are representative of two independent experiments.



*Serum IL-6 levels in rats during a turpentine oil (TO)-induced acute phase reaction*

To elucidate the possible relationship between hepatic HO-1 induction and IL-6-specific mRNA expression in injured muscle, serum IL-6 levels in TO-treated rats were measured by rat IL-6-specific enzyme-linked immunosorbent assay (ELISA). Serum IL-6 concentrations were markedly elevated during the TO-induced APR reaching maximal values 6-12 h after injection up to  $1725.785 \pm 310.985$  pg/ml and  $1277.913 \pm 383.983$  pg/ml, respectively. This corresponds to about 115 - 85-fold increase compared to control levels (Figure 18).

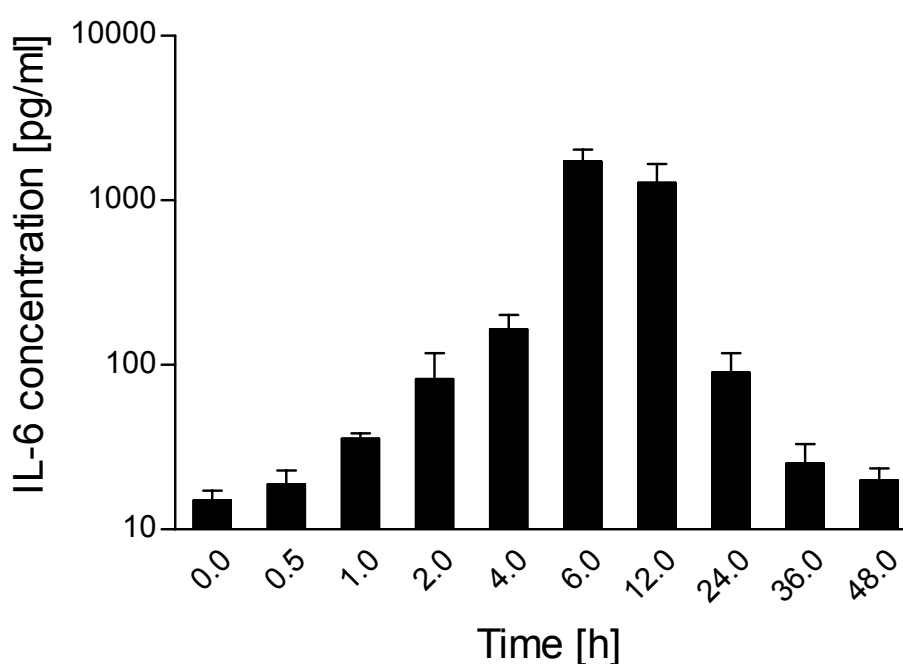


**Figure 18. Serum IL-6 levels in rats after TO administration.** An acute phase response was induced by TO injection in the rat and serum was collected at the indicated time points after injection as described in Methods. Serum IL-6 concentration was measured using a rat IL-6 specific ELISA. The results are presented as means  $\pm$  SEM (n = 3).

After 12 h, the IL-6 serum concentration in the rats under study considerably declined returning to control levels 48 h after TO injection. It should be noted that the serum IL-6 levels were already elevated 2 h after TO administration reaching more than a 5-fold increase compared to the controls. The IL-6 serum levels from TO-treated rats are accompanied by IL-6 gene expression in injured muscle tissue, confirming that inflamed muscle seems to be the only source of IL-6 in the model used.

## **4.2 Studies *in vitro*: HO-1 expression in primary cultures of rat hepatocytes treated with proinflammatory cytokines**

Hepatocytes were isolated from male Wistar rats by circulating perfusion with collagenase. The cultures were maintained at 37°C in a humid atmosphere containing 95% air/ 5% CO<sub>2</sub>. Fetal calf serum (5%) was present during the plating phase up to 4 h, afterwards the cells were cultured under serum-free conditions and treated with various proinflammatory cytokines. After washing with PBS, the cells were frozen on the plates and kept at –80°C until RNA or protein extraction. Northern blot hybridizations of total cellular RNA were performed with cDNAs specific for HO-1,  $\alpha$ 2-macroglobulin, albumin, GAPDH and with a 28S rRNA-specific oligonucleotide. Western blot analysis was carried out using antibodies against rat HO-1 and  $\beta$ -actin. The transfection experiments with various HO-1 promoter luciferase gene constructs were performed using the calcium phosphate precipitation method. HO-1 promoter controlled luciferase gene expression was assessed by detection of luciferase activity in cell lysate supernatants.

### **4.2.1 Regulation of HO-1 mRNA expression in primary rat hepatocytes by proinflammatory cytokines**

It is known that under stress conditions, HO-1 expression can be induced to a different extent in all liver cell types (Suematsu and Ishimura, 2000). Liver parenchymal cells, the hepatocytes, represent the major cell population in the liver (about 80% of total cell number) being the main target of a multiple set of mediators involved in the APR. IL-6, IL-1 $\beta$  and TNF- $\alpha$  are the most potent inducers of acute phase protein synthesis in hepatocytes (Ramadori and Christ, 1999). Considering the above mentioned statements and the fact that induction of HO-1 immunoreactive protein in the livers of TO-treated rats was attributed to the liver parenchymal cells (Figure 14B), the contribution of different cytokines to the HO-1 induction *in vitro* was evaluated using primary cultured rat hepatocytes.

#### *Dose-dependent induction of HO-1 mRNA expression in primary rat hepatocytes by proinflammatory cytokines*

Northern blot analysis of total cellular RNA isolated from primary rat hepatocytes cultured either in the absence (control) or in the presence of increasing

concentrations (0.1-100 ng/ml) of IL-6, IL-1 $\beta$  or TNF- $\alpha$  for 24 h, revealed an induction of HO-1-specific mRNA by all cytokines used in the study (Figure 19).

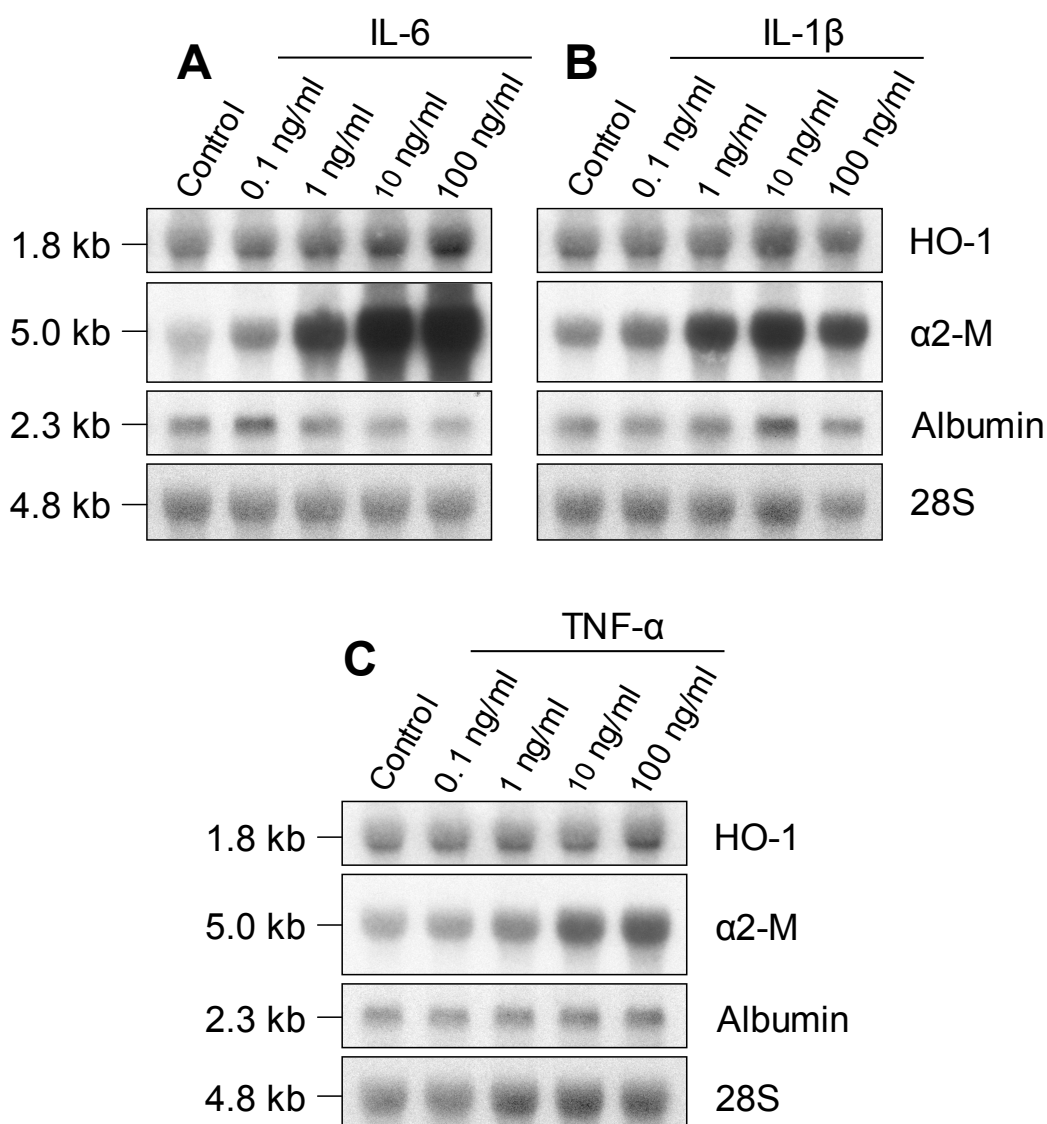


**Figure 19. Dose-dependent induction of HO-1 mRNA expression by proinflammatory cytokines in primary rat hepatocytes.** Rat hepatocytes were isolated, plated and cultured as described in Methods. After 18 h of cultivation under serum-free conditions, the medium was changed; the cells were incubated for 6 h, and afterwards cultured in the absence (Control) or the presence of increasing concentrations of IL-6 (A), IL-1 $\beta$  (B) or TNF- $\alpha$  (C) for 24 h. Total cytosolic RNA (5  $\mu$ g) from control and treated cells was subjected to Northern blot and sequentially hybridized with [ $^{32}$ P]-labeled cDNAs specific for HO-1,  $\alpha$ 2-macroglobulin ( $\alpha$ 2-M), albumin and a 28S rRNA specific oligonucleotide probe. The latter was used to control equal loading of RNA samples. The sizes of the transcripts (in kb) are indicated on the left. Data shown are representative of three independent experiments

IL-6, however, led to the strongest induction in a dose-dependent manner (Figure 19A). This cytokine-induced HO-1 expression well correlated with  $\alpha$ 2-

macroglobulin and albumin, positive and negative acute phase proteins, respectively. It should be noted that induction of  $\alpha$ 2-macroglobulin transcription was strongest in the presence of IL-6 (Figure 19A), moderate in the cells treated with IL-1 $\beta$  (Figure 19B), and the weakest induction was observed after treatment with TNF- $\alpha$  (Figure 19C), whereas albumin mRNA levels declined only after IL-6 treatment (Figure 19A) and were not affected by IL-1 $\beta$  or TNF- $\alpha$  (Figure 19B, C).

*Time-dependent induction of HO-1 mRNA expression in primary rat hepatocytes by proinflammatory cytokines*

In order to demonstrate the time-course of HO-1 induction *in vitro* by various proinflammatory cytokines, Northern blot analysis of total cellular RNA isolated from primary rat hepatocytes cultured either in the absence (control 0 h, 6 h, 12 h) or in the presence of IL-6, IL-1 $\beta$  or TNF- $\alpha$  for 10 min, 20 min, 30 min, 60 min, 3 h, 6 h, 9 h and 12 h was performed using radiolabeled HO-1 cDNA as a probe.

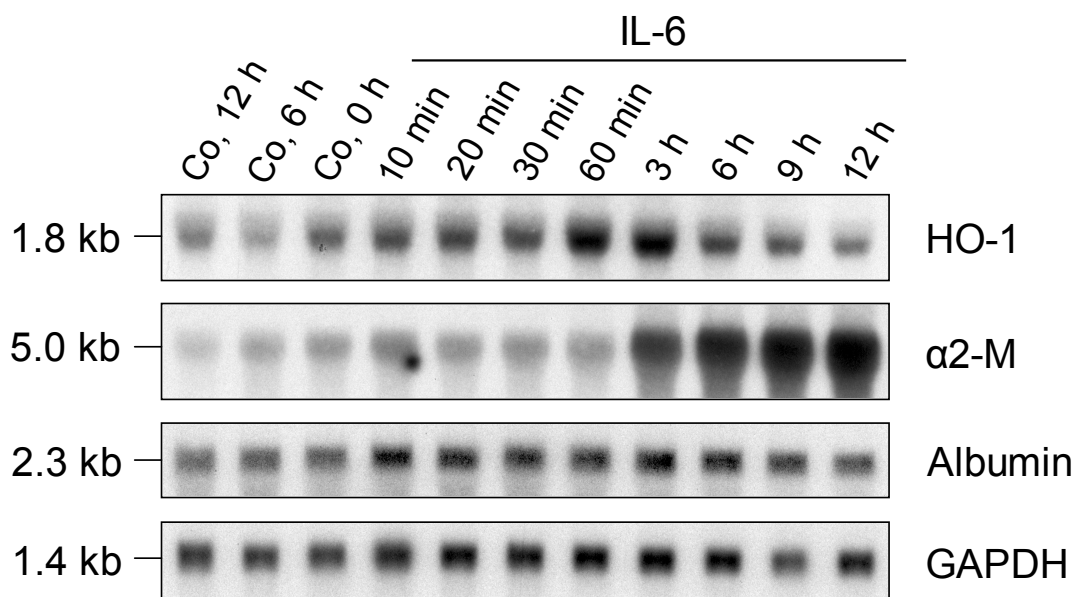


**Figure 20. Time course of IL-6 induced HO-1 mRNA expression in primary rat hepatocytes.** Rat hepatocytes were isolated, plated and cultured as described in Methods. After 18 h of cultivation under serum-free conditions, the medium was changed; the cells were incubated for 6 h, and afterwards cultured in the absence (Co) or the presence of IL-6 (500 ng/ml) for the time indicated. Total cytosolic RNA (5  $\mu$ g) from control and treated cells was subjected to Northern blot and sequentially hybridized with [ $^{32}$ P]-labeled cDNAs specific for HO-1,  $\alpha$ 2-macroglobulin ( $\alpha$ 2-M), albumin and a 28S rRNA specific oligonucleotide probe. The latter was used to control equal loading of RNA samples. The sizes of the transcripts (in kb) are indicated on the left. Data shown are representative of three independent experiments.

The strongest induction of HO-1 mRNA was observed 1-3 h after addition of IL-6 (Figure 20). Figure 20 further illustrates that the  $\alpha$ 2-macroglobulin mRNA up-regulation started already 3 h after stimulation of the cells with IL-6. Down-regulation of albumin transcripts in the cells incubated with IL-6 occurred after 12 h. In contrast to IL-6, HO-1 induction was significantly lower in IL-1 $\beta$ -stimulated rat hepatocytes (Figure 21) and negligible in TNF- $\alpha$ -treated cells (Figure 22).

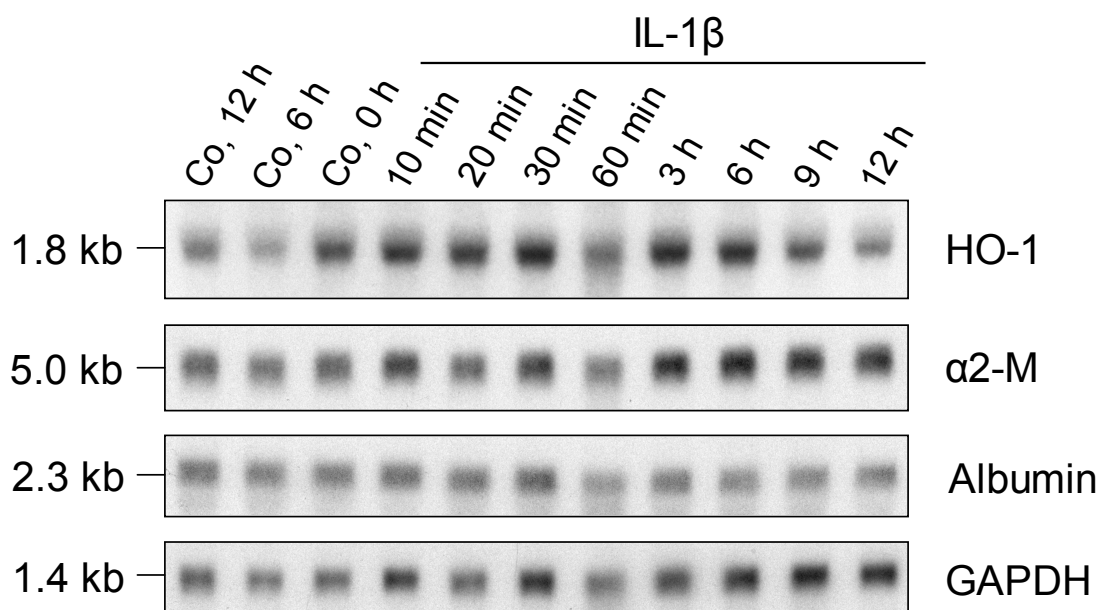


**Figure 21. Time course of IL-1 $\beta$  induced HO-1 mRNA expression in primary rat hepatocytes.** Rat hepatocytes were isolated, plated and cultured as described in Methods. After 18 h of cultivation under serum-free conditions, the medium was changed; the cells were incubated for 6 h, and afterwards cultured in the absence (Co) or the presence of IL-1 $\beta$  (500 ng/ml) for the time indicated. Total cytosolic RNA (5  $\mu$ g) from control and treated cells was subjected to Northern blot and sequentially hybridized with [ $^{32}$ P]-labeled cDNAs specific for HO-1,  $\alpha$ 2-macroglobulin ( $\alpha$ 2-M), albumin and a 28S rRNA specific oligonucleotide probe. The latter was used to control equal loading of RNA samples. The sizes of the transcripts (in kb) are indicated on the left. Data shown are representative of three independent experiments.

Hybridization with respective cDNAs did not show any relevant changes in the levels of  $\alpha$ 2-macroglobulin and albumin mRNA expression in primary rat hepatocytes after treatment with IL-1 $\beta$  or TNF- $\alpha$  (Figures 21, 22).

Taken together, the present data from the studies of HO-1 mRNA expression clearly demonstrate that among the proinflammatory cytokines used, IL-6 is the most potent inducer of HO-1 mRNA expression.

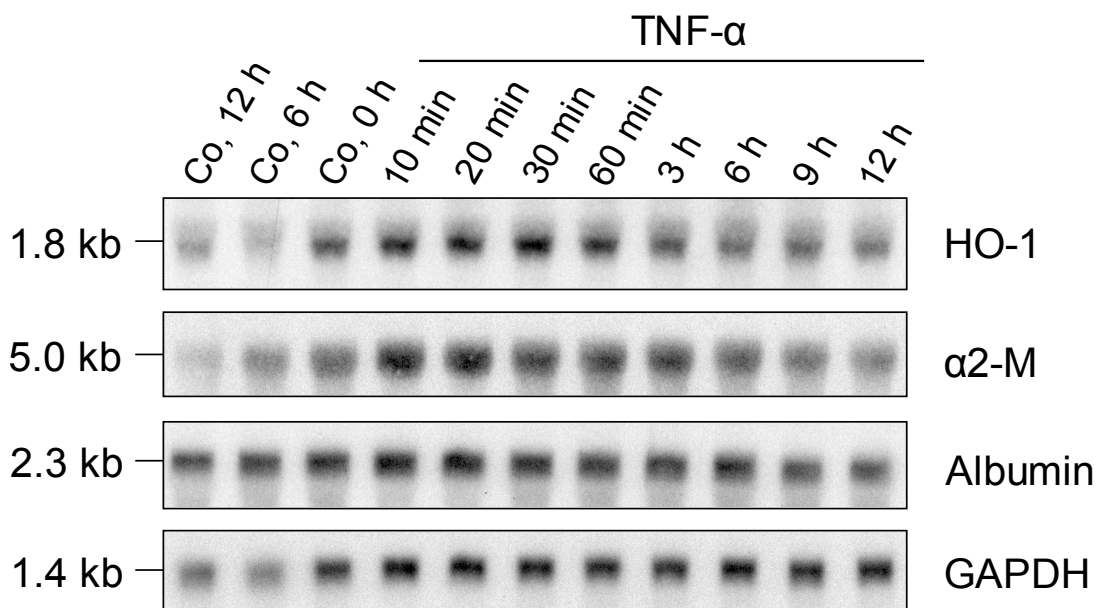


**Figure 22. Time course of TNF- $\alpha$  induced HO-1 mRNA expression in primary rat hepatocytes.** Rat hepatocytes were isolated, plated and cultured as described in Methods. After 18 h of cultivation under serum-free conditions, the medium was changed; the cells were incubated for 6 h, and afterwards cultured in the absence (Co) or the presence of TNF- $\alpha$  (50 ng/ml) for the time indicated. Total cytosolic RNA (5  $\mu$ g) from control and treated cells was subjected to Northern blot and sequentially hybridized with [ $^{32}$ P]-labeled cDNAs specific for HO-1,  $\alpha$ 2-macroglobulin ( $\alpha$ 2-M), albumin and a 28S rRNA specific oligonucleotide probe. The latter was used to control equal loading of RNA samples. The sizes of the transcripts (in kb) are indicated on the left. Data shown are representative of three independent experiments.

#### 4.2.2 Regulation of HO-1 mRNA and protein expression by IL-6 in primary rat hepatocytes

The previous experiments in primary cultures of rat hepatocytes have shown that HO-1 mRNA levels were markedly up-regulated in a dose- and time-dependent manner after treatment with IL-6. To elucidate whether IL-6-dependent HO-1 induction at the mRNA level was accompanied by changes at the protein level of HO-1 production, a new set of experiments in cultured rat hepatocytes was performed. Control and IL-6-stimulated cells were subjected in parallel to RNA and protein extraction followed by Northern and Western blot analyses, respectively. The relative induction levels of HO-1 mRNA and protein were assessed densitometrically and the values were plotted on the same graphs for better comparison.

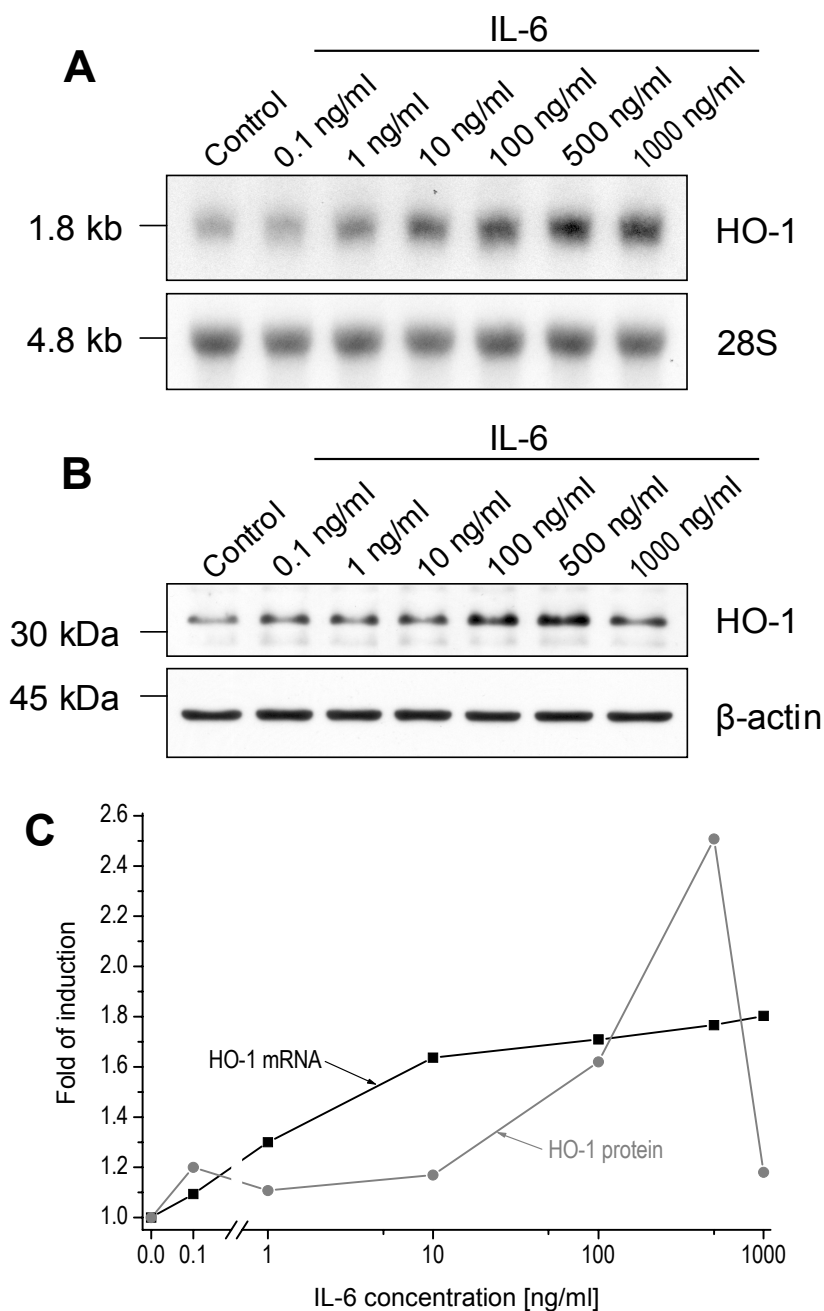


**Figure 23. Dose-dependent induction of HO-1 mRNA and protein expression by IL-6 in primary rat hepatocytes.** Rat hepatocytes were isolated, plated and cultured as described in Methods. After 18 h of cultivation under serum-free conditions, the medium was changed; the cells were incubated for 6 h, and afterwards cultured in the absence (Control) or the presence of increasing concentrations of IL-6 for 2 h (**A**) and 18 h (**B**). (**A**) Total cytosolic RNA (5  $\mu$ g) from control and treated cells was subjected to Northern blot and hybridized with [ $^{32}$ P]-labeled cDNA specific for HO-1. A 28S rRNA-specific oligonucleotide probe was used to control equal loading of RNA samples. The sizes of the transcripts (in kb) are indicated on the left. (**B**) The protein samples (15  $\mu$ g) from control and treated cells were immunoblotted and probed with a rabbit polyclonal anti-HO-1 antibody as described in Methods. Mouse monoclonal anti- $\beta$ -actin antibody was used to control equal loading of protein samples. The positions of molecular weight standards (in kDa) are indicated on the left. (**C**) The graphs represent a densitometric quantification of HO-1 mRNA (-■-) and protein (-●-) expression normalized for 28S rRNA or  $\beta$ -actin, respectively, and indicate fold of induction compared to control levels.

*Dose-dependent induction of HO-1 mRNA and protein expression by IL-6 in primary rat hepatocytes*

To define the most effective doses of the cytokine, considering both the protein and mRNA levels of subsequent HO-1 induction, treatment of primary rat hepatocytes with a broader concentration range (0.1-1000 ng/ml) was performed (Figure 23). Since HO-1 mRNA has a short half-life of 3 h (Dennerly, 2000) and in view of the fact that maximal HO-1 induction in primary hepatocytes occurred between 1 and 3 h after IL-6 stimulation (Figure 20), the cells were therefore incubated in the presence of different IL-6 concentrations for 2 h followed by subsequent RNA extraction and Northern blot hybridization. HO-1 protein has a much longer (15-21 h) half-life (Dennerly, 2000), and therefore rat hepatocytes were cultured either in the presence or absence of the indicated IL-6 concentrations for 18 h with subsequent protein extraction and Western blot analysis.

HO-1-specific transcripts in primary rat hepatocytes were markedly elevated in a dose-dependent manner, reaching maximal levels at a concentration of 500 ng/ml IL-6. HO-1 mRNA induction was about 1.8-fold compared to the unstimulated control (Figure 23A, C). The protein levels of HO-1 in hepatocytes were also dose-dependently increased after IL-6 treatment, reaching the maximum (about 2.5-fold compared to the control) at a concentration of 500 ng/ml (Figure 23B). It is notable that HO-1 protein expression dramatically declined at the IL-6 dose of 1000 ng/ml (Figure 23C), which could be due to a toxic effect of the high non-physiological dose of the cytokine.

Thus, the IL-6 dose of 500 ng/ml was considered to be appropriate for the stimulation of rat primary hepatocytes in further experiments.

*Time-dependent induction of HO-1 mRNA and protein expression by IL-6 in primary rat hepatocytes*

Primary rat hepatocytes were cultured either in the presence or absence of 500 ng/ml IL-6 for 0.5 h, 1 h, 2 h, 4 h, 6 h, 12 h, and 24 h. As revealed by Northern blot analysis, HO-1-specific mRNA was rapidly up-regulated already 1 h after treatment and reached an about 1.6-fold increase (the peak of up-regulation) compared to the respective control 2 h after treatment of primary rat hepatocytes with IL-6; thereupon the relative induction of the mRNA declined and remained at lower levels up to 24 h (Figure 24A, C).



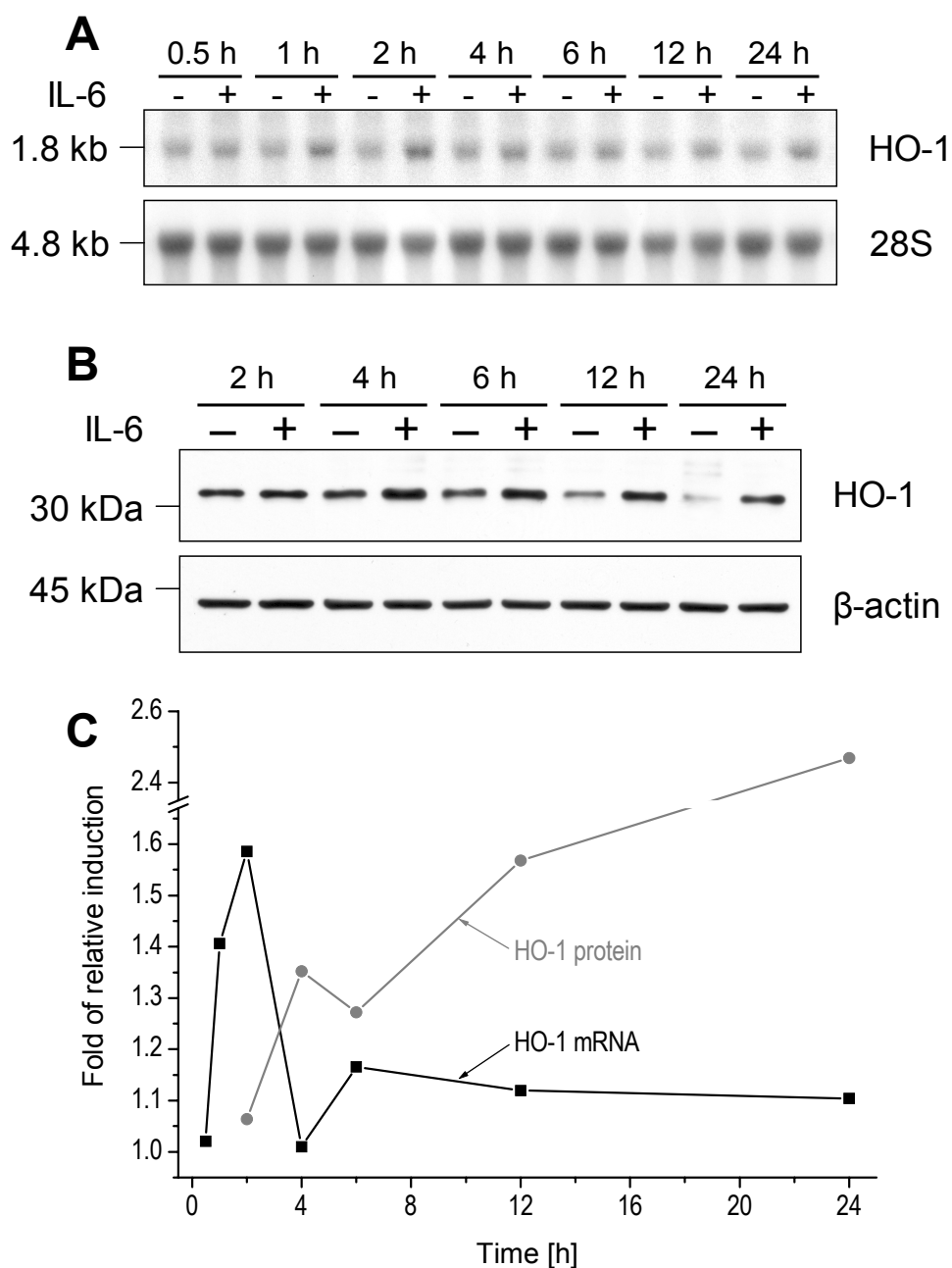


**Figure 24. Time course of IL-6-induced HO-1 mRNA and protein expression in primary rat hepatocytes.** Rat hepatocytes were isolated, plated and cultured as described in Methods. After 18 h of cultivation under serum-free conditions, the medium was changed; the cells were incubated for 6 h, and afterwards cultured in the presence of 500 ng/ml IL-6 for the time indicated. The respective controls for each time point were processed in parallel. **(A)** Total cytosolic RNA (5  $\mu$ g) from control and treated cells was subjected to Northern blot and hybridized with [ $^{32}$ P]-labeled cDNA specific for HO-1. A 28S rRNA-specific oligonucleotide probe was used to control equal loading of RNA samples. The sizes of the transcripts (in kb) are indicated on the left. **(B)** The protein samples (15  $\mu$ g) from control and treated cells were immunoblotted and probed with a rabbit polyclonal anti-HO-1 antibody as described in Methods. Mouse monoclonal anti- $\beta$ -actin antibody was used to control equal loading of protein samples. The positions of molecular weight standards (in kDa) are indicated on the left. **(C)** The graphs represent a densitometric quantification of HO-1 mRNA (■) and protein (●) expression and indicate fold of induction compared to the respective control levels.

The induction of HO-1 mRNA was accompanied by an increase of HO-1 protein (Figure 24B). The time-course of IL-6-dependent HO-1 protein induction in the cells under study appeared to be considerably different compared to that of HO-1 mRNA. Being up-regulated 2 h after stimulation with IL-6, relative levels of HO-1 protein remained elevated up to 24 h, reaching the maximal 2.5-fold induction, while the mRNA levels of HO-1 were already decreased (Figure 24C). That is in line with the previous *in vivo* experiment performed to study time-dependency of HO-1 induction at the mRNA and protein levels in rat liver after TO administration (Figure 11).

#### 4.2.3 Regulation of transfected HO-1 promoter luciferase gene constructs by IL-6 in primary rat hepatocytes

To further investigate the regulatory role of IL-6 in the HO-1 gene expression, primary cultures of rat hepatocytes were transiently transfected with luciferase gene constructs driven by various rat HO-1 promoter sequences and cultured in the presence or absence of IL-6.

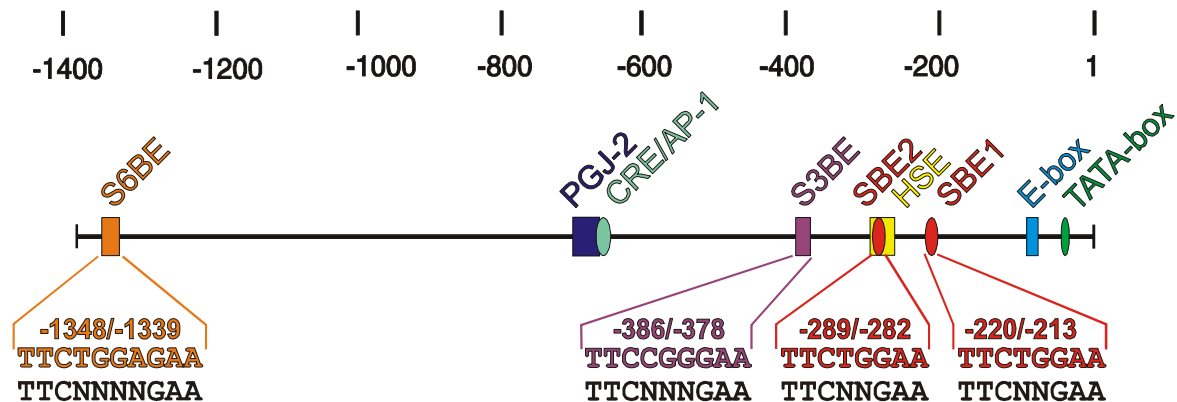


**Figure 25. Localization of putative IL-6 response elements within the rat HO-1 gene promoter.** The rat HO-1 gene promoter with the putative IL-6 response element is shown up to -1387 bp. TATA-box element; E-box, enhancer box element; HSE, heat shock response element; CRE/AP-1, cAMP response element / activator protein-1 binding site; PGJ-2, prostaglandin J<sub>2</sub> response element; SBE1, signal transducers and activators of transcription (STAT) binding element 1; SBE2, STAT binding element 2; S3BE, STAT3-like binding element; S6BE, STAT6-like binding element. Sequences of the putative STAT binding elements end their exact positions are indicated in colors. The consensus matching the respective found sequences are shown underneath in black. The promoter length is indexed on top by negative numbers in bp, starting from the transcription initiation site.

### *Sequence analysis of the rat HO-1 promoter*

To determine the sequences that might be involved in the regulation of HO-1 gene expression by IL-6 in rats, the rat HO-1 promoter sequence (Muller et al., 1987) was analyzed for similarities with the signal transducers and activators of transcription (STAT)-binding sites, well known IL-6 response elements (IL-6-RE) matching the general consensus TTC(N)<sub>2-4</sub>GAA (Seidel et al., 1995).

The sequence analysis revealed the presence of four putative binding sites for STAT transcription factors within the 1387 bp of the rat HO-1 promoter (Figure 25). The first and the second identical sequences [STAT binding element (SBE) 1, -220/-213 and SBE2, -289/-282; 5'-TTCTGGAA-3'] completely match the IL-6-RE of the murine SAA3 gene (Hattori et al., 1990) which was later shown to be bound by STAT complexes (Seidel et al., 1995).

The third motif [STAT3-like binding element (S3BE), -386/-378, 5'-TTCCGGGAA-3'] completely matches the known generalized STAT consensus sequence (Darnell, Jr., 1997; Lee et al., 2000).

The fourth found sequence [STAT6-like binding element (S6BE), -1348/-1339, 5'-TTCTGGAGAA-3'] matches a general sequence [TTC(N)<sub>4</sub>GAA] bound by STAT6 (Darnell, Jr., 1997), which is involved in IL-4 signalling (Mikita et al., 1996).

Among these four putative STAT binding sites, S3BE is of potential interest. It has been shown that activated STAT3 complexes preferentially bind to TTCN<sub>3</sub>NGAA motifs that are present in the promoter regions of APP genes (Horvath et al., 1995; Heinrich et al., 1998; Lemmink et al., 2001). Moreover, since STAT3 was reported to be activated by IL-6 in a murine model of TO-induced localized inflammation (Alonzi et al., 1998), an involvement of STAT3 in the regulation of HO-1 gene expression was further studied using an HO-1 promoter reporter gene assay.

Furthermore, in addition to JAK/STAT pathway, MAPK activation is also involved in IL-6 signalling (Heinrich et al., 2003). Since an AP-1 binding site was shown to be functionally active in the MAPK-dependent induction of rat HO-1 by arsenite (Kietzmann et al., 2003), the role of the AP-1 binding site in IL-6-dependent HO-1 gene regulation was also investigated.

### *Induction of the rat HO-1 promoter controlled luciferase expression in primary rat hepatocytes by IL-6 treatment*

To assess the transfection efficiency of primary rat hepatocytes, a reporter vector pcDNA3.1-GFP containing the GFP gene was used. The freshly isolated

hepatocytes were transiently transfected with the plasmid pcDNA3.1-GFP using the calcium phosphate precipitation method.

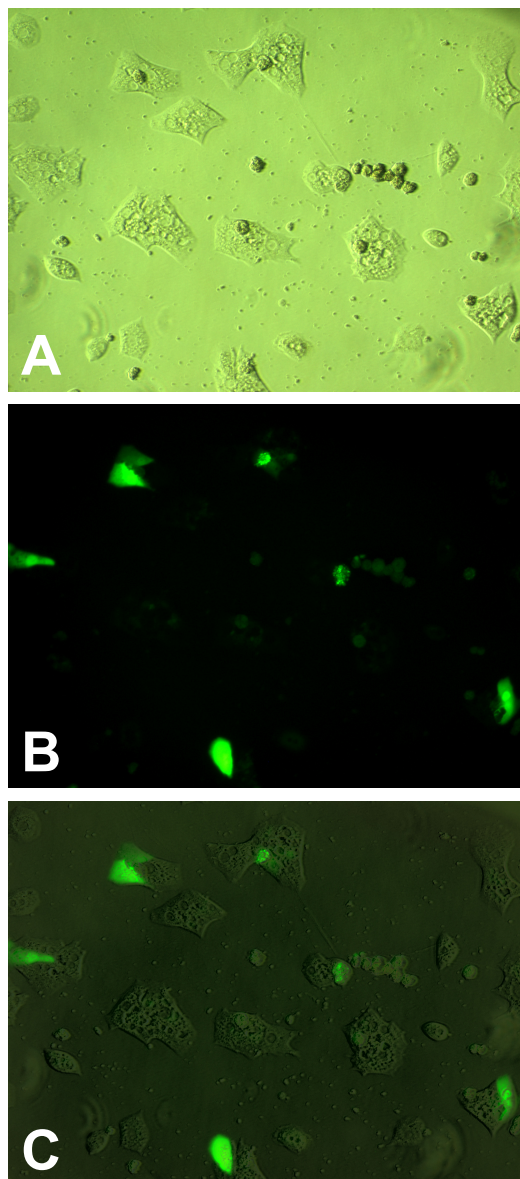


**Figure 26. Verification of transfection efficiency in primary rat hepatocytes by fluorescent microscopy using a GFP-reporter.** Freshly isolated rat hepatocytes were transiently transfected with the pcDNA3.1-GFP reporter vector containing the green fluorescent protein (GFP) gene using the calcium phosphate precipitation method. The cells were washed 5 h after transfection and incubated in serum-free medium for 24 h to allow GFP synthesis. Panel (A) represents the phase-contrast microscopy of the hepatocytes in culture; panel (B) demonstrates blue-light (470 nm filter)-stimulated GFP fluorescence in successfully transfected hepatocytes from the same view. Panel (C) represents image (B) merged with image (A) to evaluate the transfection efficiency.

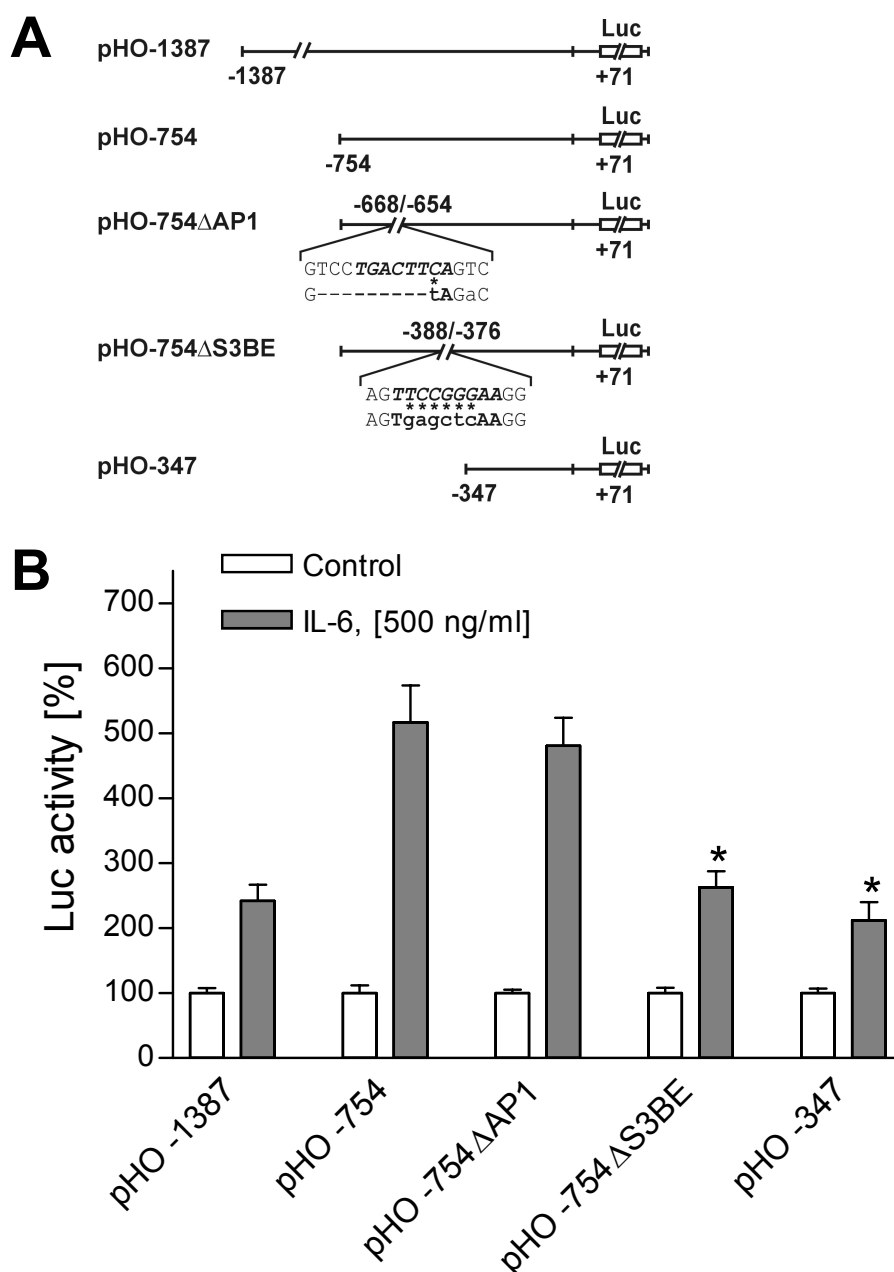


**Figure 27. Induction of the rat HO-1 promoter controlled luciferase gene expression in primary rat hepatocytes treated with IL-6.** (A) Freshly isolated rat hepatocytes were transiently transfected with luciferase (Luc) gene constructs driven by wild-type 1387, 754, and 347 bp of the rat HO-1 promoter (pHO-1387, pHO-754, and pHO-347) or the 754-bp promoter mutated at the CRE/AP-1 site (pHO-754 $\Delta$ AP1) or at the STAT3 site (pHO-754 $\Delta$ S3BE). In pHO-754 $\Delta$ AP1 and pHO-754 $\Delta$ S3BE, the wild-type HO-1 promoter sequence is shown on the upper strand, and the mutated sequence is shown on the lower strand: deleted bases are indicated by “-“, mutated bases are shown in lowercase letters and indicated by asterisks. (B) The cells were washed 5 h after transfection and further cultured under serum-free conditions. After 18 h of cultivation under serum-free conditions, the medium was changed; the cells were incubated for 6 h, and afterwards cultured in the absence (Control) or the presence of IL-6 (500 ng/ml) for 24 h. In each experiment, the percentage of Luc activity was determined relative to the pHO-1387, pHO-754, pHO-347, pHO-754 $\Delta$ AP1, or pHO-754 $\Delta$ S3BE controls, which were set equal to 100%. The values represent means  $\pm$  SEM of three independent experiments. Statistics, Student’s t-test for paired values: \*, significant difference pHO-754 $\Delta$ S3BE vs. pHO-754 and pHO-347 vs. pHO-754,  $p < 0.05$ .

After 24 h, the cells were monitored using phase-contrast and sequential fluorescent microscopy (Figure 26A, B). The transfection efficiency was evaluated from three independent experiments (10 randomly chosen views of each) using overlapped pictures obtained by phase-contrast and fluorescent microscopy from the same field of view (Figure 26C) and comprised about 30%.

To examine the molecular mechanism of HO-1 gene regulation by IL-6, primary rat hepatocytes were transfected with constructs containing 1387, 754 and 347 bp of the wild-type rat HO-1 promoter in front of the luciferase (Luc) gene (pHO-1387, pHO-754 and pHO-347, respectively). The Luc expression from pHO-1387 was up-regulated following IL-6 treatment to 242% (Figure 27). Surprisingly, when the cells were transfected with pHO-754, the IL-6-dependent induction of Luc expression comprised 517%, which was more than 2 times higher compared to pHO-1387. This might imply the presence of negative regulatory elements in the upstream region between -754 and -1387. Further, the Luc activity in pHO-347 transfected hepatocytes was induced only to 212% after IL-6 treatment, suggesting that the promoter region between -347 and -754 nucleotides is responsible for the IL-6-directed up-regulation of the rat HO-1 gene.

To investigate the functional role of the potential STAT binding site S3BE in the regulation of HO-1 gene expression by IL-6, primary rat hepatocytes were transfected with the construct pHO-754 $\Delta$ S3BE, in which 6 out of 9 bp of the motif were mutated. In rat primary hepatocytes transfected with pHO-754 $\Delta$ S3BE, the Luc activity increased only to about 262%, which was close to pHO-347 and significantly lower compared to pHO-754 (Figure 27).

In order to examine the functional activity of the AP-1 binding site in IL-6 signalling, primary rat hepatocytes were transfected with the construct pHO-754 $\Delta$ AP1, in which the whole AP-1 binding sequence was deleted (Immenschuh et al., 1998). IL-6 treatment up-regulated Luc activity in pHO-754 $\Delta$ AP1-transfected cells to 481% that was not significantly different from IL-6-dependent pHO-754 Luc induction (Figure 27).

Taken together, these results indicate that activation of the STAT pathway by IL-6 may induce the rat HO-1 gene expression mainly through the S3BE sequence in the promoter of this gene, whereas the AP-1 binding site most likely is not involved in IL-6-dependent HO-1 induction.

## 5. Discussion

The present study showed that during the acute phase reaction induced by turpentine oil injection in rats, HO-1 expression is dramatically up-regulated in the liver, the major target organ of the inflammatory response, and in the injected muscle, the site of localized inflammation. In the other internal organs investigated, only moderate changes of HO-1 expression under inflammatory conditions were observed. As revealed by immunohistochemical analysis, the induction of HO-1 in the liver was attributed mainly to hepatocytes, whereas macrophages represented the major source of HO-1 in the injured muscle. Interleukin-6 mRNA expression was found exclusively in the inflamed muscle, but its plasma level profile correlated with HO-1 mRNA and protein induction in the liver, suggesting that this cytokine plays a role in HO-1-induction. Experiments *in vitro* further supported this idea. Among the proinflammatory cytokines (IL-6, IL-1 $\beta$ , and TNF- $\alpha$ ) used for the treatment of primary cultured rat hepatocytes, IL-6 was the most potent inducer of HO-1 expression. Moreover, functional analysis of the rat HO-1 promoter revealed the presence of an active IL-6-response element (STAT binding sequence) which is involved in IL-6-dependent HO-1 gene regulation during the acute phase response.

### 5.1 Regulation of HO-1 expression in turpentine oil (TO) model of the acute phase response (APR) in rats

In the current study, TO injection in rats was used as a means to induce an APR and to investigate HO-1 regulation. The results indicate that HO-1 mRNA expression was dramatically increased in the liver by 4-6 h after TO administration with a peak at 6 h (Figure 11A). Previously, hepatic HO-1 mRNA expression in a TO model was studied by Lyoumi and colleagues (Lyoumi et al., 1998a; Lyoumi et al., 1999) along with an LPS-induced model of the APR. Using RT-PCR, they also have shown that in the liver, HO-1 specific transcripts were maximally elevated 6 h after TO administration, however, no information was provided about the protein. In the present study, not only HO-1 mRNA expression but also HO-1 protein levels were investigated. HO-1 protein was markedly up-regulated after 6 h and reached a maximum 24 h after TO injection (Figure 11B).

To find out whether the induction of HO-1 during inflammation is a liver-specific cytokine-mediated direct consequence of the APR, in the current study, in addition to the liver, extrahepatic sites of HO-1 induction were investigated for the first time. Besides the liver, which is the main target organ for the APR, the most prominent HO-1 mRNA induction occurred in skeletal muscle, where the APR was initiated by TO injection (Figure 12). In the other internal organs investigated, only moderate changes in HO-1 expression were observed (Figure 12).

It should be noted that in spite of the similarities in general signs and symptoms, different *in vivo* models of the APR are characterized by certain patterns of mediators and plasma proteins released in the course of inflammation (Fattori et al., 1994; Ramadori and Christ, 1999). For instance, an LPS model is characterized by rapid circulatory increase of the three major proinflammatory cytokines like IL-6, IL-1 $\beta$ , and TNF- $\alpha$ , causing systemic inflammation (Ulich et al., 1990; Ulich et al., 1991; Luster et al., 1994). The variety of mediators in this model makes difficult to define the role of individual cytokines in the induction of certain proteins, particularly, HO-1 in the liver. The significant advantage of TO injection over the other models of the APR implicates the circulatory increase of only one major cytokine, IL-6, whereas no increase in plasma IL-1 $\beta$  or TNF- $\alpha$  bioactivity is detected (Luheshi et al., 1997). Therefore, to investigate the IL-6 expression in the TO-induced APR was another aim of the present study.

## **5.2 Expression of IL-6 after turpentine oil (TO) administration and its possible role in HO-1 induction in the liver**

In agreement with previous observations of other groups (Luheshi et al., 1997; Tsujinaka et al., 1997; Lyoumi et al., 1998b), we demonstrated that serum IL-6 concentrations were extremely elevated after TO-injection (Figure 18). In order to find the source of IL-6 released during TO-induced APR, we studied IL-6 mRNA expression in various rat tissues. Our data have clearly demonstrated that during TO-induced APR, injured skeletal muscle was the only organ where induction of IL-6 expression was observed (Figure 17). Moreover, temporal expression of IL-6 in the muscle well correlated with circulatory IL-6 levels (Figure 18). Taking into consideration all these findings, we hypothesized that HO-1 induction observed in the livers of TO-treated rats (Figure 11) might be mediated by IL-6 as it has been



shown for other positive acute phase reactants, e. g.,  $\alpha$ 2-macroglobulin in rats (Geiger et al., 1988).

Interleukin (IL)-6 has been shown to be a potent inducer of acute phase protein synthesis *in vitro* as well as *in vivo* (Geiger et al., 1988; Castell et al., 1989; Castell et al., 1990; Heinrich et al., 1990). The pivotal role of IL-6 as a major mediator of the acute phase response (APR) in the liver was unequivocally determined after generation of IL-6-deficient mice (Poli et al., 1994). It has been shown that in the absence of IL-6, mice are unable to develop a normal inflammatory response to localized tissue damage generated by turpentine oil injection (Fattori et al., 1994; Siewert et al., 2000). Moreover, it was also reported that IL-6, but not other members of its superfamily, is primarily in charge of the hepatic APR associated with TO-induced myositis (Kaibara et al., 1998).

Remarkably, IL-6 specific transcripts appeared in the skeletal muscle 2 h after TO injection (Figure 17), whereas induction of HO-1 mRNA expression in the liver was observed 4-6 h after TO administration (Figure 71A). It should be also noted that serum IL-6 levels were already elevated by 2 h after administration of TO (Figure 18). Taken together, these data suggest that induction of HO-1 expression in the liver during APR is a consequence of the increased plasma levels of IL-6 that followed its expression at the site of inflammation. Moreover, expression profile of HO-1 in the injected muscle (Figure 12) was similar to that of IL-6 (Figure 17). Thus, a possible relationship between up-regulation of these two genes could be the subject of further investigations.

Interestingly, the serum IL-6 levels were still high 12 h after TO injection (Figure 18), while HO-1 mRNA levels in the liver were already decreased (Figure 11A). This phenomenon might be explained by the known fact that IL-6 induces down-regulation of its cognate receptor, IL-6R, *in vitro* (Hoffmann et al., 1994). Moreover, it has been demonstrated that IL-6R mRNA expression in the rat liver markedly decreased by 6-12 h after TO administration (Geisterfer et al., 1993). Therefore, it is likely that dramatic increase of IL-6 levels observed in TO-induced APR model subsequently leads to down-regulation of the IL-6R, thus abolishing the action of IL-6 in the liver when it is not required any more. It should also be noted that HO-1 mRNA has a short half-life of 3 h, whereas the protein has a much longer half-life period of 15-21 h (Srivastava et al., 1993), which is in accordance with our data (Figure 11B).

Further, in another study with TNF- $\alpha$ -knockout mice, it was concluded that TNF- $\alpha$  is a major candidate to trigger HO-1 induction in response to LPS stimulation (Oguro et al., 2002). However, that study also contains indirect evidence for possible involvement of IL-6 in the LPS-dependent induction of HO-1 mRNA in the liver. They demonstrated that in TNF- $\alpha$ -deficient mice, which were unable to respond to LPS treatment with hepatic HO-1 induction, serum IL-6 levels were considerably lower compared to wild-type mice (Oguro et al., 2002).

Thus, IL-6 is most likely a principle inducer of hepatic HO-1 expression under inflammatory conditions, particularly in the TO-induced acute phase response model.

### **5.3 Cell type specificity of HO-1 induction and its possible role in turpentine oil (TO)-induced acute phase response (APR)**

To elucidate which cell types are responsible for the TO-induced HO-1 expression in the injured muscle and in the liver, immunohistochemical analysis of these organs was performed. It has been demonstrated that within injured skeletal muscle, synthesis of HO-1 occurred mainly in the cells positive for ED1, a known marker of monocytes and macrophages, whereas muscle fibers were HO-1 negative (Figure 16). These findings are consistent with data obtained by Kampfer and colleagues, who demonstrated that infiltrated macrophages are the major source of HO-1 at the wound site in the mouse excisional model of skin repair (Kampfer et al., 2001). Based on their *in vitro* data, the authors assumed involvement of HO-1 in the regulation of macrophage-derived cytokine release (Kampfer et al., 2001). Indeed, numerous recent observations indicate a potential role of HO-1 in the down-regulation of proinflammatory cytokine expression at the site of inflammation in various model systems (Tamion et al., 2001; Tullius et al., 2002; Vicente et al., 2003; Ohta et al., 2003; Song et al., 2003a). It has been also shown, that HO-1 might provide an anti-inflammatory action *in vivo* through the down-modulation of cell adhesion molecules (Wagener et al., 2001; Soares et al., 2004), thus inhibiting leukocyte infiltration (Bussolati et al., 2004), and via promotion of non-inflammatory angiogenesis, facilitating tissue repair (Bussolati et al., 2004). Moreover, an increased leukocyte adhesion to the vessel wall and spontaneous perivascular infiltration of leukocytes in various tissues of HO-1 deficient mice has been reported before (Poss and Tonegawa, 1997).

Considering all these data and the results of the current study demonstrating that the levels of IL-6 mRNA in injured muscle were already declined, whereas HO-1 mRNA expression was still up-regulated (Figures 12 and 17), we can also speculate here about the role of HO-1 in resolution of TO-induced localized inflammation and muscular tissue repair.

Although hepatic HO-1 production under physiological and some pathological conditions is ascribed mainly to Kupffer cells, the resident liver tissue macrophages (Goda et al., 1998; Bauer et al., 1998; Kiemer et al., 2003; Song et al., 2003b), there is evidence that HO-1 could be also up-regulated under certain conditions in hepatocytes, as has been shown *in vivo* by several groups (Bauer et al., 1998; Fernandez and Bonkovsky, 1999; Bauer et al., 2003; Mostert et al., 2003).

Immunohistochemical analysis of normal rat liver carried out in the present study revealed that expression of HO-1 was attributed predominantly to Kupffer cells (Figure 14A, C), which is in compliance with the observations of other groups (Goda et al., 1998; Bauer et al., 1998). However, the dramatic induction of HO-1 immunoreactivity in the liver parenchyma after TO administration has been shown for the first time (Figure 14B). This suggests that during the inflammatory response to localized tissue injury, hepatocytes are the major source of increased HO-1 mRNA and protein expression levels observed in the livers of TO-treated rats (Figure 11).

The data regarding muscle- and liver-specific HO-1 induction in TO model of the APR might be of physiological importance, since the products of HO-1 reaction have been shown to be involved in a wide variety of cytoprotective, particularly anti-inflammatory mechanisms. Carbon monoxide (CO) regulates blood vessel tone (Morita and Kourembanas, 1995), prevents platelet activation and aggregation (Brune and Ullrich, 1987), suppresses the pro-inflammatory cytokine production and promotes increased interleukin (IL)-10 expression by macrophages both *in vitro* and *in vivo* (Otterbein et al., 2000). Moreover, CO mediates the anti-inflammatory effects of IL-10 (Lee and Chau, 2002). It was also reported that CO prevented apoptosis in several cell types, including endothelial cells, fibroblasts and hepatocytes (Otterbein et al., 2003). Biliverdin and its reduced product bilirubin both are potent antioxidants and may protect cells from oxidative injury by scavenging reactive oxygen species (Stocker et al., 1987). Biliverdin has also

been shown to inhibit human complement *in vitro* (Nakagami et al., 1993). Bilirubin provided a protective effect on the transplanted liver grafts via inhibition of lipid peroxidation in hepatocytes (Kato et al., 2003). Although reduced iron ( $\text{Fe}^{2+}$ ), released by HO-1 from the core of the heme molecule, is a potent prooxidant, the potential catalysis of oxidative reactions by this compound is limited through its chelation by iron-sequestering protein ferritin as well as via its active removal from the cell by the specific Fe-ATPase pump (Ferris et al., 1999). Both these mechanisms are potentiated by increased intracellular pool of free iron following increased HO-1 expression (Eisenstein et al., 1991; Baranano et al., 2000) and could protect the cells from apoptosis (Ferris et al., 1999; Yang et al., 2002).

Despite a number of data accumulated, the precise role of HO-1 in the APR remains to be fully defined. For instance, it has been shown that in re-oxygenated rat peritoneal macrophages, CO promoted inflammation through cGMP-dependent pathway, stimulating IL-6 and TNF- $\alpha$  synthesis (Tamion et al., 1999). On the other hand, CO was shown to mediate anti-inflammatory effects of HO-1 via MAPK activation both *in vitro*, in macrophage cell line, and *in vivo*, in LPS-induced mouse APR model (Otterbein et al., 2000). Therefore, considering these studies and based on our data concerning the HO-1 and IL-6 induction in the injured muscle and liver, we could speculate that HO-1 has a regulatory function in the APR, promoting the induction of pro-inflammatory cytokine synthesis in macrophages to trigger the defense reaction of the organism and “switching off” the APR afterwards (down-regulation of pro-inflammatory and induction of anti-inflammatory cytokines) to avoid unfavorable consequences of chronic inflammation. At the same time under inflammatory conditions, HO-1 protects hepatocytes which could become damaged due to a number of toxic metabolites.

#### **5.4 Cytokine-dependent regulation of HO-1 in cultured hepatocytes**

*In vitro* studies of primary rat hepatocytes treated with proinflammatory cytokines (Figures 19, 20, 21, 22) further confirmed the statement that IL-6 is a major regulator of acute phase protein synthesis in hepatocytes (Castell et al., 1989; Castell et al., 1990; Ramadori and Christ, 1999). Indeed, the most prominent induction of  $\alpha 2$ -macroglobulin transcript levels and the down-regulation of albumin

mRNA expression occurred in primary rat hepatocytes treated with IL-6 in both time- and dose-dependent experiments (Figures 19A and 20), whereas other proinflammatory cytokines (IL-1 $\beta$  and TNF- $\alpha$ ) had significantly lower effects on the regulation of these acute phase proteins (Figures 19B, C, 21, 22). These observations are consistent with early data reported by Andus and co-workers. They demonstrated that in primary rat hepatocytes treated with human recombinant proinflammatory cytokines, IL-6 was 27 times more potent inducer of  $\alpha$ 2-macroglobulin synthesis compared to IL-1 $\beta$  (Andus et al., 1988). Interestingly, in primary rat hepatocytes, HO-1 mRNA expression was also induced by IL-6 to a higher extent compared to other cytokines used (Figures 19A and 20).

In addition to our data obtained in primary rat hepatocytes, there is also early evidence that HO-1 is a positive acute phase reactant in a human liver-derived cell line (Mitani et al., 1992). They showed that HO-1 mRNA was time- and dose-dependently accumulated in Hep3B cells after IL-6 treatment; this accumulation of HO was essentially abolished by simultaneous treatment of the cells with actinomycin D, suggesting that the induction occurs at the transcriptional level (Mitani et al., 1992). In our study, in addition to mRNA, protein levels of IL-6-induced HO-1 expression in primary rat hepatocytes were analyzed (Figures 23B and 24B). Remarkably, HO-1 mRNA expression was up-regulated within a whole range of IL-6 concentrations used in the dose-dependent experiment, whereas HO-1 protein levels were significantly declined at the high doses of IL-6, which could be explained by the toxic effect of IL-6 at the high concentration (Figure 23C). Time-course of HO-1 mRNA expression in primary rat hepatocytes treated with IL-6 was considerably different from that of HO-1 protein (Figure 24C). Being rapidly elevated 2 h after IL-6 application, the mRNA levels of HO-1 were already declined 4 h post IL-6 treatment, whereas the relative levels of HO-1 protein remained elevated at all time points assayed (Figure 24C). This shift between the kinetics of HO-1 mRNA and protein synthesis may be explained by the different half-lives of HO-1 transcripts (3 h) and protein (15-21 h), which correlates well with our *in vivo* data (Figure 11). In this regard, it should be noted that use of primary cell cultures has an advantage over the cell lines, since they are more close to the *in vivo* conditions. Thus, the regulation of HO-1 by different proinflammatory cytokines can vary depending on the cell type examined. For instance, in non-transformed human endothelial cells, HO-1 was significantly induced by TNF- $\alpha$

and IL-1 $\alpha$ , but not by IL-6 (Terry et al., 1998), whereas in human umbilical vein endothelial cells (HUVEC cell line), treatment with TNF- $\alpha$  and LPS did not significantly induce HO-1 expression (Kronke et al., 2003).

Thus, based on our *in vitro* data, the induction of HO-1 mRNA and protein levels might be considered as an event associated with the APR and supports the role of HO-1 as an intracellular positive acute phase protein *in vivo*.

## **5.5 Molecular mechanisms of HO-1 regulation under inflammatory conditions**

The sequences of HO-1 gene 5'-flanking regions from four animal species (human, mouse, rat, and chicken) are known to date (Choi and Alam, 1996; Elbirt and Bonkovsky, 1999). Among them, the rat HO-1 gene promoter region is poorly investigated. Only four functional response elements of the rat HO-1 promoter have been characterized (Figure 2).

The JAK/STAT pathway was found to be the major signalling pathway induced by the principle mediator of the APR, IL-6, which signals via the activation of Janus kinases (JAKs) and transcription factors of the STAT family (Heinrich et al., 1998). Since we have shown that IL-6 up-regulates HO-1 mRNA and protein expression in primary rat hepatocytes (Figures 23 and 24), it was of interest to analyse the known sequence of the rat HO-1 promoter for the presence of putative STAT-binding sites (Figure 25). As early as in 1992, Mitani and colleagues discovered in the human HO-1 promoter the motif 5'-TTCTGGGAC-3' (nucleotide residues -373 to -365), sharing a significant homology with the consensus sequence found in many acute phase protein genes (Mitani et al., 1992). This consensus [TTC(N)<sub>3</sub>GAA] was later referred to as STAT binding site (Heinrich et al., 1998). This putative STAT binding site in the 5'-flanking region of human HO-1 was shown to be functional, as revealed by electrophoretic mobility shift assay (EMSA) using specific oligonucleotides (Mitani et al., 1992).

Among the putative STAT binding sites found by analysis of the rat HO-1 promoter, S3BE (STAT3-like binding element, -386/-378, 5'-TTCCGGGAA-3') that completely matches the known generalized STAT consensus sequence (Darnell, Jr., 1997; Lee et al., 2000) was considered as the most promising candidate to bind activated STAT3 (Figure 25). In turn, the pivotal role of STAT3 in transduction of the IL-6 signal was demonstrated using IL-6-deficient mice (Alonzi et al., 1998).

Furthermore, the sequence and position of S3BE in the rat HO-1 promoter is much similar to that of IL-6 response element reported by Mitani and colleagues in the promoter region of the human HO-1 gene (Mitani et al., 1992).

The functional role of the potential STAT binding site S3BE in the regulation of the rat HO-1 gene expression by IL-6 has been clearly demonstrated in the current study by means of a luciferase (Luc) reporter gene assay (Figure 27). The induction of the Luc activity measured after IL-6 treatment in primary rat hepatocytes transfected with S3BE-mutated (pHO-754 $\Delta$ S3BE) or S3BE-deleted (pHO-347) HO-1 promoter luciferase gene constructs was almost 2 times less potent compared to that in the hepatocytes transfected with the wild-type (pHO-754) rat HO-1 promoter construct (Figure 27).

In addition, functional analysis of the mouse HO-1 gene 5'-flanking region has identified a sequence motif, 5'-TTCCGGGAA-3', that conforms to the consensus IL-6-response element [TTC(N)<sub>3</sub>GAA], i. e. STAT binding site. Interestingly, transcriptional activation of the mouse HO-1 gene by IL-6 required cooperation between the 5'-distal enhancer with an AP-1 binding site and the proximal promoter enclosing the STAT binding site (Choi and Alam, 1996; Lee et al., 2000). However, in the present study, the induction of the Luc activity measured after IL-6 treatment in primary rat hepatocytes transfected with the construct pHO-754 $\Delta$ AP1, where the whole AP-1 binding sequence was deleted (Immenschuh et al., 1998), was not significantly different from that in the hepatocytes transfected with the wild-type pHO-754 construct (Figure 27). This suggests that cooperation between AP-1 and S3BE is not important for the IL-6-dependent induction of HO-1 gene in rats.

It should be noted that IL-6-dependent induction of Luc expression from pHO-754 $\Delta$ S3BE as well as pHO-347 was not completely abolished compared to the wild-type pHO-754 construct (Figure 27), indicating the potential role of SBE1 and/or SBE2 putative STAT binding sequences in IL-6-mediated HO-1 gene regulation (Figure 25). Indeed, these two identical motifs (TTCTGGAA, -289/-282 and -220/-213) completely match the IL-6-response element of the murine SAA3 gene (Hattori et al., 1990) which, as was shown later, is bound by STAT complexes (Seidel et al., 1995). Therefore, it is of interest to further investigate the roles of these two putative STAT binding sites in the regulation of rat HO-1 gene by IL-6.

Notably, following IL-6 treatment of primary rat hepatocytes, the Luc expression in the pHO-1387-transfected cells was up-regulated to a considerably lesser extent compared to the cells transfected with pHO-754 (Figure 27). This might be explained by the presence of negative regulatory elements in the upstream region between -754 and -1387. Indeed, the promoter analysis of the rat HO-1 gene revealed the presence of several putative glucocorticoid response elements (GREs) in this region (data not shown). Moreover, negative regulation of rat HO-1 gene by glucocorticoids was reported (Cantoni et al., 1991) and functional GRE in the human HO-1 promoter was identified (Lavrovsky et al., 1996; Deramaudt et al., 1999). Since the pituitary-adrenal axis is activated during the acute phase response (Ramadori and Christ, 1999), further investigations are required to elucidate the role of the putative GREs in the HO-1 gene regulation under inflammatory conditions. The lower Luc expression from pHO-1387 compared to pHO-754 might be also due to the presence of the putative STAT6 binding element (S6BE) in the longer HO-1 promoter construct (Figure 25), which may be involved in IL-4 signalling (Mikita et al., 1996). IL-4, in turn, was demonstrated to exert anti-inflammatory function by the inhibition of acute phase protein production *in vitro* (Loyer et al., 1993).

In summary, the results presented here clearly indicate that activation of the STAT pathway by IL-6 induces the rat HO-1 gene expression mainly through the S3BE sequence in the promoter of this gene.

## **5.6 Conclusions and future directions**

The present study has demonstrated that during turpentine oil-induced localized inflammation in rats, the expression of HO-1 was strongly up-regulated in injured muscle, the initiating site of the acute phase reaction, and in the liver, the major source of serum acute phase proteins. In injured muscle, the induction of HO-1 was attributed to macrophages, whereas in the liver, hepatocytes were the major source of the elevated HO-1 levels during the acute phase response.

Studies in primary rat hepatocytes further underlined the pivotal role of IL-6 in the induction of HO-1 expression under inflammatory conditions. Sequence analysis of the rat HO-1 promoter revealed the presence of several putative binding sites for transcription factors of the STAT-family, the major transducers of IL-6 signalling. Furthermore, the functional analysis of the rat HO-1 promoter by means of



luciferase reporter gene assay identified one of the putative STAT binding sites, S3BE, as an active element of the IL-6-dependent HO-1 gene regulation.

Taken together, these data indicate that HO-1 might be referred to as an intracellular positive acute phase protein that seems to play an important role in cytoprotection of hepatocytes via the products released in the heme breakdown reaction. Bilirubin is a potent antioxidant and could protect the cells against oxidative stress, carbon monoxide provides a vasodilatory effect improving hepatic microcirculation, and free iron induces synthesis of ferritin, an iron-sequestering protein with a potent protective function. Moreover, at the site of turpentine oil injection, up-regulation of HO-1 in macrophages could participate in the resolution of inflammation.

The work presented here could be the basis for the future investigations of the HO-1 gene regulation under inflammatory conditions. A functional analysis of two other putative STAT binding sites, SBE1 and SBE2, found in the rat HO-1 promoter sequence might be performed. Furthermore, the certain transcription factors from the STAT family (STAT1, STAT3, STAT5 homo- or heterodimers) that may bind to the found sequences, thus mediating IL-6-dependent HO-1 gene induction in rats, can be identified. Since IL-4 that signals via STAT6 is known to down-regulate expression of acute phase proteins, it might be of interest to investigate the involvement of S6BE, a putative binding site for STAT6, in the rat HO-1 gene regulation. The potential negative regulatory role of putative GREs found in the rat HO-1 promoter could be also elucidated.

Furthermore, to provide unequivocal evidence that induction of HO-1 *in vivo* occurs as a response to IL-6 produced at the site of inflammation, studies in IL-6 knockout mice could be carried out. The use of IL-6-receptor antagonists, neutralizing antibodies or recombinant IL-6 injection might be other approaches to further study IL-6-dependent HO-1 induction *in vivo*.

## References

1. **Alam J., Cai J., and Smith A.** Isolation and characterization of the mouse heme oxygenase-1 gene. Distal 5' sequences are required for induction by heme or heavy metals. *J.Biol.Chem.* 269: 1001-1009, **1994**.
2. **Alcaraz M.J., Fernandez P., and Guillen M.I.** Anti-inflammatory actions of the heme oxygenase-1 pathway. *Curr.Pharm.Des.* 9: 2541-2551, **2003**.
3. **Alonzi T., Fattori E., Cappelletti M., Ciliberto G., and Poli V.** Impaired Stat3 activation following localized inflammatory stimulus in IL-6-deficient mice. *Cytokine.* 10: 13-18, **1998**.
4. **Andus T., Geiger T., Klapproth J., Kunz D., Heisig M., Castell J., and Heinrich P.C.** Regulation of alpha 2-macroglobulin gene expression by interleukin-6 (BSF-2/HSF). *Tokai J.Exp.Clin.Med.* 13: 265-276, **1988**.
5. **Balla G., Jacob H.S., Balla J., Rosenberg M., Nath K., Apple F., Eaton J.W., and Vercellotti G.M.** Ferritin: a cytoprotective antioxidant strategem of endothelium. *J.Biol.Chem.* 267: 18148-18153, **1992**.
6. **Baranano D.E., Wolosker H., Bae B.I., Barrow R.K., Snyder S.H., and Ferris C.D.** A mammalian iron ATPase induced by iron. *J.Biol.Chem.* 275: 15166-15173, **2000**.
7. **Barbu V. and Dautry F.** Northern blot normalization with a 28S rRNA oligonucleotide probe. *Nucleic Acids Res.* 17: 7115- **1989**.
8. **Bauer I., Rensing H., Florax A., Ulrich C., Pistorius G., Redl H., and Bauer M.** Expression pattern and regulation of heme oxygenase-1/heat shock protein 32 in human liver cells. *Shock.* 20: 116-122, **2003**.
9. **Bauer I., Wanner G.A., Rensing H., Alte C., Miescher E.A., Wolf B., Pannen B.H., Clemens M.G., and Bauer M.** Expression pattern of heme oxygenase isoenzymes 1 and 2 in normal and stress-exposed rat liver. *Hepatology.* 27: 829-838, **1998**.
10. **Bauer M. and Bauer I.** Heme oxygenase-1: redox regulation and role in the hepatic response to oxidative stress. *Antioxid.Redox.Signal.* 4: 749-758, **2002**.
11. **Braggins P.E., Trakshel G.M., Kutty R.K., and Maines M.D.** Characterization of two heme oxygenase isoforms in rat spleen: comparison with the hematin-induced and constitutive isoforms of the liver. *Biochem.Biophys.Res.Commun.* 141: 528-533, **1986**.
12. **Brune B. and Ullrich V.** Inhibition of platelet aggregation by carbon monoxide is mediated by activation of guanylate cyclase. *Mol.Pharmacol.* 32: 497-504, **1987**.
13. **Bussolati B., Ahmed A., Pemberton H., Landis R.C., Di C.F., Haskard D.O., and Mason J.C.** Bifunctional role for VEGF-induced heme oxygenase-1 in vivo: induction of angiogenesis and inhibition of leukocytic infiltration. *Blood.* 103: 761-766, **2004**.

14. **Camhi S.L., Alam J., Otterbein L., Sylvester S.L., and Choi A.M.** Induction of heme oxygenase-1 gene expression by lipopolysaccharide is mediated by AP-1 activation. *Am.J.Respir.Cell Mol.Biol.* 13: 387-398, **1995**.
15. **Cantoni L., Rossi C., Rizzardini M., Gadina M., and Ghezzi P.** Interleukin-1 and tumour necrosis factor induce hepatic haem oxygenase. Feedback regulation by glucocorticoids. *Biochem.J.* 279 ( Pt 3): 891-894, **1991**.
16. **Castell J.V., Gomez-Lechon M.J., David M., Andus T., Geiger T., Trullenque R., Fabra R., and Heinrich P.C.** Interleukin-6 is the major regulator of acute phase protein synthesis in adult human hepatocytes. *FEBS Lett.* 242: 237-239, **1989**.
17. **Castell J.V., Gomez-Lechon M.J., David M., Fabra R., Trullenque R., and Heinrich P.C.** Acute-phase response of human hepatocytes: regulation of acute-phase protein synthesis by interleukin-6. *Hepatology.* 12: 1179-1186, **1990**.
18. **Chalfie M., Tu Y., Euskirchen G., Ward W.W., and Prasher D.C.** Green fluorescent protein as a marker for gene expression. *Science.* 263: 802-805, **1994**.
19. **Chirgwin J.M., Przybyla A.E., MacDonald R.J., and Rutter W.J.** Isolation of biologically active ribonucleic acid from sources enriched in ribonuclease. *Biochemistry.* 18: 5294-5299, **1979**.
20. **Choi A.M. and Alam J.** Heme oxygenase-1: function, regulation, and implication of a novel stress-inducible protein in oxidant-induced lung injury. *Am.J.Respir.Cell Mol.Biol.* 15: 9-19, **1996**.
21. **Christodoulides N., Durante W., Kroll M.H., and Schafer A.I.** Vascular smooth muscle cell heme oxygenases generate guanylyl cyclase-stimulatory carbon monoxide. *Circulation.* 91: 2306-2309, **1995**.
22. **Cruse I. and Maines M.D.** Evidence suggesting that the two forms of heme oxygenase are products of different genes. *J.Biol.Chem.* 263: 3348-3353, **1988**.
23. **Darnell J.E., Jr.** STATs and gene regulation. *Science.* 277: 1630-1635, **1997**.
24. **Decker K.** Biologically active products of stimulated liver macrophages (Kupffer cells). *Eur.J.Biochem.* 192: 245-261, **1990**.
25. **Dennery P.A.** Regulation and role of heme oxygenase in oxidative injury. *Curr.Top.Cell Regul.* 36: 181-199, **2000**.
26. **Deramaudt T.B., da Silva J.L., Remy P., Kappas A., and Abraham N.G.** Negative regulation of human heme oxygenase in microvessel endothelial cells by dexamethasone. *Proc.Soc.Exp.Biol.Med.* 222: 185-193, **1999**.
27. **Dore S., Takahashi M., Ferris C.D., Zakhary R., Hester L.D., Guastella D., and Snyder S.H.** Bilirubin, formed by activation of heme oxygenase-2, protects neurons against oxidative stress injury. *Proc.Natl.Acad.Sci.U.S.A.* 96: 2445-2450, **1999**.

28. **Eisenstein R.S., Garcia-Mayol D., Pettingell W., and Munro H.N.** Regulation of ferritin and heme oxygenase synthesis in rat fibroblasts by different forms of iron. *Proc.Natl.Acad.Sci.U.S.A.* 88: 688-692, **1991**.
29. **Eisenstein R.S. and Munro H.N.** Translational regulation of ferritin synthesis by iron. *Enzyme.* 44: 42-58, **1990**.
30. **Elbirt K.K. and Bonkovsky H.L.** Heme oxygenase: recent advances in understanding its regulation and role. *Proc.Assoc.Am.Physicians.* 111: 438-447, **1999**.
31. **Fattori E., Cappelletti M., Costa P., Sellitto C., Cantoni L., Carelli M., Faggioni R., Fantuzzi G., Ghezzi P., and Poli V.** Defective inflammatory response in interleukin 6-deficient mice. *J.Exp.Med.* 180: 1243-1250, **1994**.
32. **Feder L.S., Todaro J.A., and Laskin D.L.** Characterization of interleukin-1 and interleukin-6 production by hepatic endothelial cells and macrophages. *J.Leukoc.Biol.* 53: 126-132, **1993**.
33. **Feinberg A.P. and Vogelstein B.** A technique for radiolabeling DNA restriction endonuclease fragments to high specific activity. *Anal.Biochem.* 132: 6-13, **1983**.
34. **Fernandez M. and Bonkovsky H.L.** Increased heme oxygenase-1 gene expression in liver cells and splanchnic organs from portal hypertensive rats. *Hepatology.* 29: 1672-1679, **1999**.
35. **Ferris C.D., Jaffrey S.R., Sawa A., Takahashi M., Brady S.D., Barrow R.K., Tysoe S.A., Wolosker H., Baranano D.E., Dore S., Poss K.D., and Snyder S.H.** Haem oxygenase-1 prevents cell death by regulating cellular iron. *Nat.Cell Biol.* 1: 152-157, **1999**.
36. **Fey G.H. and Fuller G.M.** Regulation of acute phase gene expression by inflammatory mediators. *Mol.Biol.Med.* 4: 323-338, **1987**.
37. **Fort P., Marty L., Piechaczyk M., el S.S., Dani C., Jeanteur P., and Blanchard J.M.** Various rat adult tissues express only one major mRNA species from the glyceraldehyde-3-phosphate-dehydrogenase multigenic family. *Nucleic Acids Res.* 13: 1431-1442, **1985**.
38. **Gehring M.R., Shiels B.R., Northemann W., de Bruijn M.H., Kan C.C., Chain A.C., Noonan D.J., and Fey G.H.** Sequence of rat liver alpha 2-macroglobulin and acute phase control of its messenger RNA. *J.Biol.Chem.* 262: 446-454, **1987**.
39. **Geiger T., Andus T., Klapproth J., Hirano T., Kishimoto T., and Heinrich P.C.** Induction of rat acute-phase proteins by interleukin 6 in vivo. *Eur.J.Immunol.* 18: 717-721, **1988**.
40. **Geisterfer M., Richards C., Baumann M., Fey G., Gywnne D., and Gauldie J.** Regulation of IL-6 and the hepatic IL-6 receptor in acute inflammation in vivo. *Cytokine.* 5: 1-7, **1993**.
41. **Goda N., Suzuki K., Naito M., Takeoka S., Tsuchida E., Ishimura Y., Tamatani T., and Suematsu M.** Distribution of heme oxygenase isoforms in rat liver. Topographic basis for carbon monoxide-mediated microvascular relaxation. *J.Clin.Invest.* 101: 604-612, **1998**.

42. **Graham F.L. and van der Eb A.J.** A new technique for the assay of infectivity of human adenovirus 5 DNA. *Virology*. 52: 456-467, **1973**.
43. **Gunshin H., Mackenzie B., Berger U.V., Gunshin Y., Romero M.F., Boron W.F., Nussberger S., Gollan J.L., and Hediger M.A.** Cloning and characterization of a mammalian proton-coupled metal-ion transporter. *Nature*. 388: 482-488, **1997**.
44. **Hartsfield C.L.** Cross talk between carbon monoxide and nitric oxide. *Antioxid.Redox.Signal*. 4: 301-307, **2002**.
45. **Hattori M., Abraham L.J., Northemann W., and Fey G.H.** Acute-phase reaction induces a specific complex between hepatic nuclear proteins and the interleukin 6 response element of the rat alpha 2-macroglobulin gene. *Proc.Natl.Acad.Sci.U.S.A.* 87: 2364-2368, **1990**.
46. **Heinrich P.C., Behrmann I., Haan S., Hermanns H.M., Muller-Newen G., and Schaper F.** Principles of interleukin (IL)-6-type cytokine signalling and its regulation. *Biochem.J.* 374: 1-20, **2003**.
47. **Heinrich P.C., Behrmann I., Muller-Newen G., Schaper F., and Graeve L.** Interleukin-6-type cytokine signalling through the gp130/Jak/STAT pathway. *Biochem.J.* 334 ( Pt 2): 297-314, **1998**.
48. **Heinrich P.C., Castell J.V., and Andus T.** Interleukin-6 and the acute phase response. *Biochem.J.* 265: 621-636, **1990**.
49. **Hentze M.W. and Kuhn L.C.** Molecular control of vertebrate iron metabolism: mRNA-based regulatory circuits operated by iron, nitric oxide, and oxidative stress. *Proc.Natl.Acad.Sci.U.S.A.* 93: 8175-8182, **1996**.
50. **Hoffmann R., Henninger H.P., Schulze-Specking A., and Decker K.** Regulation of interleukin-6 receptor expression in rat Kupffer cells: modulation by cytokines, dexamethasone and prostaglandin E2. *J.Hepatol.* 21: 543-550, **1994**.
51. **Horvath C.M., Wen Z., and Darnell J.E., Jr.** A STAT protein domain that determines DNA sequence recognition suggests a novel DNA-binding domain. *Genes Dev.* 9: 984-994, **1995**.
52. **Immenschuh S., Hinke V., Ohlmann A., Gifhorn-Katz S., Katz N., Jungermann K., and Kietzmann T.** Transcriptional activation of the haem oxygenase-1 gene by cGMP via a cAMP response element/activator protein-1 element in primary cultures of rat hepatocytes. *Biochem.J.* 334 ( Pt 1): 141-146, **1998**.
53. **Immenschuh S. and Ramadori G.** Gene regulation of heme oxygenase-1 as a therapeutic target. *Biochem.Pharmacol.* 60: 1121-1128, **2000**.
54. **Immenschuh S., Tan M., and Ramadori G.** Nitric oxide mediates the lipopolysaccharide dependent upregulation of the heme oxygenase-1 gene expression in cultured rat Kupffer cells. *J.Hepatol.* 30: 61-69, **1999**.
55. **Inouye S. and Tsuji F.I.** Aequorea green fluorescent protein. Expression of the gene and fluorescence characteristics of the recombinant protein. *FEBS Lett.* 341: 277-280, **1994**.

56. **Kaibara A., Espat N.J., Auffenberg T., Abouhamze A.S., Martin D., Kalra S., and Moldawer L.L.** Interleukin 6, but not ciliary neurotrophic factor or leukaemia inhibitory factor, is responsible for the acute phase response to turpentine-induced myositis. *Cytokine*. 10: 452-456, **1998**.
57. **Kampfer H., Kolb N., Manderscheid M., Wetzler C., Pfeilschifter J., and Frank S.** Macrophage-derived heme-oxygenase-1: expression, regulation, and possible functions in skin repair. *Mol.Med*. 7: 488-498, **2001**.
58. **Kato Y., Shimazu M., Kondo M., Uchida K., Kumamoto Y., Wakabayashi G., Kitajima M., and Suematsu M.** Bilirubin rinse: A simple protectant against the rat liver graft injury mimicking heme oxygenase-1 preconditioning. *Hepatology*. 38: 364-373, **2003**.
59. **Katz J., Golden S., and Wals P.A.** Glycogen synthesis by rat hepatocytes. *Biochem.J*. 180: 389-402, **1979**.
60. **Kelly R.B., Cozzarelli N.R., Deutscher M.P., Lehman I.R., and Kornberg A.** Enzymatic synthesis of deoxyribonucleic acid. XXXII. Replication of duplex deoxyribonucleic acid by polymerase at a single strand break. *J.Biol.Chem*. 245: 39-45, **1970**.
61. **Kiemer A.K., Gerwig T., Gerbes A.L., Meissner H., Bilzer M., and Vollmar A.M.** Kupffer-cell specific induction of heme oxygenase 1 (hsp32) by the atrial natriuretic peptide--role of cGMP. *J.Hepatol*. 38: 490-498, **2003**.
62. **Kietzmann T., Samoylenko A., and Immenschuh S.** Transcriptional regulation of heme oxygenase-1 gene expression by MAP kinases of the JNK and p38 pathways in primary cultures of rat hepatocytes. *J.Biol.Chem*. 278: 17927-17936, **2003**.
63. **Kioussis D., Eiferman F., van de R.P., Gorin M.B., Ingram R.S., and Tilghman S.M.** The evolution of alpha-fetoprotein and albumin. II. The structures of the alpha-fetoprotein and albumin genes in the mouse. *J.Biol.Chem*. 256: 1960-1967, **1981**.
64. **Knittel T., Fellmer P., Neubauer K., Kawakami M., Grundmann A., and Ramadori G.** The complement-activating protease P100 is expressed by hepatocytes and is induced by IL-6 in vitro and during the acute phase reaction in vivo. *Lab Invest*. 77: 221-230, **1997**.
65. **Knook D.L. and Sleyster E.C.** Separation of Kupffer and endothelial cells of the rat liver by centrifugal elutriation. *Exp.Cell Res*. 99: 444-449, **1976**.
66. **Koizumi T., Odani N., Okuyama T., Ichikawa A., and Negishi M.** Identification of a cis-regulatory element for delta 12-prostaglandin J2-induced expression of the rat heme oxygenase gene. *J.Biol.Chem*. 270: 21779-21784, **1995**.
67. **Kolesnick R. and Golde D.W.** The sphingomyelin pathway in tumor necrosis factor and interleukin-1 signaling. *Cell*. 77: 325-328, **1994**.
68. **Kronke G., Bochkov V.N., Huber J., Gruber F., Bluml S., Furnkranz A., Kadl A., Binder B.R., and Leitinger N.** Oxidized phospholipids induce expression of human heme oxygenase-1 involving activation of cAMP-responsive element-binding protein. *J.Biol.Chem*. 278: 51006-51014, **2003**.

69. **Laemmli U.K.** Cleavage of structural proteins during the assembly of the head of bacteriophage T4. *Nature*. 227: 680-685, **1970**.
70. **Lavrovsky Y., Drummond G.S., and Abraham N.G.** Downregulation of the human heme oxygenase gene by glucocorticoids and identification of 56b regulatory elements. *Biochem.Biophys.Res.Commun.* 218: 759-765, **1996**.
71. **Lee P.J., Camhi S.L., Chin B.Y., Alam J., and Choi A.M.** AP-1 and STAT mediate hyperoxia-induced gene transcription of heme oxygenase-1. *Am.J.Physiol Lung Cell Mol.Physiol.* 279: L175-L182, **2000**.
72. **Lee T.S. and Chau L.Y.** Heme oxygenase-1 mediates the anti-inflammatory effect of interleukin-10 in mice. *Nat.Med.* 8: 240-246, **2002**.
73. **Lemmink H.H., Tuyt L., Knol G., Krikke E., and Vellenga E.** Identification of LIL-STAT in monocytic leukemia cells and monocytes after stimulation with interleukin-6 or interferon gamma. *Blood*. 98: 3849-3852, **2001**.
74. **Loyer P., Ilyin G., Abdel R.Z., Banchereau J., Dezier J.F., Campion J.P., Guguen-Guillouzo C., and Guillouzo A.** Interleukin 4 inhibits the production of some acute-phase proteins by human hepatocytes in primary culture. *FEBS Lett.* 336: 215-220, **1993**.
75. **Luckey S.W., Taylor M., Sampey B.P., Scheinman R.I., and Petersen D.R.** 4-hydroxynonenal decreases interleukin-6 expression and protein production in primary rat Kupffer cells by inhibiting nuclear factor-kappaB activation. *J.Pharmacol.Exp.Ther.* 302: 296-303, **2002**.
76. **Luheshi G.N., Stefferl A., Turnbull A.V., Dascombe M.J., Brouwer S., Hopkins S.J., and Rothwell N.J.** Febrile response to tissue inflammation involves both peripheral and brain IL-1 and TNF-alpha in the rat. *Am.J.Physiol.* 272: R862-R868, **1997**.
77. **Luster M.I., Germolec D.R., Yoshida T., Kayama F., and Thompson M.** Endotoxin-induced cytokine gene expression and excretion in the liver. *Hepatology*. 19: 480-488, **1994**.
78. **Lyoumi S., Puy H., Tamion F., Bogard C., Leplingard A., Scotte M., Vranckx R., Gauthier F., Hiron M., Daveau M., Nordmann Y., Deybach J.C., and Lebreton J.P.** Heme and acute inflammation role in vivo of heme in the hepatic expression of positive acute-phase reactants in rats. *Eur.J.Biochem.* 261: 190-196, **1999**.
79. **Lyoumi S., Puy H., Tamion F., Scotte M., Daveau M., Nordmann Y., Lebreton J.P., and Deybach J.C.** Nitric oxide synthase inhibition and the induction of cytochrome P-450 affect heme oxygenase-1 messenger RNA expression after partial hepatectomy and acute inflammation in rats. *Crit Care Med.* 26: 1683-1689, **1998a**.
80. **Lyoumi S., Tamion F., Petit J., Dechelotte P., Dauguet C., Scotte M., Hiron M., Leplingard A., Salier J.P., Daveau M., and Lebreton J.P.** Induction and modulation of acute-phase response by protein malnutrition in rats: comparative effect of systemic and localized inflammation on interleukin-6 and acute-phase protein synthesis. *J.Nutr.* 128: 166-174, **1998b**.
81. **Maines M.D.** The heme oxygenase system: a regulator of second messenger gases. *Annu.Rev.Pharmacol.Toxicol.* 37: 517-554, **1997**.

82. **Maines M.D., Mayer R.D., Ewing J.F., and McCoubrey W.K., Jr.** Induction of kidney heme oxygenase-1 (HSP32) mRNA and protein by ischemia/reperfusion: possible role of heme as both promotor of tissue damage and regulator of HSP32. *J.Pharmacol.Exp.Ther.* 264: 457-462, **1993**.
83. **Maines M.D., Trakshel G.M., and Kutty R.K.** Characterization of two constitutive forms of rat liver microsomal heme oxygenase. Only one molecular species of the enzyme is inducible. *J.Biol.Chem.* 261: 411-419, **1986**.
84. **McCoubrey W.K., Jr., Huang T.J., and Maines M.D.** Heme oxygenase-2 is a hemoprotein and binds heme through heme regulatory motifs that are not involved in heme catalysis. *J.Biol.Chem.* 272: 12568-12574, **1997a**.
85. **McCoubrey W.K., Jr., Huang T.J., and Maines M.D.** Isolation and characterization of a cDNA from the rat brain that encodes hemoprotein heme oxygenase-3. *Eur.J.Biochem.* 247: 725-732, **1997b**.
86. **McCoubrey W.K., Jr. and Maines M.D.** The structure, organization and differential expression of the gene encoding rat heme oxygenase-2. *Gene.* 139: 155-161, **1994**.
87. **Mikita T., Campbell D., Wu P., Williamson K., and Schindler U.** Requirements for interleukin-4-induced gene expression and functional characterization of Stat6. *Mol.Cell Biol.* 16: 5811-5820, **1996**.
88. **Mitani K., Fujita H., Kappas A., and Sassa S.** Heme oxygenase is a positive acute-phase reactant in human Hep3B hepatoma cells. *Blood.* 79: 1255-1259, **1992**.
89. **Morin J.G. and Hastings J.W.** Energy transfer in a bioluminescent system. *J.Cell Physiol.* 77: 313-318, **1971**.
90. **Morita T. and Kourembanas S.** Endothelial cell expression of vasoconstrictors and growth factors is regulated by smooth muscle cell-derived carbon monoxide. *J.Clin.Invest.* 96: 2676-2682, **1995**.
91. **Moshage H.** Cytokines and the hepatic acute phase response. *J.Pathol.* 181: 257-266, **1997**.
92. **Mostert V., Hill K.E., Ferris C.D., and Burk R.F.** Selective induction of liver parenchymal cell heme oxygenase-1 in selenium-deficient rats. *Biol.Chem.* 384: 681-687, **2003**.
93. **Motterlini R., Green C.J., and Foresti R.** Regulation of heme oxygenase-1 by redox signals involving nitric oxide. *Antioxid.Redox.Signal.* 4: 615-624, **2002**.
94. **Muller R.M., Taguchi H., and Shibahara S.** Nucleotide sequence and organization of the rat heme oxygenase gene. *J.Biol.Chem.* 262: 6795-6802, **1987**.
95. **Nakagami T., Toyomura K., Kinoshita T., and Morisawa S.** A beneficial role of bile pigments as an endogenous tissue protector: anti-complement effects of biliverdin and conjugated bilirubin. *Biochim.Biophys.Acta.* 1158: 189-193, **1993**.



96. **Neuzil J. and Stocker R.** Free and albumin-bound bilirubin are efficient co-antioxidants for alpha-tocopherol, inhibiting plasma and low density lipoprotein lipid peroxidation. *J.Biol.Chem.* 269: 16712-16719, **1994**.
97. **Northemann W., Braciak T.A., Hattori M., Lee F., and Fey G.H.** Structure of the rat interleukin 6 gene and its expression in macrophage-derived cells. *J.Biol.Chem.* 264: 16072-16082, **1989**.
98. **Oguro T., Takahashi Y., Ashino T., Takaki A., Shioda S., Horai R., Asano M., Sekikawa K., Iwakura Y., and Yoshida T.** Involvement of tumor necrosis factor alpha, rather than interleukin-1alpha/beta or nitric oxides in the heme oxygenase-1 gene expression by lipopolysaccharide in the mouse liver. *FEBS Lett.* 516: 63-66, **2002**.
99. **Ohta K., Kikuchi T., Arai S., Yoshida N., Sato A., and Yoshimura N.** Protective role of heme oxygenase-1 against endotoxin-induced uveitis in rats. *Exp.Eye Res.* 77: 665-673, **2003**.
100. **Okinaga S. and Shibahara S.** Identification of a nuclear protein that constitutively recognizes the sequence containing a heat-shock element. Its binding properties and possible function modulating heat-shock induction of the rat heme oxygenase gene. *Eur.J.Biochem.* 212: 167-175, **1993**.
101. **Otterbein L.E., Bach F.H., Alam J., Soares M., Tao L.H., Wysk M., Davis R.J., Flavell R.A., and Choi A.M.** Carbon monoxide has anti-inflammatory effects involving the mitogen-activated protein kinase pathway. *Nat.Med.* 6: 422-428, **2000**.
102. **Otterbein L.E. and Choi A.M.** Heme oxygenase: colors of defense against cellular stress. *Am.J.Physiol Lung Cell Mol.Physiol.* 279: L1029-L1037, **2000**.
103. **Otterbein L.E., Soares M.P., Yamashita K., and Bach F.H.** Heme oxygenase-1: unleashing the protective properties of heme. *Trends Immunol.* 24: 449-455, **2003**.
104. **Perregaux D.G. and Gabel C.A.** Post-translational processing of murine IL-1: evidence that ATP-induced release of IL-1 alpha and IL-1 beta occurs via a similar mechanism. *J.Immunol.* 160: 2469-2477, **1998**.
105. **Pillar T.M. and Seitz H.J.** Oxidative stress response induced in rat primary hepatocyte monolayers by mechanical removal of adherent cells. *Cell Tissue Res.* 295: 363-367, **1999**.
106. **Poli V., Balena R., Fattori E., Markatos A., Yamamoto M., Tanaka H., Ciliberto G., Rodan G.A., and Costantini F.** Interleukin-6 deficient mice are protected from bone loss caused by estrogen depletion. *EMBO J.* 13: 1189-1196, **1994**.
107. **Poss K.D. and Tonegawa S.** Heme oxygenase 1 is required for mammalian iron reutilization. *Proc.Natl.Acad.Sci.U.S.A.* 94: 10919-10924, **1997**.
108. **Prasher D.C., Eckenrode V.K., Ward W.W., Prendergast F.G., and Cormier M.J.** Primary structure of the *Aequorea victoria* green-fluorescent protein. *Gene.* 111: 229-233, **1992**.
109. **Ramadori G. and Armbrust T.** Cytokines in the liver. *Eur.J.Gastroenterol.Hepatol.* 13: 777-784, **2001**.

110. **Ramadori G. and Christ B.** Cytokines and the hepatic acute-phase response. *Semin.Liver Dis.* 19: 141-155, **1999**.
111. **Rizzardini M., Carelli M., Cabello Porras M.R., and Cantoni L.** Mechanisms of endotoxin-induced haem oxygenase mRNA accumulation in mouse liver: synergism by glutathione depletion and protection by N-acetylcysteine. *Biochem.J.* 304 ( Pt 2): 477-483, **1994**.
112. **Rizzardini M., Zappone M., Villa P., Gnocchi P., Sironi M., Diomede L., Meazza C., Monshouwer M., and Cantoni L.** Kupffer cell depletion partially prevents hepatic heme oxygenase 1 messenger RNA accumulation in systemic inflammation in mice: role of interleukin 1beta. *Hepatology.* 27: 703-710, **1998**.
113. **Rowell D.L., Eckmann L., Dwinell M.B., Carpenter S.P., Raucy J.L., Yang S.K., and Kagnoff M.F.** Human hepatocytes express an array of proinflammatory cytokines after agonist stimulation or bacterial invasion. *Am.J.Physiol.* 273: G322-G332, **1997**.
114. **Ryter S.W. and Choi A.M.** Heme oxygenase-1: molecular mechanisms of gene expression in oxygen-related stress. *Antioxid.Redox.Signal.* 4: 625-632, **2002**.
115. **Ryter S.W. and Tyrrell R.M.** The heme synthesis and degradation pathways: role in oxidant sensitivity. Heme oxygenase has both pro- and antioxidant properties. *Free Radic.Biol.Med.* 28: 289-309, **2000**.
116. **Schreiber G., Aldred A.R., Thomas T., Birch H.E., Dickson P.W., Tu G.F., Heinrich P.C., Northemann W., Howlett G.J., de Jong F.A., and .** Levels of messenger ribonucleic acids for plasma proteins in rat liver during acute experimental inflammation. *Inflammation.* 10: 59-66, **1986**.
117. **Seglen P.O.** Preparation of rat liver cells. 3. Enzymatic requirements for tissue dispersion. *Exp.Cell Res.* 82: 391-398, **1973**.
118. **Seidel H.M., Milocco L.H., Lamb P., Darnell J.E., Jr., Stein R.B., and Rosen J.** Spacing of palindromic half sites as a determinant of selective STAT (signal transducers and activators of transcription) DNA binding and transcriptional activity. *Proc.Natl.Acad.Sci.U.S.A.* 92: 3041-3045, **1995**.
119. **Shibahara S., Muller R., Taguchi H., and Yoshida T.** Cloning and expression of cDNA for rat heme oxygenase. *Proc.Natl.Acad.Sci.U.S.A.* 82: 7865-7869, **1985**.
120. **Shibahara S., Yoshizawa M., Suzuki H., Takeda K., Meguro K., and Endo K.** Functional analysis of cDNAs for two types of human heme oxygenase and evidence for their separate regulation. *J.Biochem.(Tokyo).* 113: 214-218, **1993**.
121. **Siewert E., Bort R., Kluge R., Heinrich P.C., Castell J., and Jover R.** Hepatic cytochrome P450 down-regulation during aseptic inflammation in the mouse is interleukin 6 dependent. *Hepatology.* 32: 49-55, **2000**.
122. **Smith P.K., Krohn R.I., Hermanson G.T., Mallia A.K., Gartner F.H., Provenzano M.D., Fujimoto E.K., Goeke N.M., Olson B.J., and Klenk D.C.** Measurement of protein using bicinchoninic acid. *Anal.Biochem.* 150: 76-85, **1985**.

123. **Soares M.P., Seldon M.P., Gregoire I.P., Vassilevskaia T., Berberat P.O., Yu J., Tsui T.Y., and Bach F.H.** Heme oxygenase-1 modulates the expression of adhesion molecules associated with endothelial cell activation. *J.Immunol.* 172: 3553-3563, **2004**.
124. **Song R., Kubo M., Morse D., Zhou Z., Zhang X., Dauber J.H., Fabisiak J., Alber S.M., Watkins S.C., Zuckerbraun B.S., Otterbein L.E., Ning W., Oury T.D., Lee P.J., McCurry K.R., and Choi A.M.** Carbon monoxide induces cytoprotection in rat orthotopic lung transplantation via anti-inflammatory and anti-apoptotic effects. *Am.J.Pathol.* 163: 231-242, **2003a**.
125. **Song Y., Shi Y., Ao L.H., Harken A.H., and Meng X.Z.** TLR4 mediates LPS-induced HO-1 expression in mouse liver: role of TNF-alpha and IL-1beta. *World J.Gastroenterol.* 9: 1799-1803, **2003b**.
126. **Srivastava K.K., Cable E.E., Donohue S.E., and Bonkovsky H.L.** Molecular basis for heme-dependent induction of heme oxygenase in primary cultures of chick embryo hepatocytes. Demonstration of acquired refractoriness to heme. *Eur.J.Biochem.* 213: 909-917, **1993**.
127. **Stocker R., Yamamoto Y., McDonagh A.F., Glazer A.N., and Ames B.N.** Bilirubin is an antioxidant of possible physiological importance. *Science.* 235: 1043-1046, **1987**.
128. **Streetz K.L., Wustefeld T., Klein C., Manns M.P., and Trautwein C.** Mediators of inflammation and acute phase response in the liver. *Cell Mol.Biol.(Noisy.-le-grand).* 47: 661-673, **2001**.
129. **Suematsu M. and Ishimura Y.** The heme oxygenase-carbon monoxide system: a regulator of hepatobiliary function. *Hepatology.* 31: 3-6, **2000**.
130. **Tamion F., Richard V., Bonmarchand G., Leroy J., Lebreton J.P., and Thuillez C.** Induction of heme-oxygenase-1 prevents the systemic responses to hemorrhagic shock. *Am.J.Respir.Crit Care Med.* 164: 1933-1938, **2001**.
131. **Tamion F., Richard V., Lyoumi S., Hiron M., Bonmarchand G., Leroy J., Daveau M., Thuillez C., and Lebreton J.P.** Induction of haem oxygenase contributes to the synthesis of pro-inflammatory cytokines in re-oxygenated rat macrophages: role of cGMP. *Cytokine.* 11: 326-333, **1999**.
132. **Taylor J.L., Carraway M.S., and Piantadosi C.A.** Lung-specific induction of heme oxygenase-1 and hyperoxic lung injury. *Am.J.Physiol.* 274: L582-L590, **1998**.
133. **Tenhunen R., Marver H.S., and Schmid R.** The enzymatic conversion of heme to bilirubin by microsomal heme oxygenase. *Proc.Natl.Acad.Sci.U.S.A.* 61: 748-755, **1968**.
134. **Tenhunen R., Marver H.S., and Schmid R.** Microsomal heme oxygenase. Characterization of the enzyme. *J.Biol.Chem.* 244: 6388-6394, **1969**.
135. **Tenhunen R., Marver H.S., and Schmid R.** The enzymatic catabolism of hemoglobin: stimulation of microsomal heme oxygenase by hemin. *J.Lab Clin.Med.* 75: 410-421, **1970**.
136. **Terry C.M., Clikeman J.A., Hoidal J.R., and Callahan K.S.** Effect of tumor necrosis factor-alpha and interleukin-1 alpha on heme oxygenase-1 expression in human endothelial cells. *Am.J.Physiol.* 274: H883-H891, **1998**.

137. **Towbin H., Staehelin T., and Gordon J.** Electrophoretic transfer of proteins from polyacrylamide gels to nitrocellulose sheets: procedure and some applications. *Proc.Natl.Acad.Sci.U.S.A.* 76: 4350-4354, **1979**.
138. **Tsujinaka T., Kishibuchi M., Yano M., Morimoto T., Ebisui C., Fujita J., Ogawa A., Shiozaki H., Kominami E., and Monden M.** Involvement of interleukin-6 in activation of lysosomal cathepsin and atrophy of muscle fibers induced by intramuscular injection of turpentine oil in mice. *J.Biochem.(Tokyo)*. 122: 595-600, **1997**.
139. **Tullius S.G., Nieminen-Kelha M., Buelow R., Reutzel-Selke A., Martins P.N., Pratschke J., Bachmann U., Lehmann M., Southard D., Iyer S., Schmidbauer G., Sawitzki B., Reinke P., Neuhaus P., and Volk H.D.** Inhibition of ischemia/reperfusion injury and chronic graft deterioration by a single-donor treatment with cobalt-protoporphyrin for the induction of heme oxygenase-1. *Transplantation*. 74: 591-598, **2002**.
140. **Ulich T.R., Guo K.Z., Irwin B., Remick D.G., and Davatelis G.N.** Endotoxin-induced cytokine gene expression in vivo. II. Regulation of tumor necrosis factor and interleukin-1 alpha/beta expression and suppression. *Am.J.Pathol.* 137: 1173-1185, **1990**.
141. **Ulich T.R., Guo K.Z., Remick D., del C.J., and Yin S.M.** Endotoxin-induced cytokine gene expression in vivo. III. IL-6 mRNA and serum protein expression and the in vivo hematologic effects of IL-6. *J.Immunol.* 146: 2316-2323, **1991**.
142. **Verma A., Hirsch D.J., Glatt C.E., Ronnett G.V., and Snyder S.H.** Carbon monoxide: a putative neural messenger. *Science*. 259: 381-384, **1993**.
143. **Vicente A.M., Guillen M.I., Habib A., and Alcaraz M.J.** Beneficial effects of heme oxygenase-1 up-regulation in the development of experimental inflammation induced by zymosan. *J.Pharmacol.Exp.Ther.* 307: 1030-1037, **2003**.
144. **Wagener F.A., Eggert A., Boerman O.C., Oyen W.J., Verhofstad A., Abraham N.G., Adema G., van K.Y., de W.T., and Figdor C.G.** Heme is a potent inducer of inflammation in mice and is counteracted by heme oxygenase. *Blood*. 98: 1802-1811, **2001**.
145. **Wagner C.T., Durante W., Christodoulides N., Hellums J.D., and Schafer A.I.** Hemodynamic forces induce the expression of heme oxygenase in cultured vascular smooth muscle cells. *J.Clin.Invest.* 100: 589-596, **1997**.
146. **Wang R., Wang Z., and Wu L.** Carbon monoxide-induced vasorelaxation and the underlying mechanisms. *Br.J.Pharmacol.* 121: 927-934, **1997**.
147. **Wang S. and Hazelrigg T.** Implications for bcd mRNA localization from spatial distribution of exu protein in *Drosophila* oogenesis. *Nature*. 369: 400-403, **1994**.
148. **Wilks A.** Heme oxygenase: evolution, structure, and mechanism. *Antioxid.Redox.Signal.* 4: 603-614, **2002**.
149. **Wunder C. and Potter R.F.** The heme oxygenase system: its role in liver inflammation. *Curr Drug Targets.Cardiovasc.Haematol.Disord.* 3: 199-208, **2003**.

150. **Yang D.C., Jiang X., Elliott R.L., and Head J.F.** Antisense ferritin oligonucleotides inhibit growth and induce apoptosis in human breast carcinoma cells. *Anticancer Res.* 22: 1513-1524, **2002**.
151. **Yoshida T. and Kikuchi G.** Purification and properties of heme oxygenase from rat liver microsomes. *J.Biol.Chem.* 254: 4487-4491, **1979**.
152. **Zucker S.D., Goessling W., and Hoppin A.G.** Unconjugated bilirubin exhibits spontaneous diffusion through model lipid bilayers and native hepatocyte membranes. *J.Biol.Chem.* 274: 10852-10862, **1999**.

## Acknowledgements

I want to express gratitude to Professor Giuliano Ramadori for the opportunity he gave me to work in this department and for his encouragement to perform this study. I deeply appreciate the time he spent supervising and teaching me.

I am thankful to Professor Rüdiger Hardeland for reviewing my PhD thesis and to Professor Kurt von Figura for being my coreviewer.

I am thankful to Professor Gerhard Burckhardt, a leader of GRK 335, for giving me the opportunity to be a scholar in the frame of GRK “Clinical, Cellular and Molecular Biology of Internal Organs”, and for his help in every respect.

I am grateful to Dr. Thomas Kietzmann and Dr. Anatoly Samoylenko for their help and cooperation. I appreciate their helpful advices and the time they spent discussing our results.

My sincere thanks to Dr. Jozsef Dudas for his cooperation, practical advices and answering all my questions. I am thankful to Ruslan Novosyadlyy for his contribution to my project and cooperativeness.

I want to give my special thanks to Renate Klages for help in organizing of my work and for her constant wholehearted support in every respect.

I am very thankful to Dr. Silke Cameron for proof-read and corrections of the manuscript.

I am thankful to Missis Zachmann for help with isolation of hepatocytes and to Anke Herbst for teaching me laboratory techniques.

I thank Buba, Abdul, Velasco and all other colleagues, with whom I worked day by day in the department, for the creation of scientific working atmosphere.

My very special thanks to Dasha for her support in all respects.

## Curriculum Vitae

Name	Kyrylo Tron
Date of birth	26.07.1977
Place of birth	Zhytomyr, Ukraine
Citizenship	Ukraine
1984 – 1994	School education Kiev, Ukraine
1995 – 2000	University Study Biological faculty Kiev National Taras Shevchenko University Kiev, Ukraine
1999	Bachelor diploma with honors Degree: Bachelor of Science in biology, teacher of biology Defense of Bachelor scientific project “The comparative characteristic of the methods of human microplasminogen purification”
2000	Master diploma with honors Degree: Master of Science in biology, biochemistry, University teacher of biology Defense of Master scientific project “Isolation and study of tyrosine protein kinases from rat splenocytes under irradiation”
2000 – 2001	PhD Student Department of biochemistry Kiev National Taras Shevchenko University Kiev, Ukraine
March 2001 – May 2004	Experimental work for the present dissertation in Department of Gastroenterology and Endocrinology of Georg-August University Clinic (Göttingen) in the frame of GRK 335 “Clinical, Cellular and Molecular Biology of Internal Organs“